Nonlinear Cyclic Truss Model for Beam-Column Joints of Non-ductile RC Frames

Jeremy Thomas Bowers

Thesis submitted to the faculty of the Virginia Polytechnic Institute and State University in partial fulfillment of the requirements for the degree of

Master of Science
In
Civil Engineering

Ioannis Koutromanos, Chair
Finley A. Charney
Roberto T. Leon

6/24/14
Blacksburg, VA

Keywords: Reinforced Concrete, Beam-Column Joints, Seismic Analysis

Nonlinear Cyclic Truss Model for Beam-Column Joints of Non-ductile RC Frames

Jeremy Thomas Bowers

ABSTRACT

Reinforced concrete (RC) moment frames comprise a significant portion of the built environment in areas with seismic hazards. The beam-to-column joints of these frames are key components that have a significant impact on the structure's behavior. Modern detailing provides sufficient strength within these joints to transfer the forces between the beams and the columns during a seismic event, but existing structures built with poor detailing are still quite prevalent. Identifying the need and extent of retrofits to ensure public safety through nondestructive means is of primary importance. Existing models used to analyze the performance of RC beam-to-column joints have either been developed for modern, well-detailed joints or are simplified so that they do not capture a broad range of phenomena.

The present study is aimed to extend a modeling technique based on the nonlinear truss analogy to the analysis of RC beam-to-column joints under cyclic loads. Steel and concrete elements were arranged into a lattice truss structure with zero-length bond-slip springs connecting them. A new steel model was implemented to more accurately capture the constitutive behavior of reinforcing bars. The joint modeling approach captured well the shear response of the joint. It also provided a good indication of the distribution of forces within the joint.

The model was validated against three recently tested beam-column subassemblies. These tests represented the detailing practice of poorly-detailed RC moment frames. The analytical results were in good agreement with the experimental data in terms of initial stiffness, strength and damage pattern through the joint.

Acknowledgements

"Where there is no guidance, a people falls, but in an abundance of counselors there is safety."

- Proverbs 11:14

I would like to thank those who have helped guide me in this process. To my fellow student, Mohammadreza Gargari, I would like to show my appreciation for the advice and assistance he gave along the way. I would also like to thank Professor Roberto Leon for the impromptu meetings where he shared invaluable years of experience and Professor Finley Charney for the counsel he gave. I must give a special thanks to my advisor, Professor Ioannis Koutromanos, who spent countless hours teaching, counseling, and spurring me on to further apply myself. Finally, I must give praise to God, through whose strength I have been able to complete this work.

Table of Contents

List of Figures

List of Tables

Chapter 1. Introduction

1.1 Background

Reinforced concrete (RC) buildings comprise a significant portion of the built environment in the United States due to their relatively low cost and flexibility in building form. Lateral loads in RC buildings can be resisted by two types of lateral load resisting systems: shear walls or moment frames. Moment frames are assemblies of beams and columns connected by beam-to-column joints. This type of system leaves a greater amount of open floor space within the building interior, which is much more attractive from an architectural point of view. This system also relies heavily on the ability of the beam-to-column joint to transfer the moment due to lateral loads between the columns and the beams. Brittle failure leading to a sudden, drastic decrease in strength can be a dire consequence of insufficient loading capacity and ductility within this joint. For this reason, more stringent requirements have been placed on the detailing of beam-to-column joints since the mid-1970's in order to ensure that the joint has adequate strength and in case of yielding, can undergo a relatively large amount of deformation without a complete loss of strength. These newer beam-to-column joint details are referred to as ductile, whereas those resulting in poor system deformation capacity are referred to as nonductile.

Many current RC structures, especially older structures and structures built in areas with less frequent seismic activity, still maintain nonductile detailing. The high vulnerability of RC moment frame buildings with nonductile beam-to-column joints (nonductile RC frames) has been made apparent during the relatively moderate recent earthquakes in Northridge, California, and Kocaeli (Izmit), Turkey. In the 1994 Northridge earthquake there were several building collapses, including the collapse of the Kaiser Permanente building pictured in Figure 1.1. This collapse can be traced primarily to the failure of the nonductile beam-to-column connection in

the building corner, as seen in Figure 1.1b (Hassan et al., 2010). Figure 1.2 pictures the partial building collapse of a nonductile RC frame during the 1999 Izmit earthquake in which there is relatively little damage within the framing elements, but high damage within the beam-to-column joint (Sezen et al., 2000). The series of earthquakes that struck Christchurch, New Zealand, from 2010-2012 are another reminder of the massive damage and loss of life that can be caused by the inadequate performance of poorly detailed RC structures. Several nonductile RC frames showed signs of damage within the beam-to-column joints and this damage contributed to the partial or full collapse of certain buildings (Leon et al., 2014).

Nonductile RC frames, having been the norm of construction prior to the advent of system ductility requirements in the 1971 American Concrete Institute (ACI) building code (ACI, 1971), comprise a large portion of the existing structures in the U.S. In California alone, there is an estimated 40,000 nonductile concrete buildings (Comartin et al., 2008), in spite of relatively frequent significant seismic events. In the Central and Eastern U.S., where significant seismic events are less frequent, this number increases dramatically. Though they are less frequent in this part of the country, the extent of a significant seismic event would be much more devastating due to the lessened capability of the bedrock to disperse seismic energy. Compared with the 1994 Northridge earthquake, which had a magnitude of 6.7, the magnitude 6 earthquake that struck Saint Louis in 1895 had a much farther reaching area of damage, as seen in Figure 1.3. If a similar earthquake were to strike the Central or Eastern U.S. today, the results would be disastrous (Filson et al., 2003).

The high vulnerability of nonductile RC frames to earthquake events forces the consideration of applying seismic retrofits to existing structures. A rational retrofit strategy requires the reliable determination of the vulnerability corresponding to a given level of seismic

a) Partial building collapse

b) Close up of beam-to-column joint failure

Figure 1.1 Partial collapse of Kaiser Permanente building during 1994 Northridge earthquake. Hassan, W. M., Park, S., Lopez, R. R., Mosalam, K. M., and Moehle, J. P. (2010), "Seismic Response of Older-Type Reinforced Concrete Corner Joints." Proceedings of the 9th U.S. National and 10th Canadian Conference on Earthquake Engineering, Toronto, Ontario, Canada, Paper No. 1616. Photo used under fair use, 2014.

a) Partial building collapse

b) Close up of beam-to-column joint failure

Figure 1.2 Partial building collapse during 1999 Izmit earthquake. Sezen, H., Elwood, K. J., Whittaker, A. S., Mosalam, K. M., Walace, J. W., and Stanton, J. F., (2000), "Sezen - Structural Engineering Reconnaissance of the August 17, 1999, Kocaeli (Izmit), Turkey, Earthquake." *Report No. PEER-2000/09*, Berkeley, CA. Photos used under fair use, 2014.

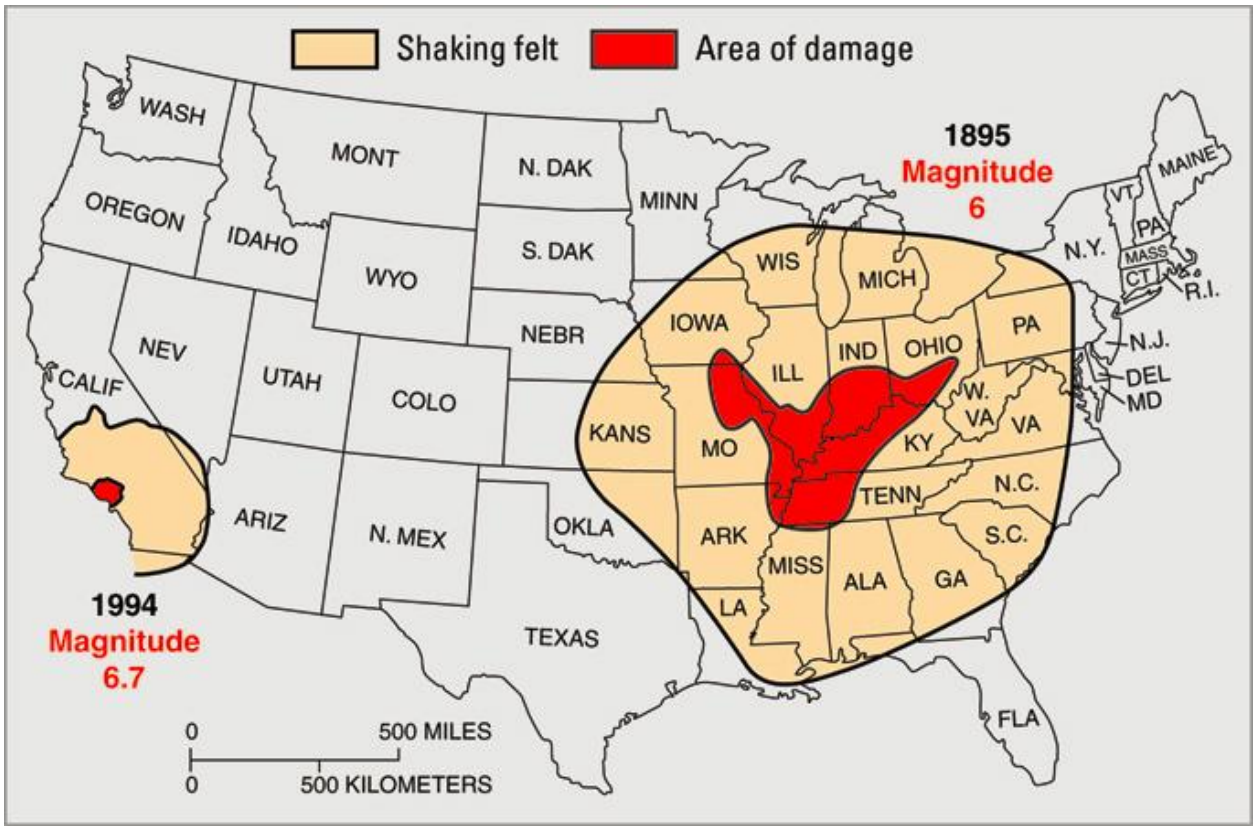

Figure 1.3 Damage areas of the 1994 Northridge earthquake and the 1895 St. Louis earthquake. Filson, J. R., McCarthy, J., Ellsworth, W. L., and Zoback, M. L. (2003), "The USGS earthquake hazards program in NEHRP—Investing in a safer future." *USGS Fact Sheet 017-03*, Reston, VA. Figure used under fair use, 2014.

demand, the latter expressed in terms of a deformation history. The aim of this research is to computationally assess the performance of existing nonductile RC frames undergoing seismic loads to determine the degree and necessity of seismic retrofits.

1.2 Thesis Scope

This thesis aims to the establishment of a modeling approach that adequately describes the behavior of nonductile beam-to-column joints. Whereas a great deal of research has been undertaken to assess the performance of well-detailed joints under cyclic loading, the prevalence of poorly-detailed joints necessitates an effort to properly model their behavior. Beam-to-column joint damage is typically caused by shear stresses within the joint which leads to diagonal

cracking and crushing of the concrete along principal stress planes, and is manifested as spalling of the concrete on the joint core surface, as pictured in Figure 1.4. Tests have shown that the concrete compressive strength and confinement, the steel reinforcement details, and the bond strength have significant influence on joint behavior, and the compressive strut and panel truss have both been described as primary shear force transfer mechanisms.

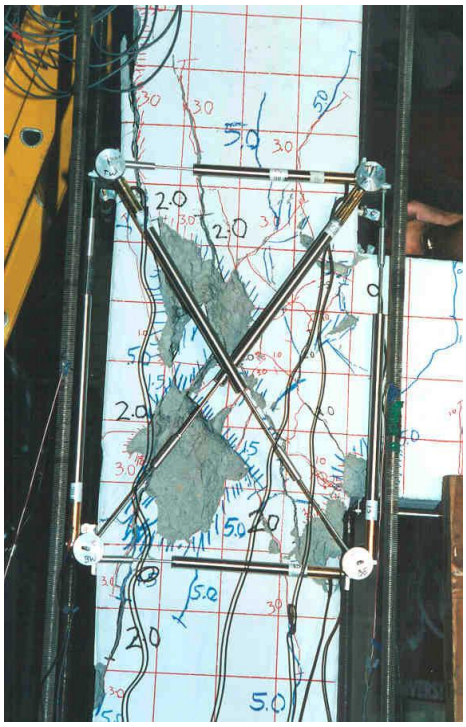

Figure 1.4 Concrete spalling within beam-to-column joint core. Pantelides, C., Hansen, J., Nadauld, J., and Reaveley, L. (2002), "Assessment of Reinforced Concrete Building Exterior Joints with Substandard Details." *Report No. PEER-2002/18,* Berkeley, CA. Photo used under fair use, 2014.

The vast majority of analytical models currently available are either empirical in nature, and thus should not be applied to cases not directly related to the physical testing on which they are based, or mechanistic, based primarily on considerations of mechanics. The mechanistic model described herein represents behavior by nonlinear truss elements, directly modeling steel, concrete, and reinforcement bond-slip elements based on their respective cyclic constitutive relationships, and capturing the two primary shear force transfer mechanisms by assembling these elements into a truss structure. The modeling scheme has been implemented in the OpenSees analysis platform (McKenna et al., 2005). A nonlinear steel constitutive model by Dodd and Restrepo-Posada (1995) has also been implemented to improve on the accuracy of the standard bilinear models used for steel reinforcement.

Beam-to-column connections can be categorized by their in-plane geometry as interior, exterior, or knee joints, as seen in Figure 1.5. An interior joint has beams framing in on both sides and columns framing in on both the top and the bottom, whereas an exterior joint only has a beam framing in on one side and columns framing in on both the top and the bottom. A knee joint has a single beam and a single column framing into the joint. Both interior and exterior joints have been selected to validate the proposed model

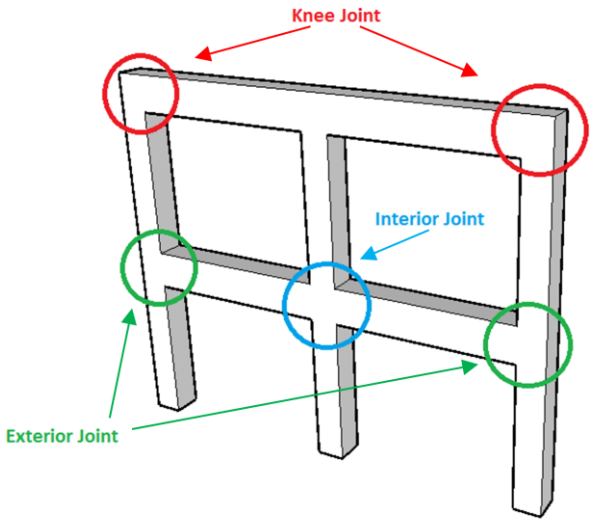

Figure 1.5 Connection types

1.3 Thesis Outline

Chapter 2 presents an overview of experimental tests of RC beam-to-column connections under cyclic loading, existing empirical beam-to-column connection models, and existing mechanistic beam-to-column connection models.

Chapter 3 describes the proposed methodology for the simulation of beam-to-column joints, based on the nonlinear truss analogy for reinforced concrete. Modeling scheme configurations and constitutive relationships for the concrete and reinforcing steel are described. The addition of a bond-slip model and confinement effects caused by the vertical confining pressure due to the column axial load are also discussed.

Chapter 4 gives a validation of the proposed model based on quasi-static experimental tests of nonductile interior and exterior beam-to-column connections. The effects of bond-slip and concrete confinement are also investigated.

Chapter 5 presents the conclusions of the present study and provides recommendations for future research.

Chapter 2. Literature Review

2.1 Description of Joint Behavior

Many tests have been conducted to observe the seismic behavior of reinforced concrete frame (RCF) beam-to-column joints. Paulay et al. (1978) have suggested two primary shear transfer mechanisms to describe this behavior: the diagonal concrete strut and the panel truss, illustrated in Figure 2.1. The concrete strut relies solely on the compressive response of a diagonal strut extending from one upper corner to the opposite lower corner within the concrete of the joint. The panel truss, however, relies on reinforcing steel to transfer the horizontal and vertical components of shear through tension. Both mechanisms contribute to the system simultaneously, with the compression strut having a greater influence prior to joint yielding because the reinforcing elements have not yet been fully activated. Once first yield occurs, behavior is highly dependent on the bond between concrete and reinforcement. When bond is poor, the strut mechanism continues to govern behavior beyond the first yield, but when good

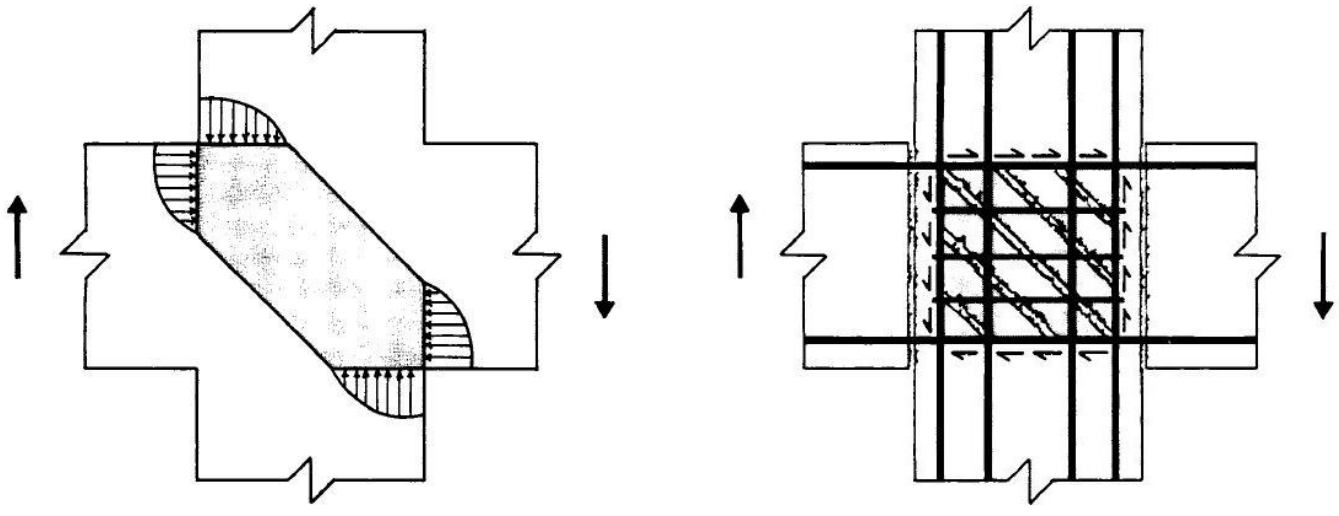

a) Concrete compressive strut mechanism b) Panel truss mechanism

Figure 2.1 Joint shear transfer mechanisms. Leon, R. (1990), "Shear Strength and Hysteretic Behavior of Interior Beam-Column Joints." ACI Structural Journal 87(1), 3-11. Figures used under fair use, 2014.

bond is achieved, the panel truss mechanism is dominant.

Ehsani and Wight (1985) tested 6 experiments of exterior beam-to-column joints, varying the transverse steel reinforcement ratio within the connections. Design values for the joint transverse reinforcement ratios were calculated based on the draft recommendations of ACI Committee 352 (ACI, 1985). Actual joints were then built with joint transverse reinforcement ratios that ranged from 74% to 99% of these design values. The objective was primarily to show that a less congested joint design may still be adequate in many cases. These tests showed that the beam-column flexural strength ratio had a significant effect on the location of the flexural hinge, either well within the beam or in the beam at the column face. For tests with low flexural strength ratios, where flexural hinges formed in the beam at the face of the column, transverse reinforcement ratio had little effect. However, when flexural hinges formed well within the beam, the transverse reinforcement ratio significantly improved the ductility of the joint. Loss of shear stiffness within the joint was largely attributed to slipping of the reinforcing bars. This issue was exacerbated by the formation of flexural hinges near the column faces.

Leon (1989) performed four half-scale tests to assess the effects of variable anchorage lengths and nominal joint shear stress on joint performance. The importance of capturing shear force-deformation behavior was emphasized, as it has a high influence on joint behavior when the beam steel development length is less than 24 bar diameters. Leon (1990) suggested that this shear behavior was highly dependent on the level of bond between the anchored reinforcement and the concrete, as well as the amount of contact between the joint and the beam at the interface of the two. For joints with little or no joint transverse reinforcement, he found that the diagonal compressive strut was the primary shear force transfer mechanism.

The effects of cyclic loading on interior and exterior beam-to-column joints of gravity load-designed frames have been experimentally investigated by Beres et al. (1991, 1992, 1996). Their tests have shown that the column axial load had a significant influence on the joint behavior. In the interior joints, this load had a positive effect, with higher compressive loads leading to increased stiffness and capacity. It was noted that this increased vertical compressive force within the joint improved the bond between concrete and reinforcement. In the exterior joints, however, the existence of column axial load precipitated the propagation of shear cracks within the joint. Column longitudinal reinforcement diameter, quantity, and arrangement were shown to have little effect on joint behavior. The presence of transverse beams loaded in compression had a negligible effect in interior joints, but did affect the behavior of exterior joints. In joints with discontinuous beam longitudinal reinforcement, pull out of the embedded beam steel was a major contributing factor to failure. It was also noted that spalling of concrete on the face of the joint lead to the buckling of column longitudinal reinforcement.

Pagni and Lowes (2004) compiled 21 specimen results from 5 sets of experimental tests to identify damage state development in nonductile reinforced concrete frames during seismic excitations and potential repair methods to restore the frames to pre-damaged states. The study found that the following factors have the greatest influence on cyclic joint response: nominal joint shear stress demand, transverse steel ratio, bond stress demand of longitudinal beam reinforcement, embedment of beam reinforcement, column axial load, and column splice location. A total of ten damage states were identified:

1. Flexural cracking at the beam-joint interface,
2. Cracking within the joint,
3. Yielding of longitudinal beam reinforcement,

4. Spalling of concrete at joint surface,
5. Deterioration of joint shear strength
6. Extension of joint cracks into beam and/or column,
7. Concrete crushing in joint core,
8. Buckling of column longitudinal reinforcement,
9. Loss of beam longitudinal reinforcement anchorage within the joint core,
10. Pull-out of beam longitudinal reinforcement.

After the onset of joint surface spalling, joint shear strength begins to degrade. Pagni and Lowes suggest that yielding of longitudinal beam reinforcement has a great influence on deterioration of bond strength because of the Poisson effect; tensile lengthening of the reinforcement in the longitudinal direction causes a reduction of cross section in the transverse directions.

A large database (139 connections) has been constructed by Kim and LaFave (2006) to allow the detections of common characteristics among these experiments and facilitate the calibration of analytical models. Experiments included interior, exterior, and knee joints and the following five parameters were investigated:

1. Concrete compressive strength
2. Joint panel geometry (characterized by the ratios of beam height to column width and beam depth to column depth)
3. Confinement of joint by beam longitudinal, column longitudinal, and joint transverse reinforcement
4. Column axial compression
5. Bond demand level of the beam and column longitudinal reinforcement

As joint shear strength was the primary focus of the study, all five parameters were compared with either the joint shear stress or the joint shear strain at three distinct points, illustrated in Figure 2.2. The first point (point A) was taken as the point of first significant change in tangent stiffness, considered to be the onset of joint shear cracking, pictured in Figure 2.3. Point B was taken as the point of next significant change in tangent stiffness, assumed to be caused by a yielding of the joint reinforcement. Point C was taken as the point of maximum shear stress, at which the initiation of concrete crushing is likely occurring, leading to the extreme concrete crushing seen in Figure 2.4. It was found that the concrete compressive strength had the greatest influence on joint shear strength, as seen in Figure 2.5, with the correlation coefficients between the concrete compressive concrete and the joint shear strength in certain types of joints exceeding 0.9. It was also noted that the compressive strength affects the bond formed between concrete and reinforcement, having an added effect on behavior. Confinement of the joint was also shown to be of some importance, though not as critical as compressive strength. However, axial load in the column, bond of the longitudinal reinforcement, and joint geometry were shown to have minimal effect. As this study focused largely on well confined joints with at least some transverse reinforcement, it is suspected that findings concerning the negligible effect of reinforcement bonding (and subsequently column axial load, as this has an effect on bond level) may not be applicable. The high influence of compressive strength and confinement may be of significance, however.

Park and Mosalam (2009) have examined the results of sixty two tests to determine the major factors affecting the shear strength of nonductile exterior beam-to-column joints and to develop both empirical and mechanistic models to predict joint behavior. The effects of joint

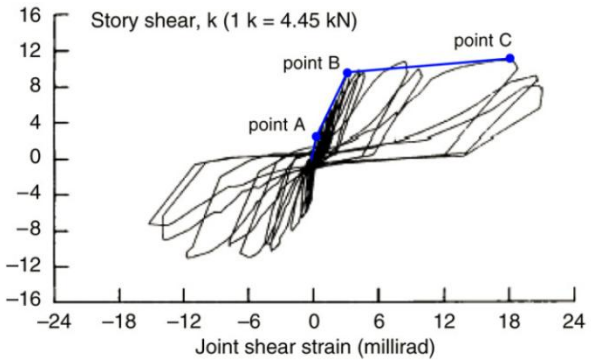

Figure 2.2 Shear stress-strain points. Kim, J., and LaFave, J. (2006), "Key influence parameters for the joint shear behaviour of reinforced concrete (RC) beam-column connections." *Engineering Structures 29, 2523-2539.* Figure used under fair use, 2014.

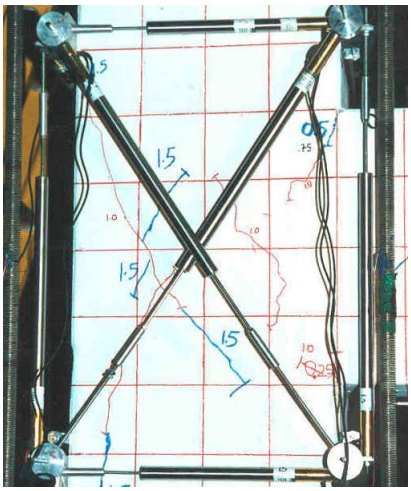

Figure 2.3 Formation of joint shear cracks. Pantelides, C., Hansen, J., Nadauld, J., and Reaveley, L. (2002), "Assessment of Reinforced Concrete Building Exterior Joints with Substandard Details." *Report No. PEER-2002/18,* Berkeley, CA. Photo used under fair use, 2014.

Figure 2.4 Crushing within joint core. Pagni, C., and Lowes, L. (2004), "Predicting Earthquake Damage in Older Reinforced Concrete Beam-Column Joints." *Report No. PEER-2003/17,* Berkeley, CA. Photo used under fair use, 2014.

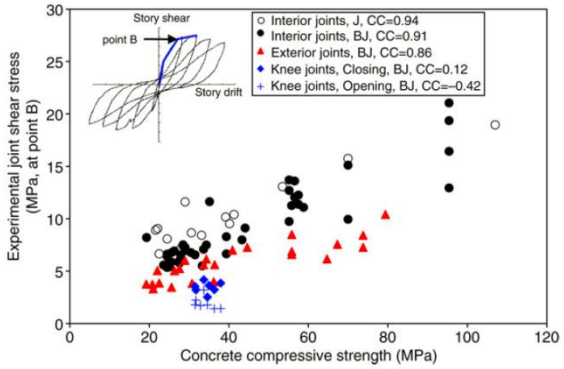

Figure 2.5 Joint shear stress vs. concrete compressive strength. Kim, J., and LaFave, J. (2006), "Key influence parameters for the joint shear behaviour of reinforced concrete (RC) beam-column connections." *Engineering Structures 29, 2523-2539.* Figure used under fair use, 2014.

aspect ratio, beam reinforcement, and column axial load were identified as of primary significance.

From the above references, it has been determined that the following mechanisms should be captured by a model in order for it to sufficiently describe behavior:

- Bond between concrete and reinforcement
- Flexural hinging at the interfaces of the joint and the beams or columns

- Diagonal compressive strut mechanism of joint
- Panel truss shear mechanism of joint

2.2 Joint Models

A variety of analytical models have been formulated to describe the behavior of reinforced concrete beam-to-column joints. Simplified models are either empirical, i.e., they are meant to reproduce the experimentally observed behavior in terms of joint force/deformation, or mechanics-based, i.e., they describe the mechanics of the salient response mechanisms. The former are relatively simple models that rely on calibrated springs to represent behavior, essentially applying curve fitting to overall joint behavior. They can present good agreement with the tests on which they are based, but it is unlikely that these models will be extendable to varying cases. The latter mechanistic models are more appealing because of their potential to be used in a wide array of settings. These models attempt to capture the individual mechanisms that describe behavior rather than being calibrated based on a curved fit to the overall joint behavior. They tend to be limited primarily by generalizing assumptions that neglect certain aspects of behavior in the name of simplicity. Whereas simplicity can be advantageous, especially in design, it must not be pursued to the detriment of accuracy.

2.2.1 Empirical Joint Models

Alath and Kunnath (1995) developed a simple empirical joint model based on the experiments of Beres et al. (1992). This model employs a single spring at the intersection of the beam and column centerlines with rigid end zones in the immediate vicinity of the joint, as seen in the scissor model in Figure 2.6. A tri-linear shear vs. strain model is used to define the nonlinear behavior, and the effects of reinforcement, bond-slip, confinement, or concrete behavior are not explicitly accounted for.

Biddah and Ghobarah (1999) described the effects of shear deformation and bond-slip with separate spring elements. For the simulation of an interior joint, two bond-slip springs and one shear spring were required, as shown in Figure 2.7. For the simulation of an exterior joint, one bond-slip spring and one shear spring represent behavior. An idealized tri-linear constitutive model was described based on a softening truss model for monotonic behavior, while cyclic behavior was defined by a multi-linear hysteretic model that neglected pinching due to concrete cracking and crushing of concrete immediately surrounding reinforcement. These constitutive models are not deemed sufficient to describe material behavior.

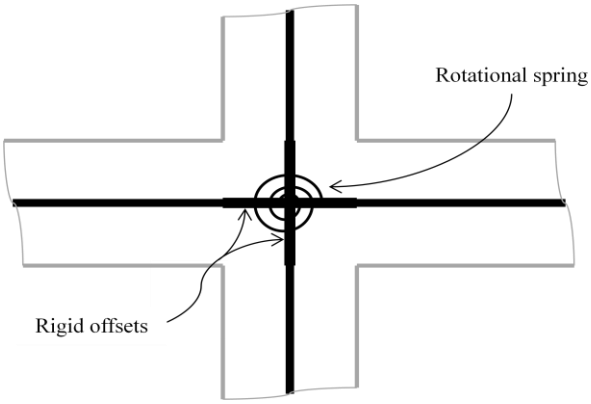

Figure 2.6 Scissor model

Pampanin et al. (2003) developed a scissor model similar to the one proposed by Alath and Kunnath (1995), but also included lumped plasticity at the beam ends. The moment-rotation constitutive model for the joint was based on bilinear shear deformation-principal tensile stress relationships. The major improvement over Alath and Kunnath (1995) was the inclusion of pinching in the hysteretic behavior due to bond-slip and shear cracking within the joint.

Anderson et al. (2008) developed a more involved scissor model based on experimental tests carried out at the University of Washington. A tri-linear envelope representing 3 distinct levels of stiffness was combined with a multi-linear cyclic model, which had the ability to include degradation of stiffness and strength. This model also lacks objectivity and extrapolation of results to more general cases is not advisable.

Park and Mosalam (2009) developed a semi-empirical moment-curvature relationship that is applied to a scissor model based on a single diagonal compression strut to resist joint shear. Joint strength is calculated as a function of the joint aspect ratio and the amount of longitudinal beam reinforcement (classified by the beam reinforcement index), neglecting column axial load. Joint aspect ratio is the only parameter affecting maximum and minimum joint shear strength, but between these values the shear strength is linearly proportional to the beam reinforcement index. This model was only developed for exterior and knee joints.

Birely et al. (2011) proposed a model with a rigid joint with rigid offsets, at the end of which there are two springs connected in series to the beams on either side of the joint, as seen in Figure 2.8. The model incorporates a lumped-plasticity beam-column element with the two springs representing the moment-rotation response of the joint and the moment-rotation response of the beam. No consideration is made for nonlinearity in the column. Eleven different research regimens totaling 45 different beam-to-column joint specimens, which all used normal weight, non-high-strength concrete in interior joints, were used to calibrate the model. It was not considered appropriate to extend this model to further specimen types.

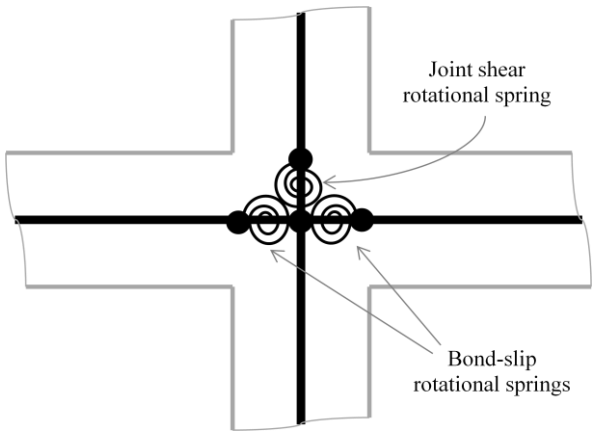

Figure 2.7 Joint model by Biddah and Ghobarah (1999)

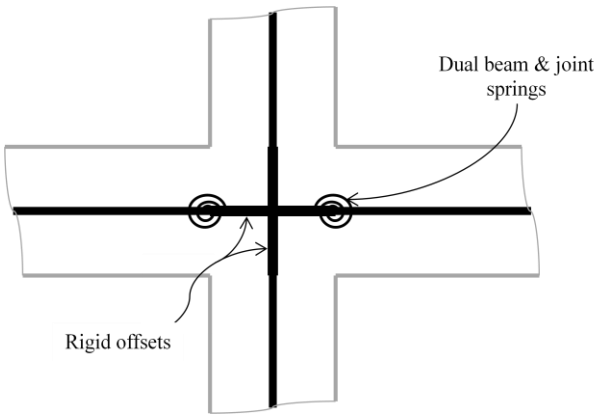

Figure 2.8 Joint model by Birely et al. (2011)

2.2.2 Mechanistic Joint Models

Filippou et al. (1983) proposed an analytical joint model similar to a fiber section beam model, as seen in Figure 2.9. The cross section of the joint was divided into several layers, each representing either steel reinforcement or concrete. Nonlinear constitutive models were used to represent the behavior of these layers, with the Menegotto-Pinto relationship representing steel and a model developed by Filippou representing the concrete. This concrete model bases crack closure (and thus the onset of regaining compressive strength) on the crack width in a given layer, but does not account for any tensile strength in the concrete. A bond stress-slip model developed by Ciampi et al. (1981) is used to account for the incompatibility of steel and concrete strains. Thus, the model by Filippou et al. (1983) can handle the effects of bond-slip and concrete flexural cracking; however, it does not account for any of the effects of shear within the joint and thus is ultimately deemed unsatisfactory.

An analytical model utilizing the modified compression field theory (MCFT), pictured in Figure 2.10, has been developed by Lowes and Altoontash (2003). This model defines a 4-sided shear panel based on MCFT connected to 4 rigid interface members. The panel-interface

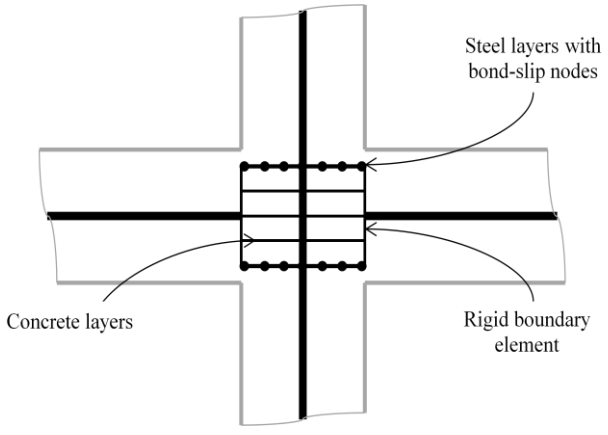

Figure 2.9 Joint model by Filippou et al. (1983)

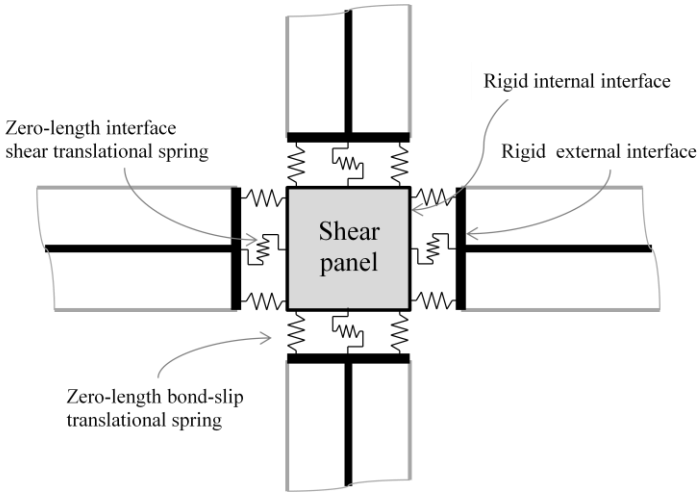

Figure 2.10 General model used by Lowes, Altoontash, and Mitra

connection is accomplished through 3 zero-length spring elements on each side: one at each corner to represent bar-slip behavior and one at the center to represent beam-joint interface shear. The elastic interface shear spring accounts for crack openings at the faces of the joint. A bar stress vs. slip relationship, shown in Figure 2.11, was developed for this model primarily based on experiments conducted by Lowes (1999) and Eligehausen et al. (1983). Bar stress increases fairly quickly until the steel yields, at which point there is a dramatic decrease in stiffness. Once the slip reaches the "slip limit" of 0.1 in. (3mm), strength decreases linearly to the residual stress. As can be seen in the comparison of the bond-slip model to test results in Figure 2.12, this model has decent agreement with cyclic behavior, though it has poor agreement under monotonic loading. A single multi-linear uniaxial load-deformation model was developed to describe the hysteretic behavior of the various materials. By varying the input parameters, constitutive relationships were defined for the shear panel and the bar-slip. The shear panel is treated as a single entity, thus giving it a sort of "black box" nature that does not allow for the extraction of information about individual

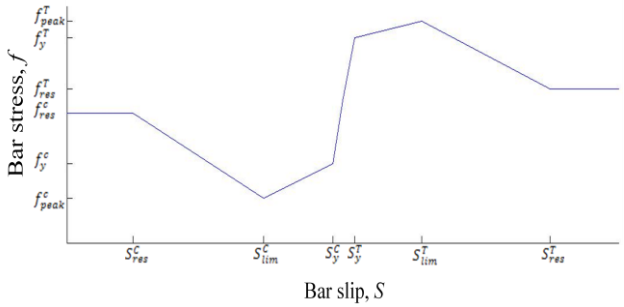

Figure 2.11 Lowes and Altoontash (2003) bond-slip envelope curve

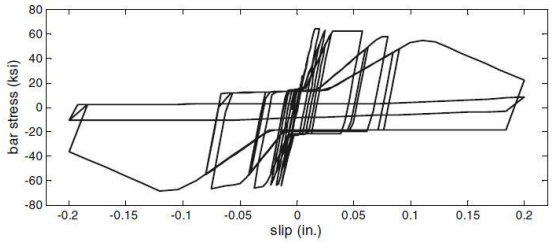

a) Simulated results

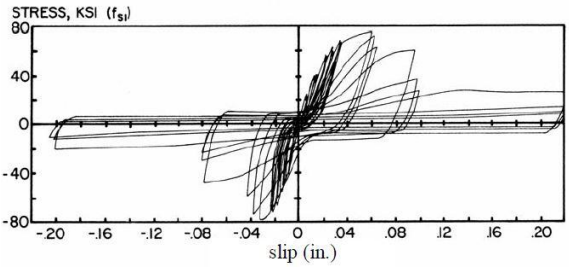

b) Experimental results

Figure 2.12 Verification of bond-slip model. Lowes, L., Mitra, N., and Altoontash, A. (2004), "A Beam-Column Joint Model for Simulating the Earthquake Response of Reinforced Concrete Frames." *Report No. PEER-2003/10*, Berkeley, CA. Figures used under fair use, 2014.

contributions to failure. The use of MCFT assumes at least a moderate amount of transverse reinforcement within the joint.

Mitra and Lowes (2007) refined the Lowes and Altoontash (2003) model by making three major adjustments: replacing MCFT with a diagonal compression-strut mechanism to represent the shear panel, slightly altering the placement of the bond-slip springs to better represent true specimen geometry, and altering the constitutive model for the bond-slip springs. The concrete strut within the joint carries the entire shear load. The contribution of steel reinforcement is only considered in relation to confinement of the core; the only relation of steel to the model is the resultant force orthogonal to the compression strut. No consideration is made for axial deformations or buckling of the reinforcement. The constitutive model for the springs was altered so that convergence issues in computation could be avoided. In the Lowes and Altoontash model, the loss of strength due to reaching the slip limit would result in a negative slope. In this model, however, the loss of strength is handled by the hysteretic model. As the model is cycled to increasing slip, the stiffness is decreased so that a higher amount of slip results in lower bond forces.

As these models (Lowes and Altoontash, 2003, and Mitra and Lowes, 2007) were developed to be used more with modern RC beam-to-column connections, it was assumed that the joints are well confined. For this reason, these models are not considered suitable for the analysis of joint in old, poorly detailed RC frames.

Shin and LaFave (2004) suggested a rectangular joint subassembly consisting of rigid links pinned at the corners, as seen in Figure 2.13. One corner is assigned three bilinear rotational springs superimposed to represent shear behavior. Rotational springs are also placed at the joint-beam interfaces to represent bond-slip. The three shear springs are combined to create a

multi-linear envelope based on MCFT and hysteretic behavior calibrated from experimental data. It was assumed that this model would be applied to ductile moment frames, for which MCFT is intended. Assumed confinement of the joint core gives this model little applicability to poorly-detailed beam-to-column joints.

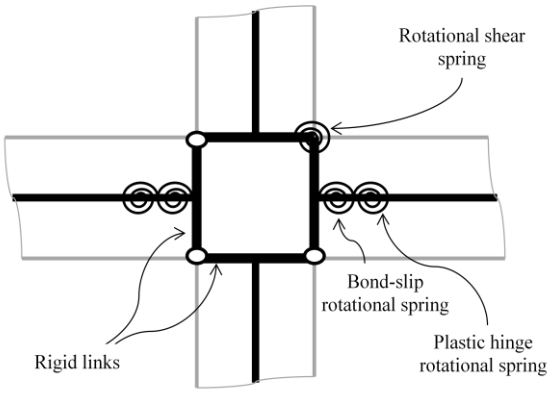

Figure 2.13 Joint model by Shin and LaFave (2004)

Park and Mosalam (2009) developed a model to predict the behavior of exterior joints. This model assumes beam longitudinal reinforcement is bent at 90°. Two diagonal struts, illustrated in Figure 2.14, are assumed to resist the entirety of the shear: one between the bend of the beam reinforcement and the concrete compression blocks in the opposite corner (ST1) and another between that opposite corner and the concrete surrounding the horizontal portion of that same beam reinforcement (ST2). This latter strut is a result of the bond between the reinforcement and the concrete. Joint shear failure is assumed to initiate at the node of the upper beam reinforcement bend because this is where anchorage of that reinforcing bar is assumed and is the location of greatest crack width. A fraction factor, α, is determined to define the contribution of ST1 to shear resistance, while the remainder is attributed to ST2. To represent bond deterioration, as tensile stress increases in the beam reinforcement, α increases. As in the phenomenological model by Park and Mosalam (2009) described earlier, this model was designed only for exterior joints and confinement in the joint and axial load in the column are neglected.

A joint model based primarily on the principal tensile stress has been proposed by Sharma et al. (2011). This model, pictured in Figure 2.15, combines 3 hinges with a centerline

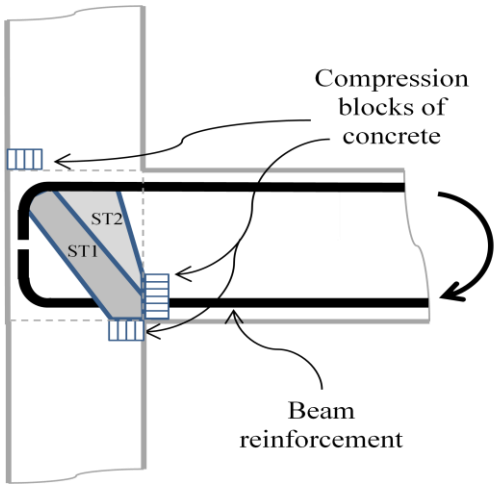

Figure 2.14 Diagonal struts of mechanistic joint model by Park and Mosalam (2009)

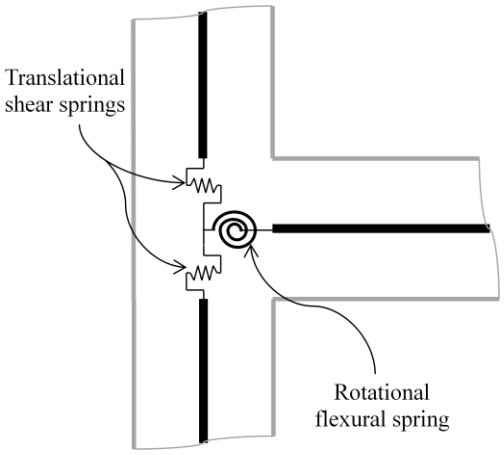

Figure 2.15 Joint model by Sharma et al. (2011)

model to describe behavior of exterior beam-to-column joints. Two constitutive models were developed to relate the principal tensile stress and the shear deformation within the joint: one relationship for joints with both top and bottom beam reinforcement bars bent in and one for joints with top beam reinforcement bent in and bottom beam reinforcement embedded 6 in. straight into the joint. These constitutive relationships are illustrated in Figure 2.16. The relationships of beam moment to joint shear strain and column shear to joint shear strain (and thus to the deformation at the joint-column interface) are found through an iterative procedure using the aforementioned principal tensile stress-shear deformation constitutive relationships. In order to extend this model to further joint types, additional principal tensile stress-joint shear deformation relationships must be developed. Bond-slip in the model is not directly modeled. It also does not allow for the evaluation of the causative effects of individual components to failure.

More refined 2-dimensional finite element models have been pursued (Noguchi, 1981, Pantazopoulou and Bonacci, 1993, Kashiwazaki et al., 1996, Baglin and Scott, 2000). These models utilize 2-dimensional quadrilateral or triangular elements to represent concrete, along

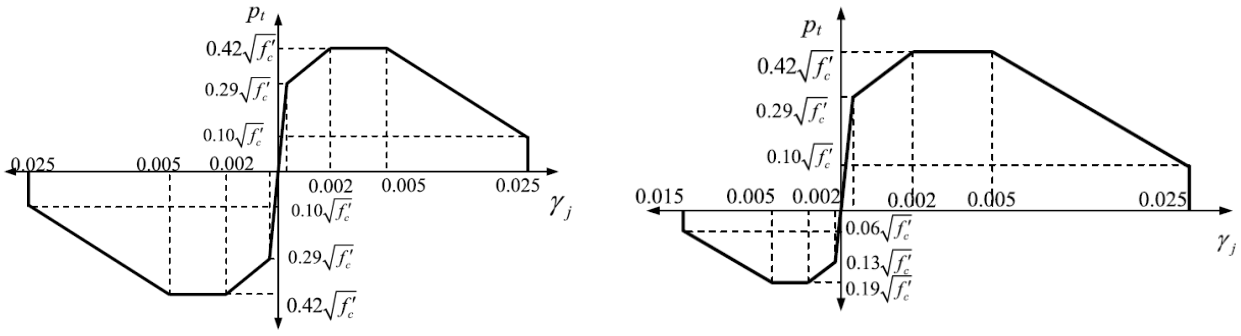

a) Both beam reinforcement bars bent in

b) Top beam bar bent in, bottom beam bar embedded 6 in straight into joint

Figure 2.16 Principal tensile stress-joint shear deformation constitutive relations. Sharma, A., Eligehausen, R., and Reddy, G. (2011), "A new model to simulate joint shear behavior of poorly detailed beam-column connection in RC structures under seismic loads, Part I: Exterior joints." *Engineering Structures* 33, 1034-1051. Figures used under fair use, 2014.

with biaxial constitutive relationships, and either 2-dimensional or truss elements to represent reinforcing steel. Bond-slip and concrete cracking, if accounted for explicitly, are modeled using zero-length contact elements or, in the case of concrete cracking, smeared crack elements. In order to accurately traverse highly nonlinear constitutive relationships, some models, such as the one seen in Figure 2.17 require up to 100 concrete elements within the joint panel alone. Cyclic loading is not conducted with these models because of the high computational expense. In monotonic loading, these models do not capture well the degradation in the response after joint shear cracking, as shown in Figure 2.18. The computational expense and complexity of such models makes them difficult to implement when modeling the overall response of a building structure.

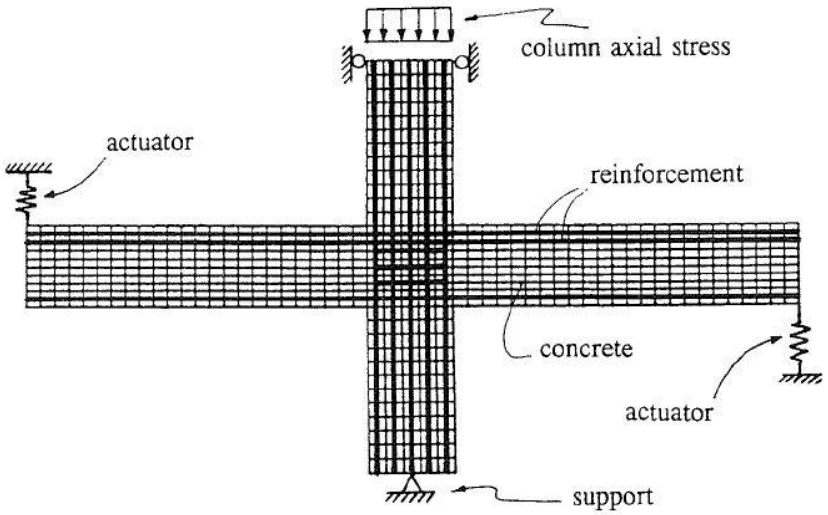

Figure 2.17 Finite element model. Pantazopoulou, S. J., and Bonacci, J. F. (1994), "On earthquake-resistant reinforced concrete frame connections." Canadian Journal of Civil Engineering 21, 307-328. Figure used under fair use, 2014.

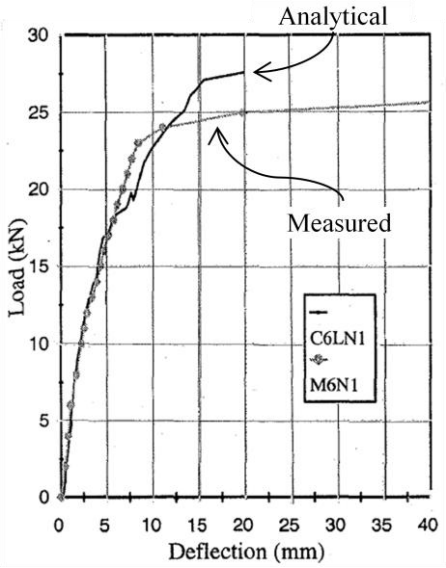

Figure 2.18 Load-deflection response of finite element joint model compared with measured response. Baglin, R. H., and Scott, P. S. (2000), "Finite Element Modeling of Reinforced Concrete Beam-Column Connections." *ACI Structural Journal* 97(6), 886-894. Figure used under fair use, 2014.

Chapter 3. Analysis Methodology

3.1 Introduction

An RC beam-to-column joint model must adequately capture physical joint behavior. In the case of mechanistic models, the applicable force transfer mechanisms and material properties must be included to attain model accuracy. The force transfer mechanisms within beam-to-column joints include: bond-slip between concrete and reinforcing steel, the diagonal compression strut, and the panel truss. The existing mechanistic models described previously rely, in one form or another, on broad simplifying assumptions that neglect aspects of these force transfer mechanisms. In some cases, these assumptions neglect shear deformations all together. In others, they do not adequately capture the effects of the shear failure mechanisms in poorly detailed joints.

The model proposed herein relies on a nonlinear truss structure to capture the diagonal components of the diagonal compressive strut and panel truss shear transfer mechanisms. Zero-length springs connecting steel and concrete elements capture the reinforcement bond-slip relationship. Concrete truss elements are defined by a nonlinear concrete constitutive stress-strain model developed and a new implementation of a uniaxial stress-strain law for steel reinforcement is used to define the steel truss elements.

3.2 Description of Nonlinear Truss Analogy for Beam-to-Column Joints

The modeling approach is based on the work of Panagiotou and Restrepo (2011). Diagonal concrete elements represent the primary shear resistance mechanism, with vertical and horizontal concrete and steel elements to account for axial resistance. The bond-slip is modeled with nonlinear zero-length springs connecting the concrete and steel elements. A general layout

of the model applied to an interior beam-column joint is shown in Figure 3.1d, along with the hypothetical joint that it would represent, shown in Figure 3.1a. Horizontal and vertical concrete elements create many truss cells, each of these cells containing two orthogonal diagonal concrete struts. An example of one of these cells is given in Figure 3.1b and the size of these cells will henceforth define the mesh size of the model. It is advantageous to have these cells as close to square as possible, for reasons that will be explained below.

For ease of modeling, it is suggested that the mesh size remain constant within a joint model. The mesh size will thus be defined as a fraction of the size of the joint core, which is bounded top and bottom by the beam reinforcing bars and left and right by the outer column reinforcing bars. This can be seen in Figure 3.1c, which shows the truss assemblage of an exterior joint superimposed on its reinforcing schematic. The outer longitudinal beam and column reinforcing bars must be modeled so that they exactly overlay the physical specimen, otherwise the effective diagonal compressive strut will not be appropriately defined and will vary depending on the mesh size.

The cross-sectional areas of the steel truss elements are calculated based on the amount of reinforcing steel in the system. As is illustrated in Figure 3.1c, the transverse reinforcing steel elements do not exactly overlay the physical specimen. To account for this, the cross-sectional areas of the transverse steel elements are determined in order to give the correct transverse reinforcing steel ratio. As the longitudinal steel elements are modeled exactly, their areas can be taken directly from the physical specimen.

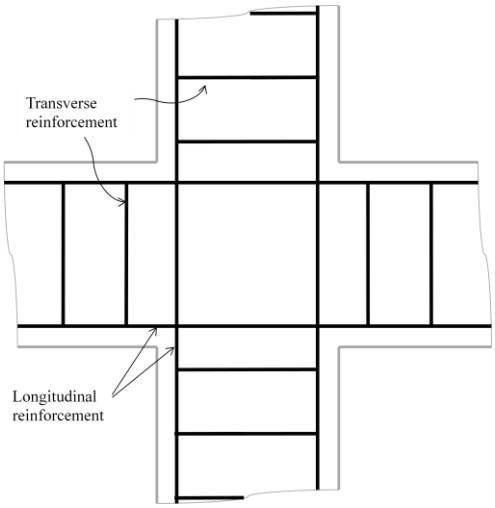

a) Interior joint physical layout

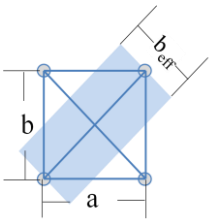

b) Concrete truss cell

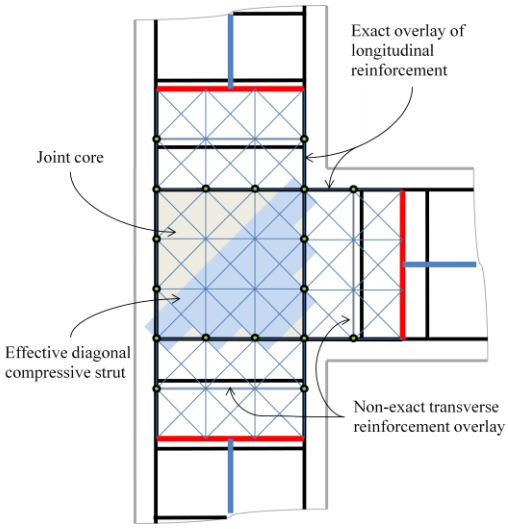

c) Exterior joint truss assemblage over specimen reinforcing schematic

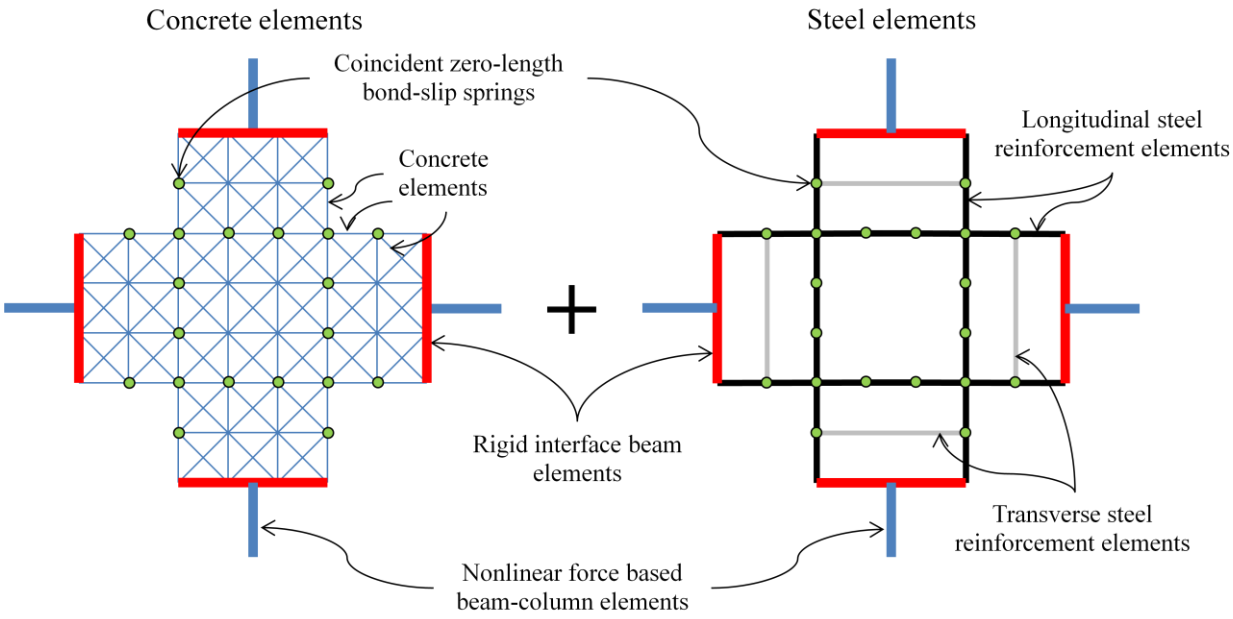

d) Corresponding components of interior joint model layout

Figure 3.1 Proposed model layout

The cross-sectional areas of the concrete truss elements are obtained as the product of the tributary width and of the out-of-plane thickness, *w*. The effective width of diagonal elements, b_{eff}, is determined from the vertical component, *b*, and horizontal component, *a*, of the element such that: $b_{eff} = \frac{b^2}{\sqrt{a^2+b^2}}$, as illustrated in Figure 3.1b. The area of the diagonal elements then

becomes $A_d = w * b_{eff}$. For horizontal and vertical concrete elements, the effective width is found as the tributary width of a given element. The cross sectional area of the cover concrete is included in the horizontal and vertical concrete elements that coincide with the exterior longitudinal steel reinforcement.

The interface of the joint and the adjacent beam or column is modeled as a rigid beam-column element. This is done in order to maintain the assumption that within the beams and columns plane sections remain plane and perpendicular to the deformed centerline of that framing element.

3.2.1 Concrete Model

The concrete elements are defined using the constitutive model proposed by Lu and Panagiotou (2013) found in Figure 3.2. The model has been defined for both confined and unconfined concrete. In confined concrete, two distinct branches are defined in compression prior to reaching the compressive strength: a quadratic curve up to the unconfined compressive

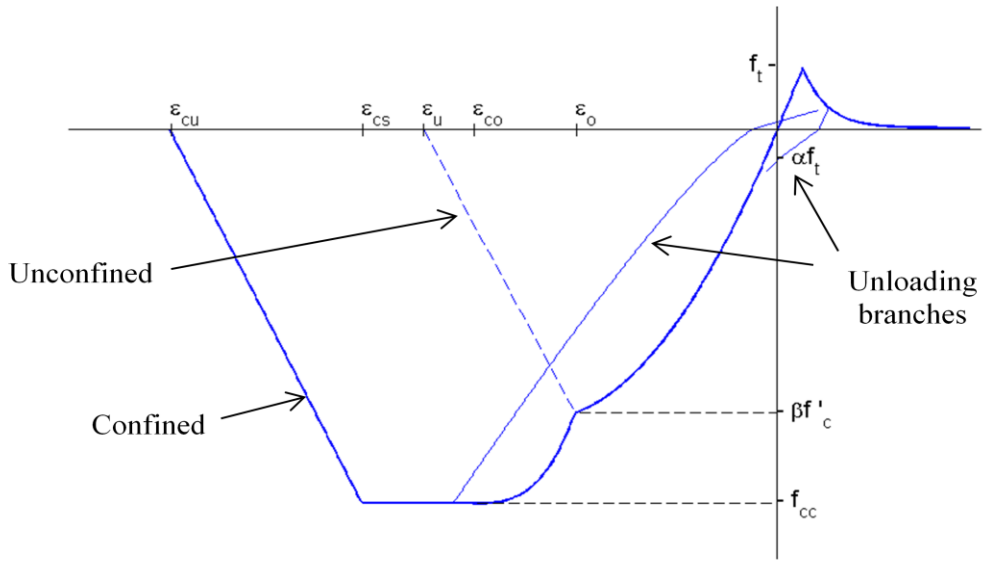

Figure 3.2 Lu and Panagiotou (2013) uniaxial stress-strain law for concrete

strength, f'_c, at the unconfined peak strain, ε_o, followed by a cubic curve up to the confined compressive strength, f_{cc}. There is then a plateau extending from the confined peak strain, ε_{co}, to the ultimate compressive strain, ε_{cs}. This is followed by linear softening to zero stress at a strain of ε_{cu}. Unconfined concrete follows the same path up to the unconfined compressive strength, at which point linear softening occurs until stress is reached at a strain of ε_u. Unloading from compression is accomplished by a nonlinear curve until zero stress is reached. Once zero stress is reached, a linear branch extends to the point of maximum prior tensile strain, and then the tension curve is rejoined.

The tensile response of the model is equivalent for both confined and unconfined concrete. The response is elastic until cracking, which is defined by the tensile strength of the concrete. For horizontal and vertical concrete elements the tensile strength is assumed to be $f_t = 0.33\sqrt{f'_c}$ (f_t and f'_c in MPa), whereas the diagonal concrete elements have no tensile strength. Following the elastic branch, a sharp peak leads to softening either by tension stiffening or as defined by a tri-linear relationship (not shown). Unloading in tension is comprised of three linear branches. The first has a slope equivalent to the initial modulus, E_c, and is defined from the point of reversal to the point of zero stress. The second branch extends down to a point of zero strain and a stress of $-\alpha f_t$, where $\alpha = 0.5$. The final branch reconnects to the point of maximum prior compressive strain, at which point the compressive skeleton curve is rejoined.

The performance of nonlinear structural elements with softening branches is highly dependent on the element mesh length (see Panagiotou et al., 2012, for further details). To account for this mesh size effect, the compressive degrading branch is made steeper as the element length increases. This is accomplished by altering the values of ε_u in unconfined concrete and ε_{cu} in confined concrete.

3.2.2 Transverse Strain Effect in Concrete

For diagonal concrete elements, transverse strain effect is taken into account as per Vecchio and Collins (1986). As transverse strain, ε_n, is increased in the tensile direction, the compressive strength of the material decreases according to the multiplier β. β is defined by a tri-linear relationship with the transverse strain, as seen in Figure 3.3. Compressive (negative) values of ε_n give a β value of 1 and thus have no effect on behavior. In order to measure transverse strain, four nodes must be defined for a single element. From these four nodes, two will define a concrete truss element and two will define a zero-stiffness gauge element, also pictured in Figure 3.3. It is advised to define the two transverse gauge nodes at locations that will give an orthogonal gauge element in order to produce an accurate approximation of ε_n. In general, as the diagonal elements are part of a cell, the two transverse nodes will be taken as the remaining two nodes in the cell. For this reason, it is advantageous to create a close-to-square meshing of the concrete. The effect of element length is also accounted for in the transverse strain effect. As the length of the concrete strut element increases, the values of ε_{int} and ε_{res} decrease.

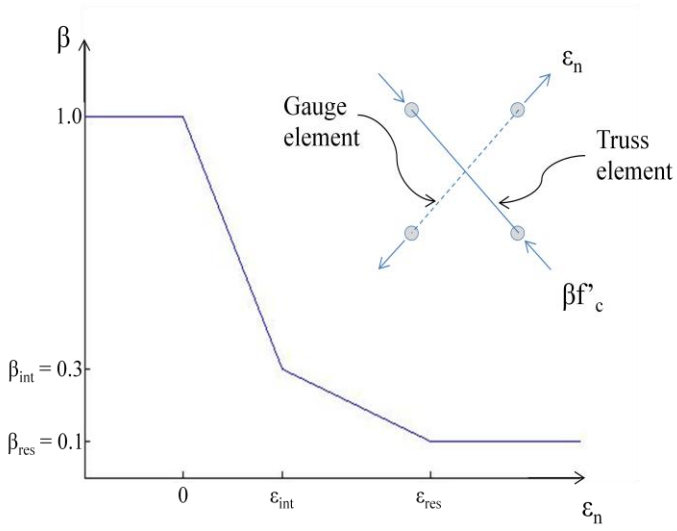

Figure 3.3 Transverse strain strength reduction factor

3.3 Enhancements to Truss Modeling Approach for Beam-to-Column Joints

Three enhancements have been made to the nonlinear truss analogy modeling scheme for beam-to-column joints. Confining pressure due to column axial load is used to calculate the

confinement parameters of concrete, a new uniaxial stress-strain law for reinforcing steel is implemented to improve accuracy, and the bond-slip effect is included by the use of zero-length springs.

3.3.1 Effective Concrete Confinement Due to Axial Column Load

It has been observed (Paulay and Scarpas, 1981, Beres et al., 1996, Pantelides et al., 2002) that column axial load has a positive effect on strength and ductility of beam-to-column connections. To account for this effect, the value of column axial stress, f_a, is used to define the partial confinement of certain concrete elements. Figure 3.4a shows a concrete core with a vertical column axial stress applied to it. This stress is assumed to have a confining effect on both horizontal and diagonal elements. The confining pressure for horizontal elements is taken as f_a and for diagonal elements it is taken as $f_a \cos\theta$, where θ is the angle of inclination for that element, as seen in Figure 3.4. The confined compressive strength, f_{cc}, and strain, ε_{co}, are found based on the expressions of Mander et al. (1988) and follow the equations:

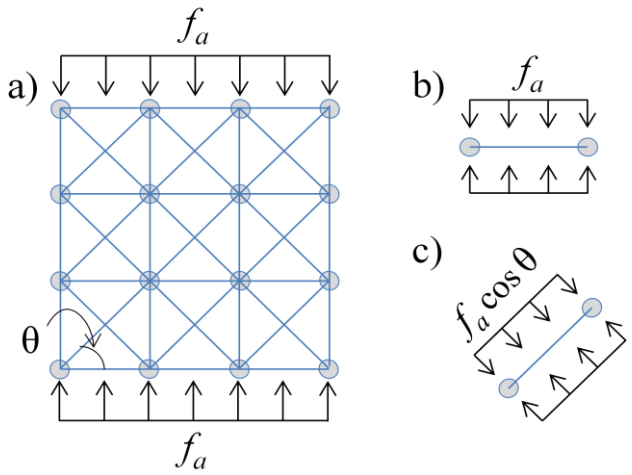

Figure 3.4 Concrete confinement pressure
a) Joint core confined by column axial stress,
b) Level of confinement in horizontal elements,
c) Level of confinement in diagonal elements

$$f_{cc} = f'_c\left(-1.254 + 2.254\sqrt{1+\frac{7.94 f_{tr}}{f'_c}} - 2\frac{f_{tr}}{f'_c}\right) \qquad \text{(Eq 3.1)}$$

$$\varepsilon_{co} = \varepsilon_o\left[1+5\left(\frac{f_{cc}}{f'_c}-1\right)\right] \qquad \text{(Eq 3.2)}$$

$$f_{tr} = \begin{cases} f_a & \text{for horizontal elements} \\ f_a \cos\theta & \text{for diagonal elements} \end{cases} \quad \text{(Eq 3.3)}$$

where f_{tr} is the transverse confining pressure. The ultimate concrete compressive strain, ε_{cs}, is set equal to ε_{co}. This is because the plateau in the model proposed by Mander et al. (1988) is meant to extend to the point when the first confining hoop fractures, whereas there are no confining hoops within the joints of the specimens investigated in this study.

3.3.2 New Implementation of a Uniaxial Model for Steel Reinforcement

The stress-strain constitutive models developed for reinforcing steel to date are either overly simple or else difficult to calibrate to test data. The typical bilinear models, such as the Menegotto-Pinto stress-strain law for reinforcing steel, give a poor representation of behavior, with no distinction made between the yield plateau and strain hardening regime. Those models that do account for this distinction are calibrated based on the initial strain hardening modulus, which can be difficult to determine from test data. For these reasons, the constitutive law for steel proposed by Dodd and Restrepo-Posada (1995) has been selected for the reinforcing elements and has been implemented as the uniaxial material model DoddRestr in the OpenSees analysis platform (McKenna et al. 2005). It is an accurate model that requires a fairly limited number of parameters to be calibrated. The elastic region, yield plateau, nonlinear strain hardening, and post-peak softening are all defined within the skeleton curve. The Bauschinger effect (captured within the nonlinear Bauschinger branch) is also accounted for within multiple different types of unloading and reloading curves. The key features of this model can be found in Figure 3.5.

In order to account for differences between the compressive and tensile portions of the curve, this model operates within the natural coordinate system. Whereas the engineering coordinate system assumes a constant cross section and length to define the stress and strain of

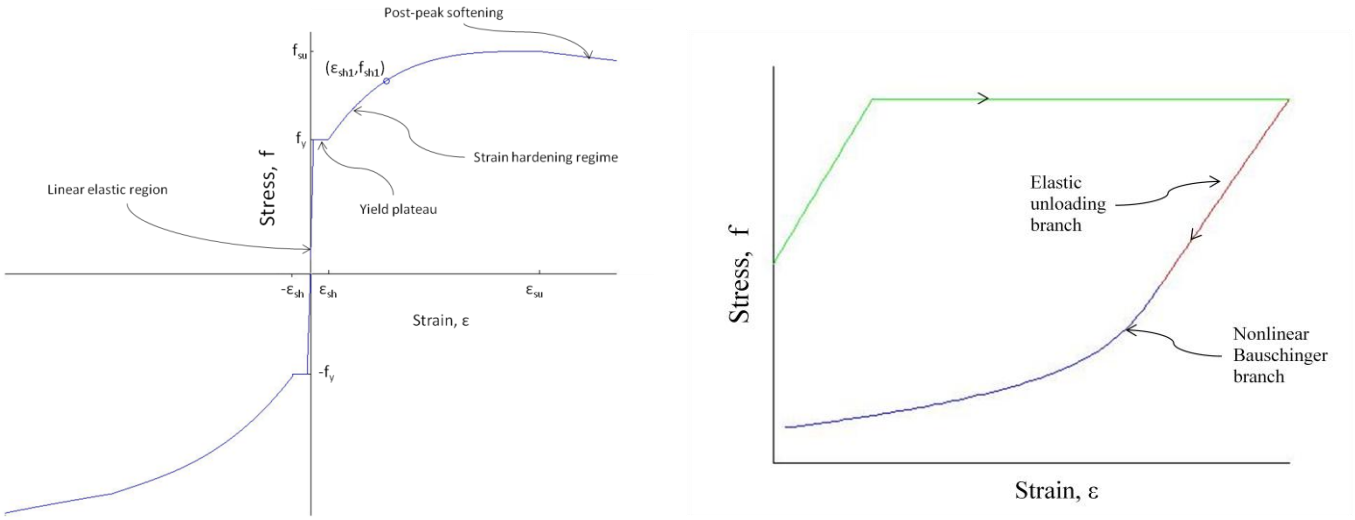

a) Skeleton curve b) Hysteretic behavior

Figure 3.5 Dodd and Restrepo-Posada (1995) constitutive law for steel

an element, the natural coordinate system is based on the instantaneous cross section and length of the reinforcement. These instantaneous parameters are calculated assuming that the element maintains constant volume as it is stretched or compressed. By basing the reinforcement stress on the instantaneous cross section, increased compressive strength can be accomplished.

The material parameters are entered in engineering stress-strain space. The model then converts the inputs to natural coordinates to perform the constitutive operations before converting the output parameters (stress and tangent modulus) back to engineering coordinates. Natural strain is related to engineering strain as:

$$\varepsilon' = \ln(1+\varepsilon) \qquad \text{(Eq 3.4)}$$

And natural stress is related to engineering stress as:

$$\sigma' = \sigma(1+\varepsilon) \qquad \text{(Eq 3.5)}$$

As shown in Figure 3.5a, the skeleton curve consists of three major branches: the linear elastic portion, the yield plateau, and the strain hardening regime and post-peak softening branch. The linear elastic portion maintains a constant slope equal to young's modulus up to the yield

stress, f_y, when the yield plateau is entered. The yield plateau is a zero stiffness region that has a constant stress equal to f_y. ε_{sh} then marks the onset of the strain hardening regime, which is defined as a nonlinear curve that reaches the ultimate strength, f_{su}, with zero-slope at the ultimate strain, ε_{su}. The exponent, P_{sh}, used to describe the curve of the strain hardening regime is calibrated based on an arbitrary point along the curve, (ε_{sh1}, f_{sh1}). This allows for a simple and accurate calibration based on experimental test data. Continued softening of the model beyond the ultimate strength accounts for the post-peak behavior of the steel, leading to a negative-slope degrading branch.

Unloading and reloading reversals are distinguished into these categories, namely, major, minor, and simple, as shown in Figure 3.6. Any unloading branch whose reversal point occurs within the non-elastic range of the skeleton curve is a major reversal, as seen in Figure 3.6b. Major reversals are comprised of a linear unloading branch and a nonlinear branch that represents the Bauschinger effect (the Bauchinger branch). Reversals within the yield plateau will eventually reconnect to a skeleton curve that has been shifted to account for plastic strains. Reversals within the strain hardening regime simply target the opposite ultimate stress-strain point, which has also been shifted to account for plastic strains. Major reversals can also be triggered within the nonlinear Bauschinger branch of another major reversal if the difference in stress between the two reversals is greater than $2f_y$. These types of major reversals behave very similarly to those which occur within the strain hardening regime.

If a reversal occurs within a major reversal such that the stress difference between the two reversals is less than $2f_y$, it is considered a minor reversal, as seen in Figure 3.6c. Minor reversals are also comprised of a linear branch and a curved Bauschinger branch. There are now two reversal points of immediate importance: the point from which the minor reversal began

(point 2 in Figure 3.6c) and the point from which the major reversal began (point 1 in Figure 3.6c). The major reversal was initiated within either the skeleton curve or another major reversal, referred to as the master branch. The minor reversal is always aiming to reconnect to the master branch at point 1. Thus, minor reversals can never cause an increase in the plastic strain of the reinforcing bar.

Any reversal that occurs within the Bauschinger curve of a minor reversal is classified as a simple reversal. As with minor reversals, simple reversals have both a linear and a curved Bauschinger branch and there can also be no increase in plastic strain accrued within a simple

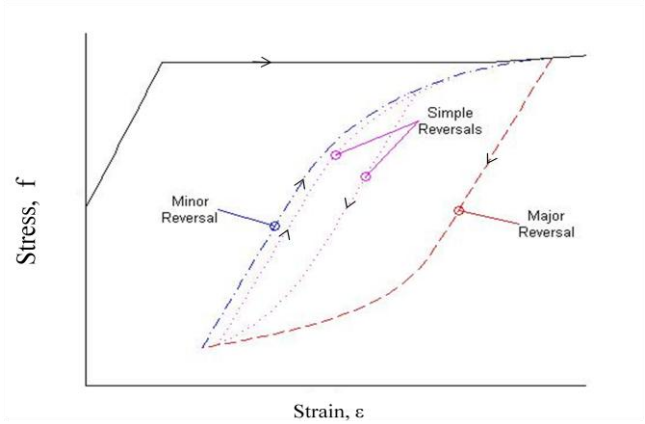

a) Relationships between reversals

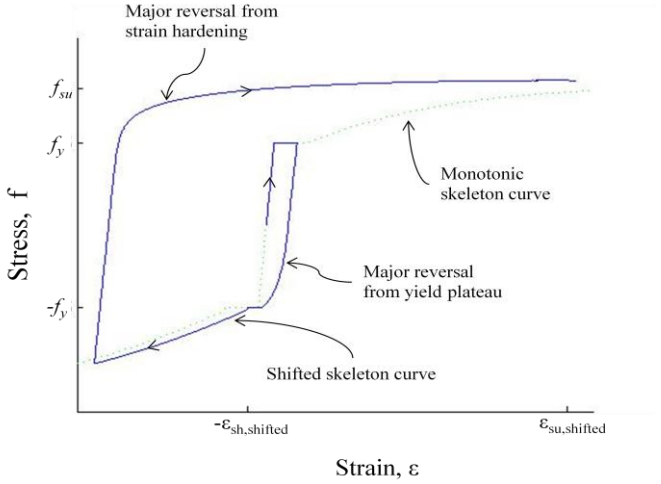

b) Major reversal load path

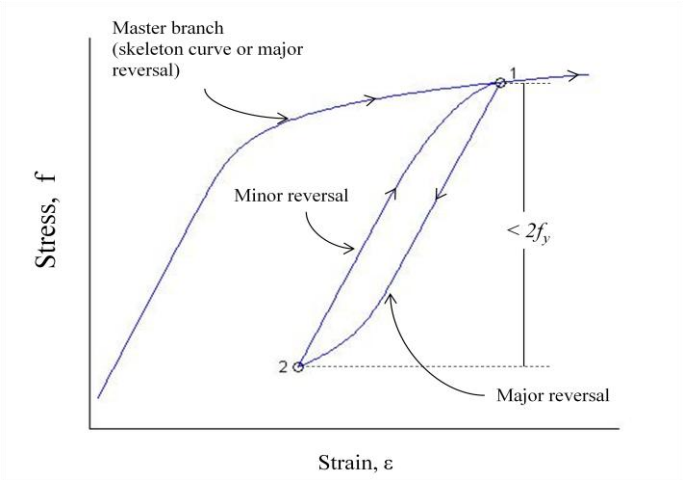

c) Minor reversal load path

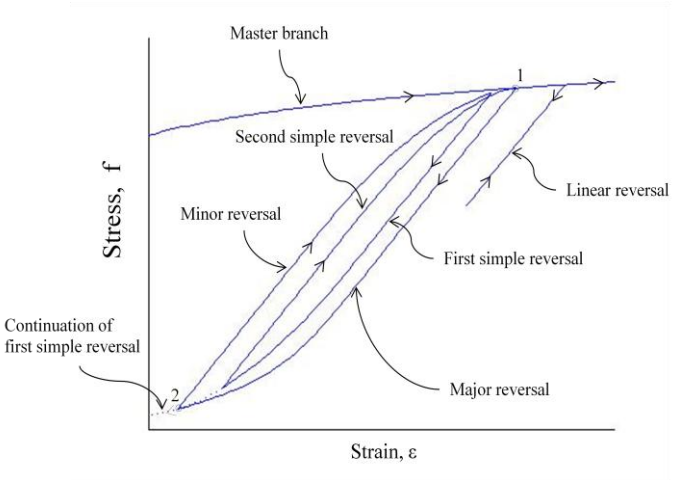

d) Simple and linear reversal load paths

Figure 3.6 Loading reversals

reversal. Simple reversals can also be initiated by a reversal within the curved branch of another simple reversal. These reversals aim to reconnect to either the major reversal from which their minor reversal initiated from (point 2) or to the master branch (point 1). This can be seen in Figure 3.6d where the first simple reversal is aiming to reconnect to the major reversal and the second simple reversal is aiming to reconnect to the master branch.

As has been discussed, all reversals have an initial linear elastic portion. If a reversal occurs within one of these regions, the model traces back along this linear portion until the prior reversal point is reached, as seen in Figure 3.6d. Once this reversal point is reached, the previous branch is rejoined.

The Bauschinger effect for the three types of reversals (major, minor, and simple) is accounted for using the same nonlinear equation with a differing exponential coefficient: P_{major} for major reversals and P_{minor} for minor and simple reversals. P_{major} varies based on the amount of plastic strain. Because the Bauschinger portion of minor and simple reversals is fairly short, P_{minor} was calibrated based on test data and is set as a constant value of 0.35.

The implemented model has been designed to give added control to the user. In order to allow for a more accurate calibration, the exponential coefficients P_{major} and P_{minor} have been included as input parameters. If measurements of the cyclic stress-strain behavior for the reinforcing steel are taken, the variation of the P_{major} coefficient can significantly improve the model accuracy.

The implementation of the constitutive law follows the type of branch the model is in at any given point during cyclic loading: the skeleton curve, major reversals, minor reversals, or simple reversals loading in either the tensile or compressive directions. This allows for rigorous model tracking when a reversal occurs, ensuring accuracy when simulating physical behavior.

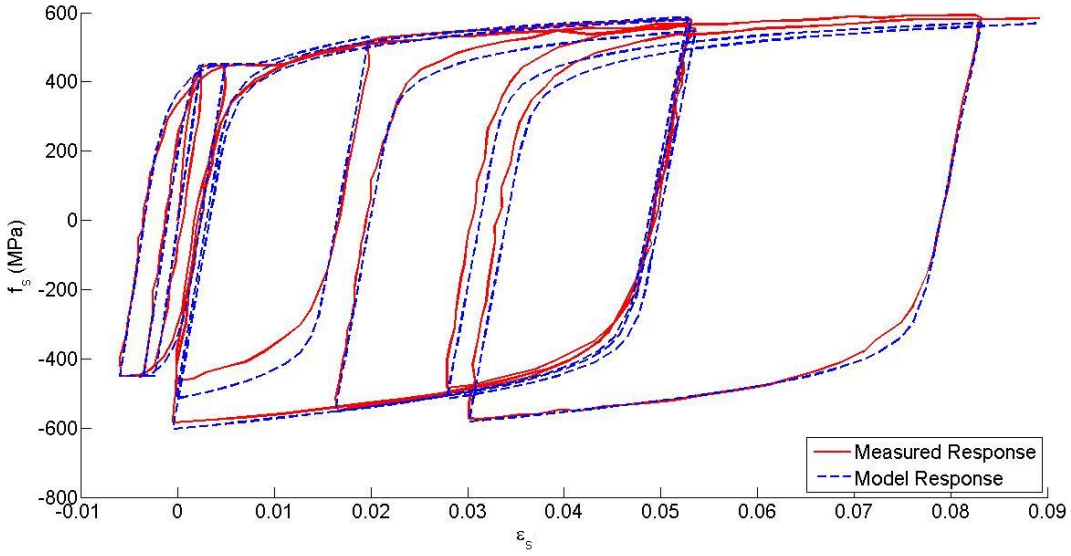

Figure 3.7 Measured and simulated cyclic stress-strain response of steel model

Table 3.1 Calibrated Steel Material Properties for Steel Coupon

f_y (MPa)	f_u (MPa)	ε_{sh} (%)	ε_u (%)	E_s (GPa)	ε_{sh1} (%)	f_{sh1} (%)	P_{major}	P_{minor}
450	640	1.2	20	190	3	560	0.1	0.35

The nonlinear branch representing the Bauschinger effect in the various reversals is solved using a full Newton-Raphson iterative algorithm. If the Newton-Raphson algorithm is unable to converge, a simple bisection algorithm is employed to solve the nonlinear equation. The full source code for this model can be found in Appendix A.

The model has been verified against the results of quasi-static cyclic tests of deformed reinforcing bars performed by Restrepo et al. (1994). Testing of a 16mm diameter grade 430 steel coupon (HX15) is compared to simulated results in Figure 3.7. Calibrated material properties can be found in Table 3.1. Good agreement is achieved between the model and the measured data.

3.3.3 Bond-Slip Model

The reinforcing bar bond force-slip displacement constitutive model chosen was developed by Mitra and Lowes (2007), as seen in Figure 3.8. Bond-slip is modeled using zero-

length translational springs to connect coincident steel and concrete nodes with the uniaxial material BarSlip, which is available in OpenSees.

There are three distinct, linear branches of the envelope of the model: an elastic branch, a yielded branch, and a post-ultimate branch. The stiffness of the elastic branch is based on the elastic modulus of the reinforcing steel. Once first yield of the steel has occurred, the yielded branch is entered and the stiffness is reduced based on the hardening modulus of the steel, assuming a bilinear steel stress-strain relationship. This is maintained until the ultimate strength of the steel is reached, initiating a near-zero-stiffness plateau. Constant positive stiffness is maintained to aid in model convergence. In tension, the yielded reinforcing bar has very little bond with the concrete because of Poisson's effect. Thus, there is very little strength gain after reinforcing bar yielding occurs and the yielded branch and post-ultimate branch can merge, as is illustrated in Figure 3.8.

Hysteretic behavior is also comprised of three linear branches: an initial unloading branch, a very shallow branch to account for material pinching, and a reloading branch, as seen in Figure 3.8. The material pinching branch is included to represent crushing in the concrete immediately surrounding the rebar. Material softening is accounted for within the hysteretic behavior; damage parameters reduce the bond strength based on the maximum deformation experienced by the material as cycling occurs. More information on this model can be found in Lowes et al. (2004) and Mitra and Lowes (2007).

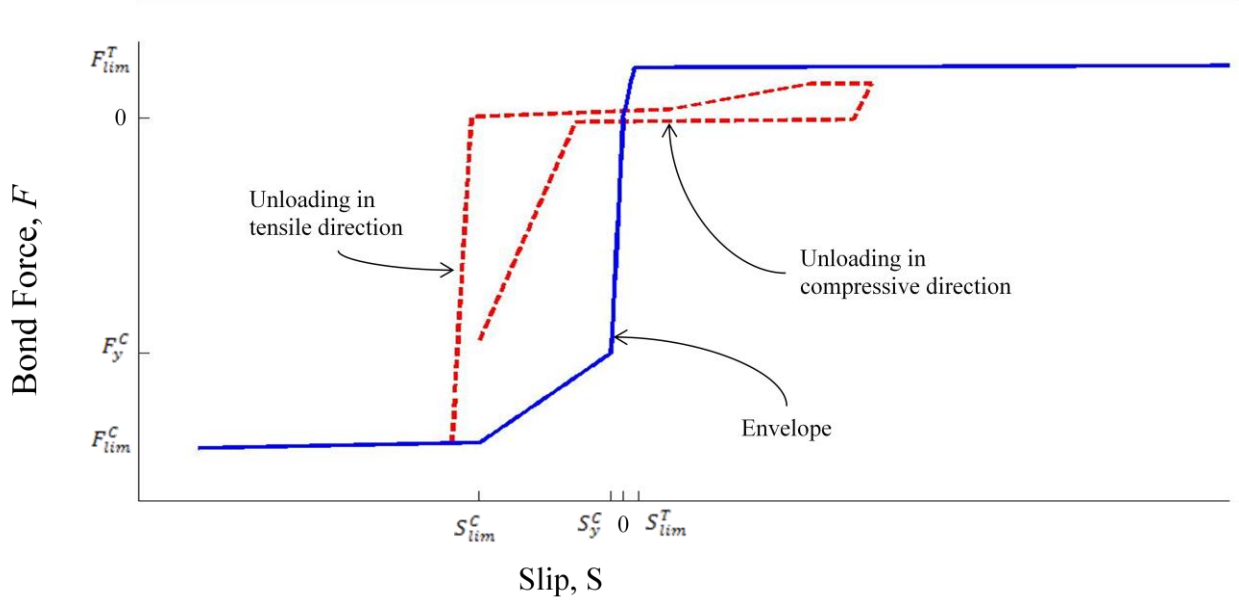

Figure 3.8 Bond-slip model by Mitra and Lowes (2007)

Chapter 4. Validation of Analysis Methodology

Validation of the model described herein is accomplished by comparing the force-displacement responses of the model to experimental test results. The model was built in the OpenSees nonlinear structural analysis computer program (McKenna et al., 2005). Two-dimensional nonlinear static analyses using a Newton-Raphson iterative solution scheme were performed on a 3.47 GHz Intel Xeon processor and took roughly ten minutes. Quasi-static tests of beam-column subassemblies detailed to approximate the standards of practice in reinforced concrete moment frame construction prior to the advent of joint ductility requirements were selected for this study. Three tests were selected to compare against: two interior beam-column subassemblages tested by Alire (2002) and an exterior beam-column subassemblage tested by Pantelides et al. (2002).

4.1 Analysis of Interior Beam-to-Column Joints

The testing scheme of four interior beam-column subassemblages undertaken by Alire (2002) was intended to support the development of modeling techniques for nonductile beam-to-column joints. In an earlier study (Mosier, 2000), it was found that moment frame construction prior to 1967 typically lacked transverse reinforcement within the joints. Thus, Alire approximated pre-1967 building standards for these tests. Specimens PEER-0850 and PEER-0995 are selected for this study. The first specimen had good ductility but ultimately failed due to a combination of slipping of the bond of the beam reinforcing bars and joint shear cracking, whereas the second specimen had significant shear cracking early in the test and failed due to crushing within the concrete core.

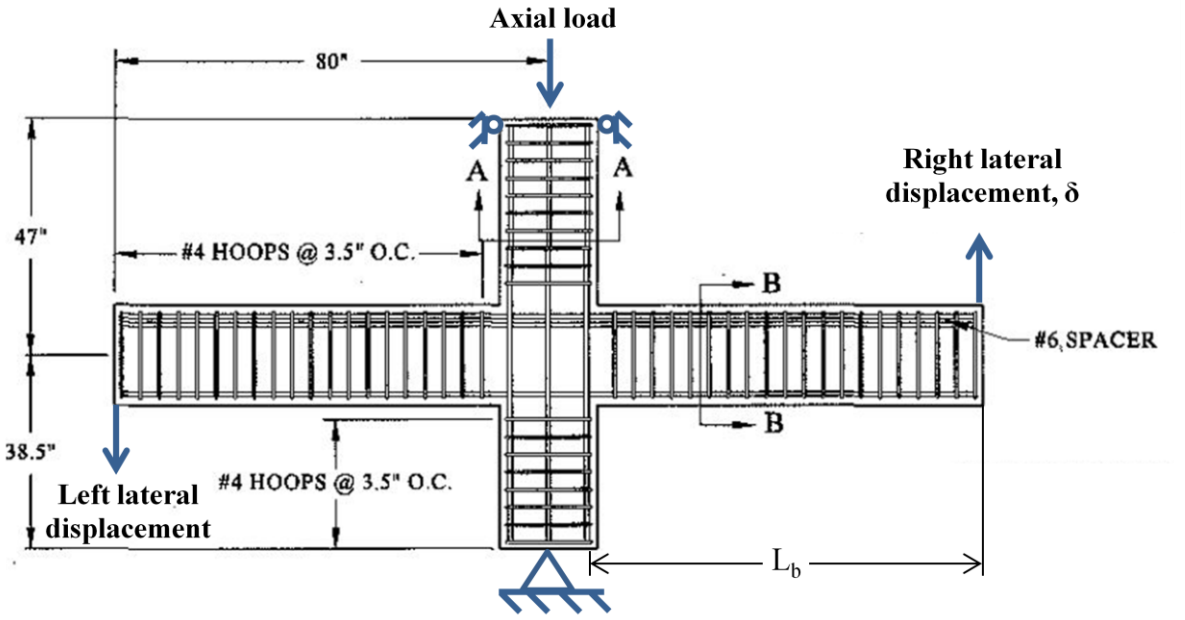

a) Interior joint dimensions

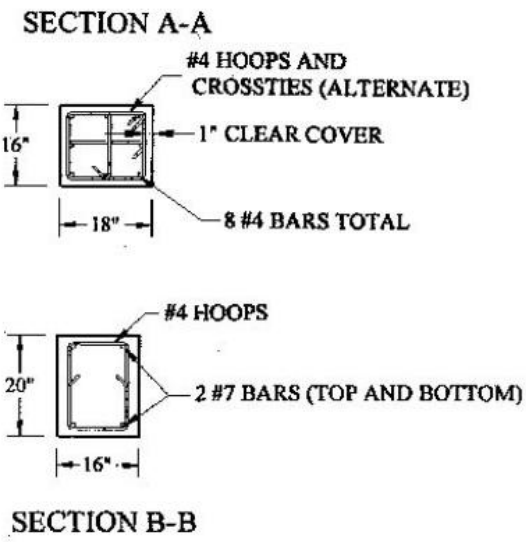

b) Reinforcement detailing for specimen 1

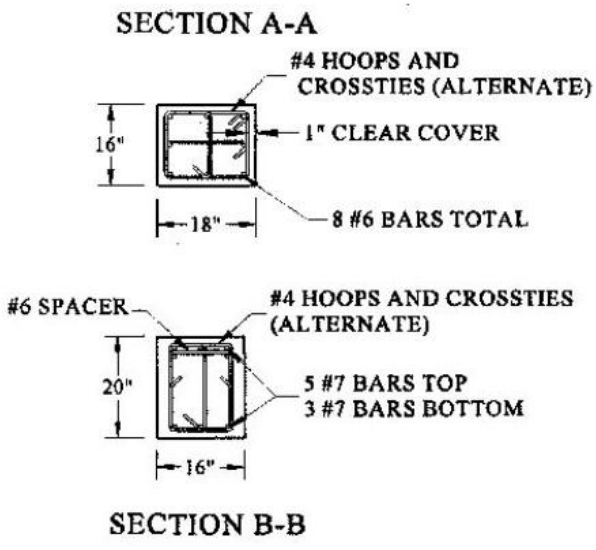

c) Reinforcement detailing for specimen 2

Figure 4.1 Reinforcement detailing of interior beam-column assemblies. Alire, D. (2002), "Seismic Evaluation of Existing Unconfined Reinforced Concrete Beam-Column Joints." *M.S. Thesis*, University of Washington, Seattle, WA, 306pp. Figures used under fair use, 2014.

4.1.1 Specimen Descriptions

Detailing for both joints can be found in Figure 4.1. They are 2/3 scale planar beam-column assemblages with no transverse beams framing into the joint. The beams and columns

have cross-sectional dimensions of 20”x16” and 18”x16”, respectively, and 1” concrete cover. The beams and columns were designed to ensure that beam longitudinal steel would yield prior to column longitudinal steel, maintaining a column moment-to-beam moment flexural strength ratio ($\Sigma M_c/\Sigma M_b$) greater than 1.5. Sufficient transverse hoop reinforcement was supplied to prevent shear failures within the beams and columns, though no transverse reinforcement was supplied within the joint. Longitudinal reinforcement was continuous from end to end to avoid splice failures. The specimens were cast and stored horizontally, then lifted into place to be tested vertically.

The specimens were built with varying concrete compressive strengths and target joint shear stresses. The first interior specimen was built with normal strength concrete, having a compressive strength on the day of testing (f'_c) of 5,070 psi. The second was built with high strength concrete with a compressive strength of 8,767 psi. The normalized target joint shear strengths ($v_{jt}/\sqrt{f'_{ct}}$) were 5.70 for the first interior joint and 8.50 for the second. The steel reinforcement for the two specimens was selected to achieve these targets. The beams of the second interior joint were built significantly stronger than those of first, with longitudinal reinforcement consisting of five No. 7 bars on top and three No. 7 bars on bottom in the second interior joint, whereas the first was reinforced with two No. 7 bars top and bottom. The column reinforcement of the first joint consisted of eight No. 4 bars and the column reinforcement of second consisted of eight No. 6 bars, spaced evenly as seen in Figure 4.1. With the exception of the beam-to-column connections, transverse reinforcement was consistently No. 4 bars spaced at 3.5” on center. The reinforcing steel material properties were presented in terms of the Raynor steel constitutive model (Raynor, 2000). These properties have been calibrated to the Dodd-

Restrepo (1995) steel constitutive model and can be found in Table 4.1 along with a comparison of the model to the experimental data, found in Figure 4.2.

The loading conditions of the two specimens were identical. An axial load of 0.1*f'cAg* was applied to the columns. This represented an estimated average of the axial loading that pre-1967 RC moment frame columns were designed to experience. Cyclic lateral loading was applied vertically in opposite directions at the beam ends (see Figure 4.4a). Ten different drift levels were applied, as detailed in Table 4.2. Each subsequent drift loading level was comprised

Table 4.1 Alire Reinforcement Properties

	No. 4 bars	No. 6 bars	No. 7 bars
f_y (ksi)	77.8	73.2	73.1
F_u (ksi)	1021.7	123.4	123.5
E_s (ksi)	33,190	31,463	31,619
ε_{sh}	0.59%	0.66%	0.45%
ε_u	8%	12%	9%
f_{sh1} (ksi)	105.9	105.6	108.8
ε_{sh1}	3%	3.5%	3.5%

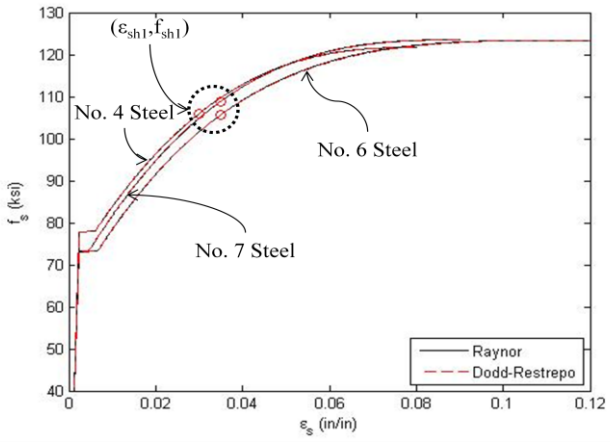

Figure 4.2 Comparison of experimental data to Dodd-Restrepo steel constitutive model

Table 4.2 Alire Displacement History

Drift Level	Drift Ratio (%)	Displacement at Beam End (in)
1	0.1	0.07
2	0.25	0.18
3	0.5	0.36
4	0.75	0.54
5	1	0.72
6	1.5	1.08
7	2	1.44
8	3	2.16
9	4	2.88
10	5	3.60

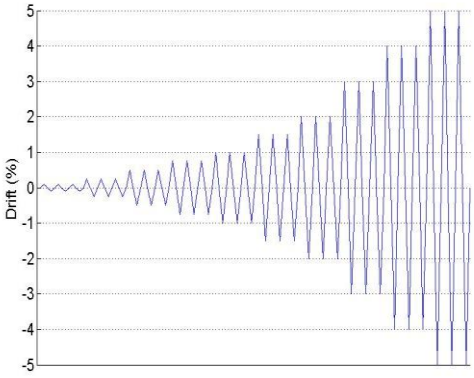

Figure 4.3 Applied drift history for the specimens tested by Alire (2002)

of three positive and three negative cycles, as seen in Figure 4.3. The drift ratio was calculated as $\theta = \delta / L_b$, where δ is the vertical displacement at the beam tip and L_b is the length of the beam, shown in Figure 4.1.

4.1.2 Model Descriptions

The specimens have been modeled similarly for both cases, using single elements for the beams and columns and a refined joint subassembly. The full model layout, along with the bounds of the concrete specimen, can be found in Figure 4.4a. The beam and columns have been modeled with nonlinear force-based beam-column elements. The top node of the upper column has been fixed against horizontal translation and a load has been applied in the vertical direction to simulate the axial column load. The bottom node of the lower column has been pinned. The horizontal reaction at this node will be used to determine the column shear. The lateral cyclic load will be applied vertically at the outer nodes of both beams, where the positive directions are as indicated in Figure 4.4a.

The nonlinear truss joint subassembly is detailed in Figure 4.4b and c, with varying steel and concrete truss element cross-sectional areas given in Figure 4.4b. A four cell by four cell mesh was selected for the joint cores, leading to a cell height of 4.5”, a cell width of 4”, and an angle of inclination of 48.4°. Horizontal and diagonal concrete elements are given differing material properties to represent the appropriate level of vertical confining pressure due to the column axial load. Vertical concrete elements receive no confining benefit due to the column axial load. Varying zero-length bond-slip spring material types are dependent on location and surface area of reinforcing bars at a given reinforcing layer. For the first joint, beam-longitudinal, column-longitudinal, and transverse steel elements are defined using No. 7, No.4, and No. 4 steel

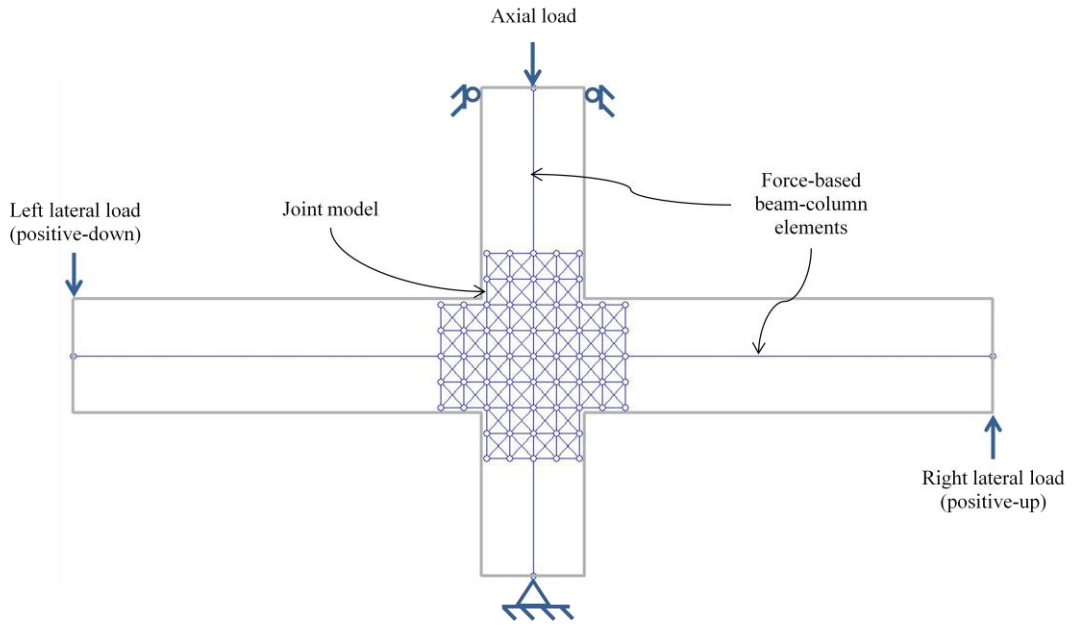

a) Full model layout

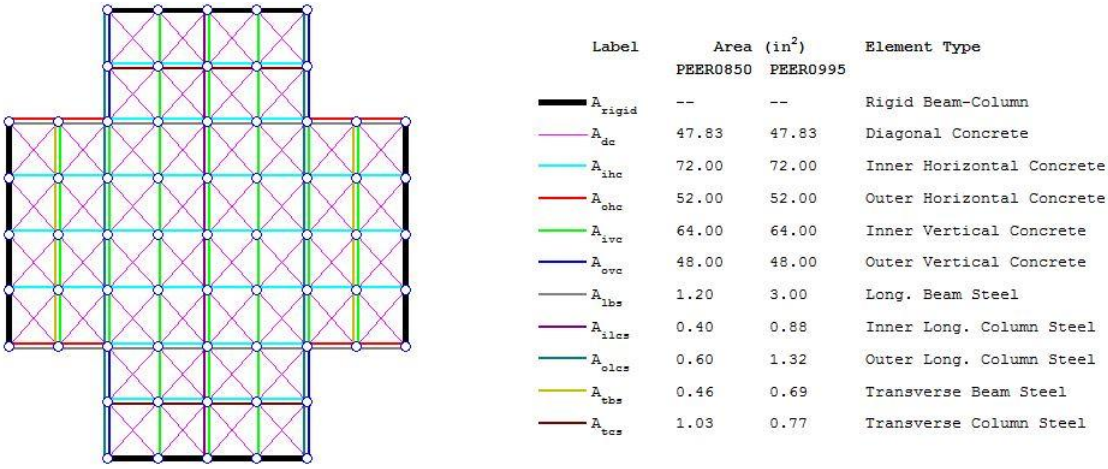

b) Joint element labels by area

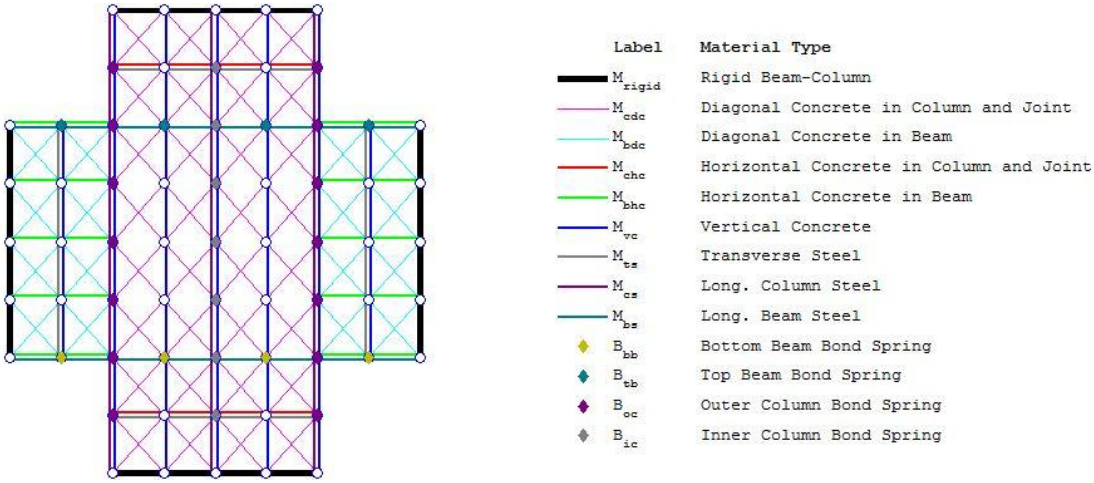

c) Element labels by material type

Figure 4.4 Interior joint model layout

reinforcement material properties, respectively; for the second, No. 7, No. 6, and No. 4 reinforcement material properties are used to define these elements, respectively.

The testing equipment used for the test included gauges to measure shear strain. The total shear strain, denoted as engineering shear strain in Figure 4.5, was approximated as the change in angle, θ. The angle, θ, is calculated based on the law of cosines using the change in length of diagonal gauges across the joint core and vertical and horizontal gauges around the edges of the joint core, as seen in Figure 4.6. The joint shear strain is calculated for all four joint corners and averaged, where, for example, the lower left corner is calculated as:

$$\gamma_{xy} = \alpha_0 - \cos^{-1}\left(\frac{(A+V1)^2 + (B+H2)^2 - (C+D1)^2}{2*(A+V1)*(B+H2)}\right) \quad \text{(Eq 4.1)}$$

and α_o is the initial angle of the corner.

The joint shear stress, v_j, is considered to be based on the column shear, V_c, and is calculated by the equation:

$$v_j = \frac{V_c}{A_j} * \left[\frac{L_c}{jd} * \left(1 - \frac{h_c}{L_b}\right) - 1\right] \quad \text{(Eq 4.2)}$$

where A_j is the joint area, L_c is the length of the column, L_b is the length of the beam, jd is the internal moment arm, and h_c is the height of the column, as illustrated in Figure 4.7. The joint area is equal to the cross-sectional area of the column in both cases. The internal moment arm is found from the tension and compression couple based on the tension reinforcement and concrete compression block in the beam.

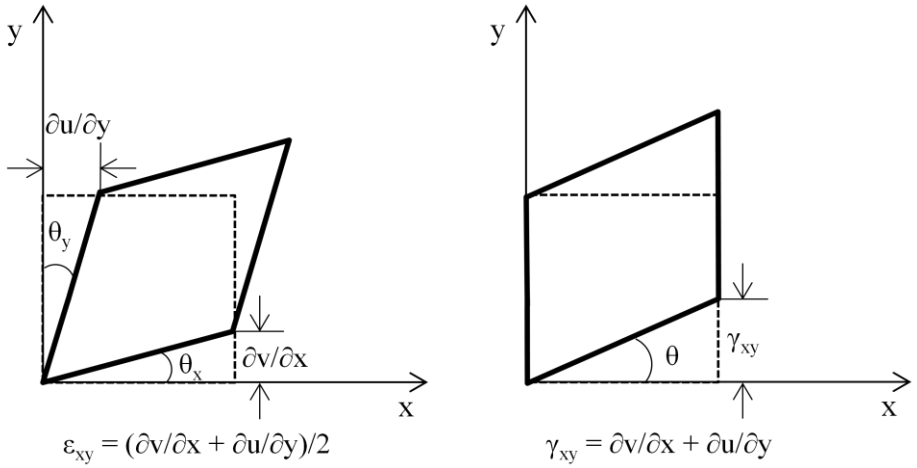

a) Shear strain tensor b) Engineering shear strain

Figure 4.5 Types of shear strain

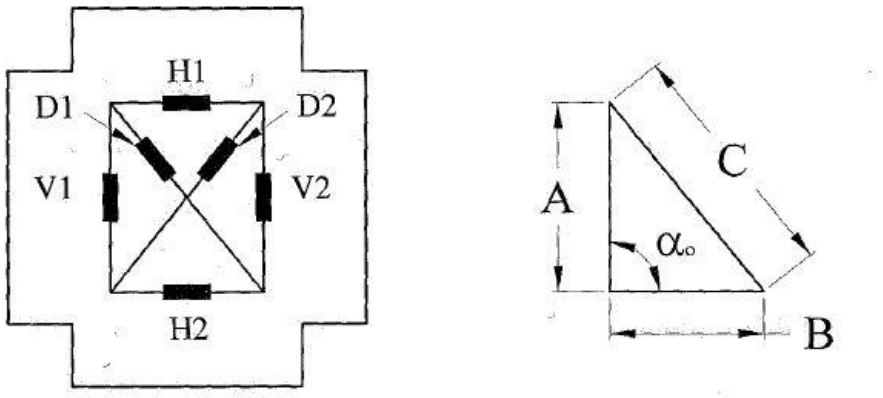

a) Shear strain instrumentation b) Isolated triangle

Figure 4.6 Measurement of shear strain. Alire, D. (2002), "Seismic Evaluation of Existing Unconfined Reinforced Concrete Beam-Column Joints." *M.S. Thesis*, University of Washington, Seattle, WA, 306pp. Figures used under fair use, 2014.

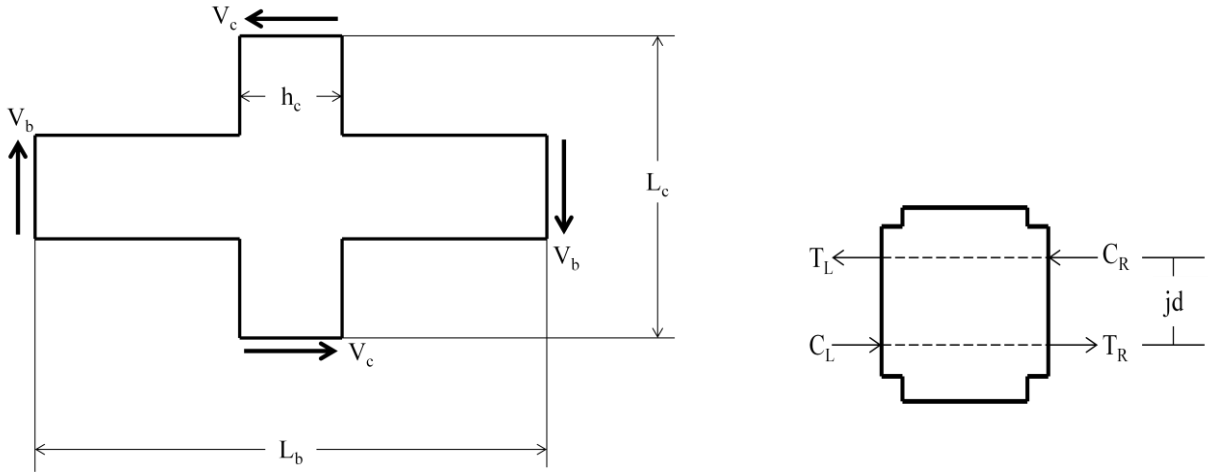

a) Beam-column subassemblage with shear forces acting on it b) Tension and compression force couples

Figure 4.7 Description of joint shear stress parameters

4.1.3 .Discussion of Results

Figure 4.8 compares the column shear-interstory drift relationships of the experimental results of the first interior joint and its simulated response. Initial stiffness, strength, and ductility are well predicted, with the model giving a simulated cyclic peak strength that is 2.3% higher than the measured peak strength. The predicted drift at which the onset of beam reinforcement steel yielding occurs is within 0.5% drift of the point when beam steel yielding occurred in the test. The first crushing of concrete along the compression strut in the simulation, seen in Figure 4.10, occurred within the same drift loading cycle as the spalling of concrete observed during the test, seen in Figure 4.9. Good agreement is found between these damage patterns. Extreme

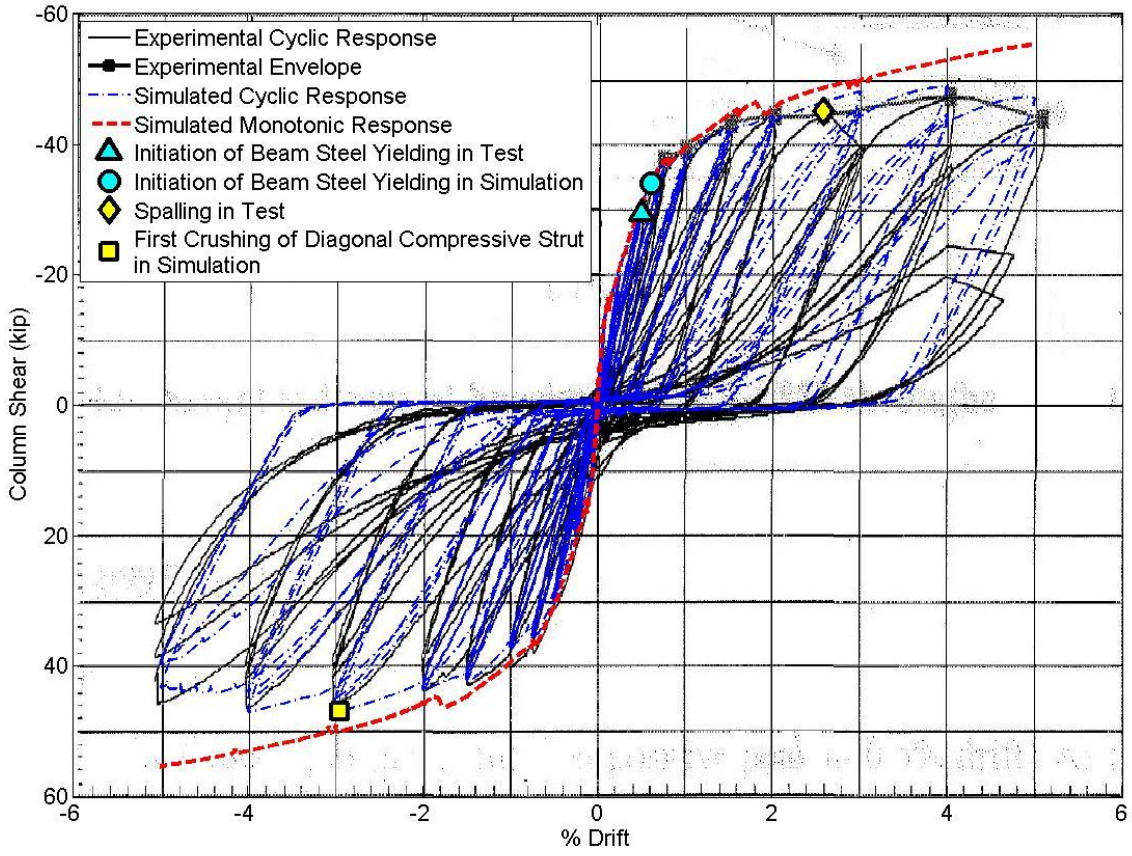

Figure 4.8 Column shear force-drift responses for the first inter joint

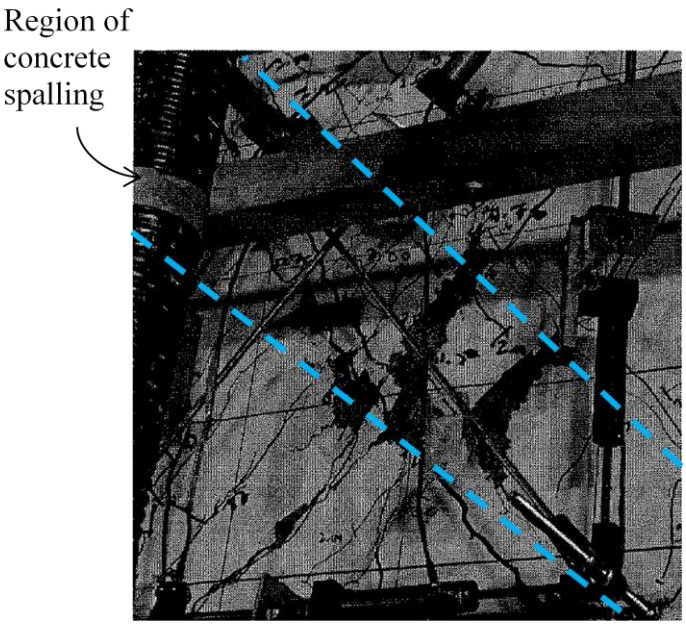

Figure 4.9 Observed concrete spalling at 3% drift. Alire, D. (2002), "Seismic Evaluation of Existing Unconfined Reinforced Concrete Beam-Column Joints." *M.S. Thesis*, University of Washington, Seattle, WA, 306pp. Photo used under fair use, 2014.

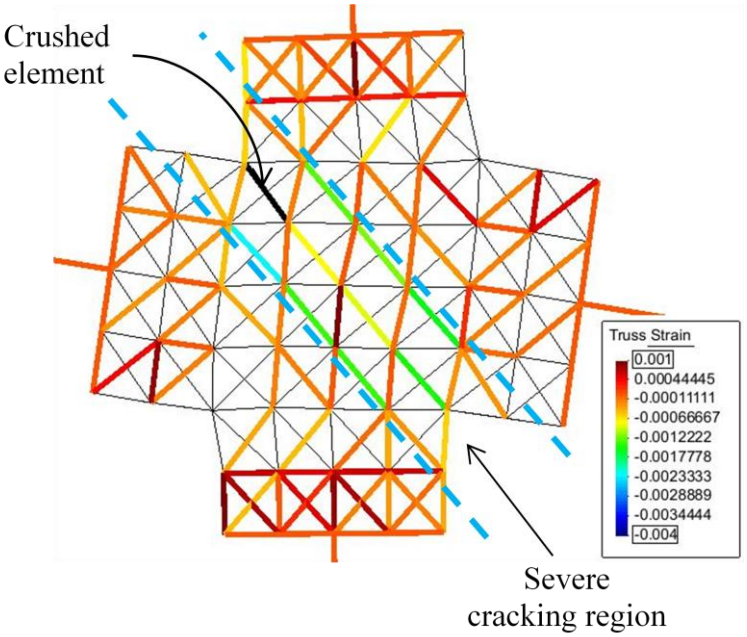

Figure 4.10 Simulated concrete crushing during 3% drift load level

spalling of the joint concrete occurred in the first cycle of the 5% drift load level of the test, leading to a loss of strength in subsequent cycles. Because concrete spalling is not explicitly accounted for in the model, this strength loss is not well captured.

Figure 4.11 gives a comparison of the joint shear stress-joint shear strain responses of the test and the analysis for the first joint up to the 3% drift loading level. Multiple rigs were set in place to measure joint shear strain during the test. At the 3% drift loading level and shortly thereafter there were large discrepancies between the measurements of these rigs and these measurements were deemed unstable. Thus, the joint shear stress-joint shear strain measurements were only reported up to the 3% drift level. The model under-predicts the initial modulus, but roughly approximates the peak joint strength. Large pinching in the simulated response indicates that these deformations are highly dependent on bond-slip, which represents well the reported physical phenomena.

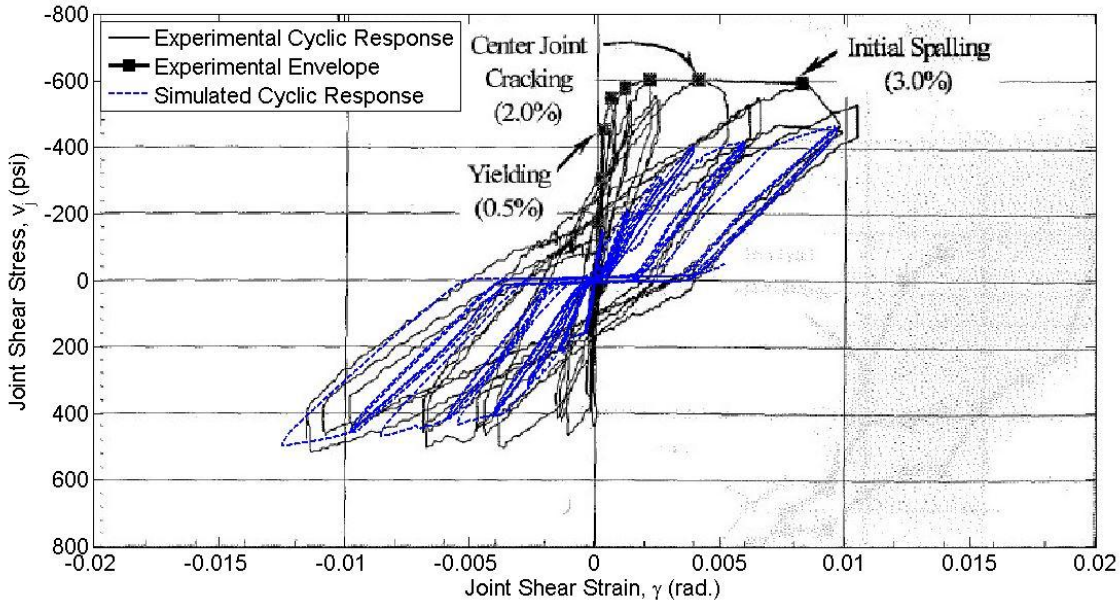

Figure 4.11 Joint shear stress-joint shear strain responses for the first interior joint.

Figure 4.12 compares the column shear-drift results of the second interior joint from the experimentally measured response against the simulated cyclic and monotonic model responses.Initial stiffness and strength are well captured by the model on the positive side of the response, though ductility is somewhat over predicted. As illustrated in Figure 4.13b, the initiation of center joint cracking and concrete cracking at the reinforcing embedment is evident in the model at 0.5% drift, as was observed during testing, pictured in Figure 4.13a. The observed crack pattern at 3% drift, pictured in Figure 4.13c, shows signs of severe diagonal cracking within the joint and concrete cracking at the points of reinforcing embedment in the corners. As is illustrated in Figure 4.13d, the model well captures this behavior at 3% drift. Beam steel yielding occurred within the 1% drift loading levels in both the model and the physical test. However, the occurrence of concrete crushing in the simulation came at a higher drift level than joint concrete spalling in the test because of the additional strength gained by the concrete confinement effect. As in the first interior specimen, spalling of the joint concrete lead to

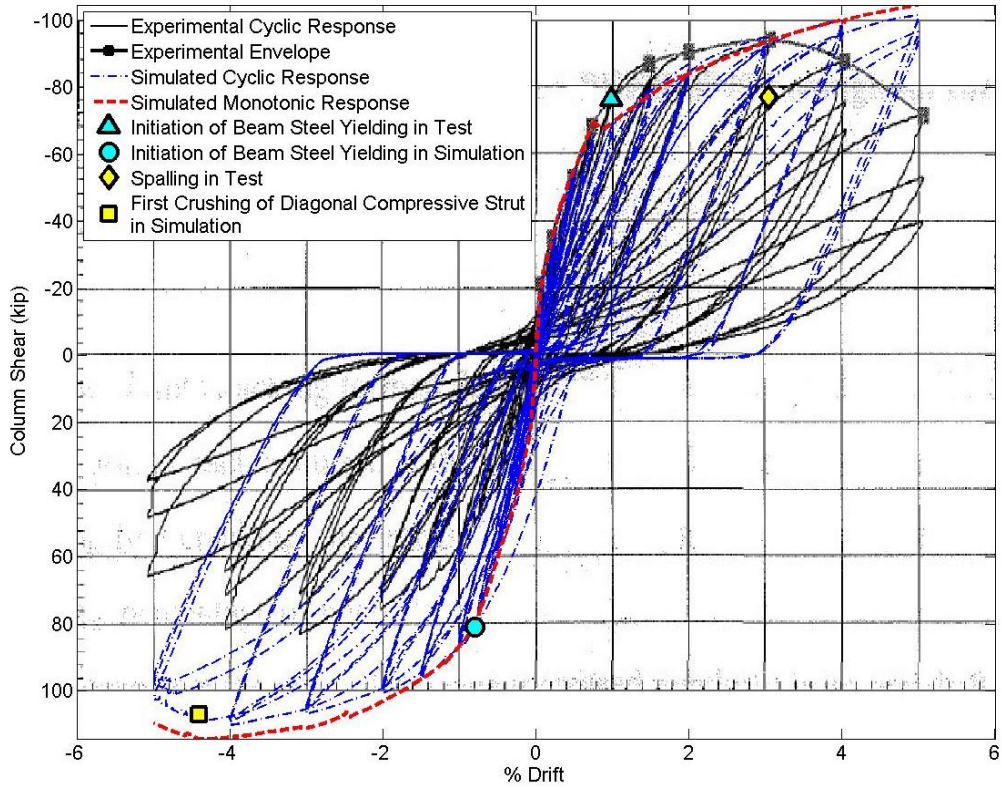

Figure 4.12 Column shear force-drift responses for the second interior joint.

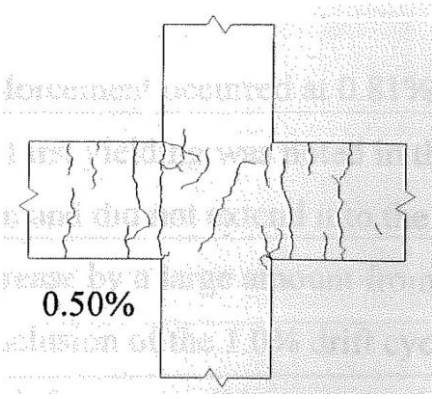

a) Observed crack pattern at 0.5% drift

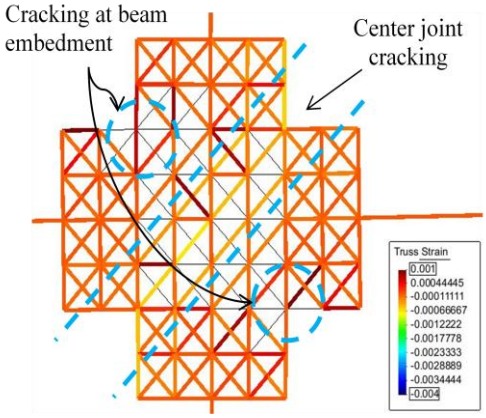

b) Simulated crack pattern at 0.5% drift

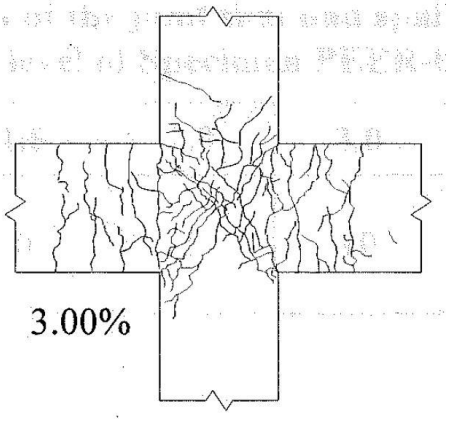

c) Observed crack pattern at 3% drift

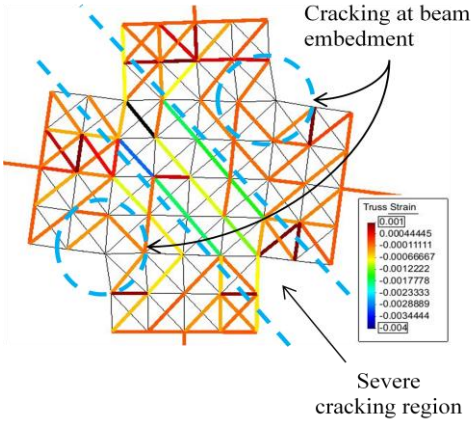

d) Simulated crack pattern at 3% drift

Figure 4.13 Crack patterns of second interior joint. Alire, D. (2002), "Seismic Evaluation of Existing Unconfined Reinforced Concrete Beam-Column Joints." *M.S. Thesis*, University of Washington, Seattle, WA, 306pp. Figures used under fair use, 2014.

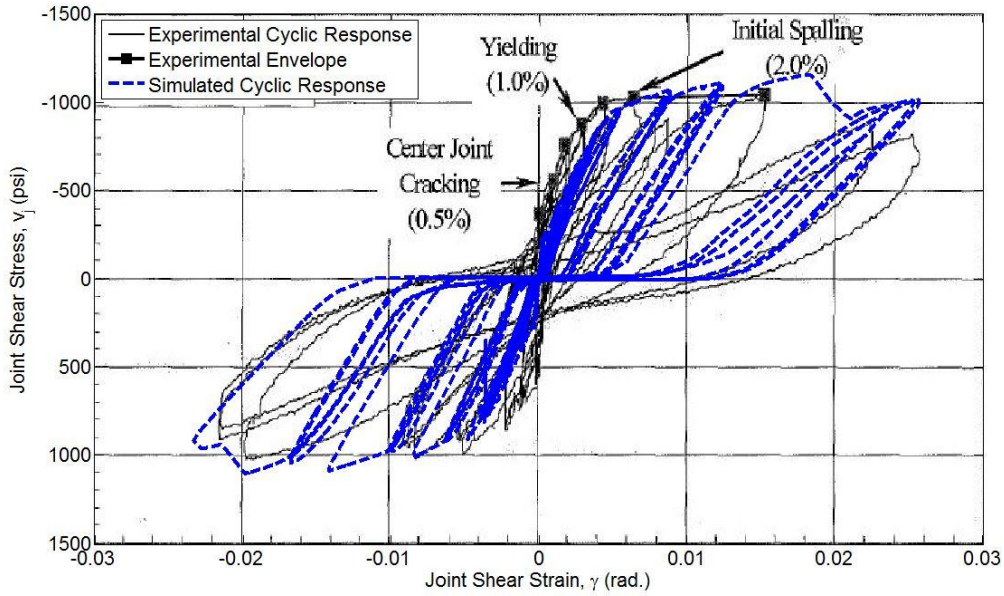

Figure 4.14 Joint shear stress-joint shear strain responses for the second interior joint

decreased strength in subsequent cycles, eventually leading to buckling of the longitudinal column bars and a loss of any confining effects provided by these bars. This bar buckling is not accounted for by the model.

Figure 4.14 compares the cyclic joint shear stress-joint shear strain relationship of the experimentally measured response and the simulated joint model response for the second joint. Up through the 3% drift load level where measured results were given, good agreement is found between the measured and simulated joint shear stress-joint shear strain relationship in terms of strength and ductility. As in the test, the simulated response remained fairly elastic up through the first two drift loading levels.

4.2 Analysis of Exterior Beam-to-Column Joint

Pantelides et al. (2002) tested six full-scale exterior beam-column subassemblages. The focus of the study was on poorly detailed joints typical of moment frame construction prior to the

mid-1970s. The effects of embedment type and concrete axial load level were of particular interest. Three types of bottom reinforcing bar embedment were tested: a straight embedment of 6", a straight embedment of 14", and a 180° hooked embedment; all top reinforcing bars were embedded 180° hooks. Column axial load level was defined as the axial compressive load, *P*, as a percentage of the axial load capacity, $f'_c A_g$. For all three types of embedment, two levels of column axial load were tested: 10 and 25%. The fifth test unit is selected for investigation in this study because of its obvious failure due to joint shear failure as opposed to bottom bar pullout.

4.2.1 Specimen Description

The exterior joint was designed to induce a failure within the beam-to-column joint prior to beam or column failure. A flexural strength ratio ($\Sigma M_c/M_b$) of 1.85 ensured that any plastic hinging would occur within the beam rather than the joint. The beam and columns were constructed with sufficient transverse reinforcement to prevent shear failure, as well as extra transverse reinforcement placed at the beam and column ends where constraints and loads would be applied, as is detailed in Figure 4.15. No transverse reinforcement was placed within the joint. Longitudinal reinforcement in the beam consisted of four No. 9 bars both top and bottom embedded into the joint with 180° hooks. Longitudinal reinforcement in the column was continuous end to end and consisted of four No. 8 bars on the out-of-plane column faces. No longitudinal reinforcement was included on the in-plane column faces because this would have led to unwanted additional confinement within the joint. Reinforcement material properties can be found in Table 4.3. No information was given on the shape of the strain hardening regime; thus, intermediate strain hardening points were assumed in order to give reasonable curves. The concrete had a compressive strength of 4,596 psi on the day of the test.

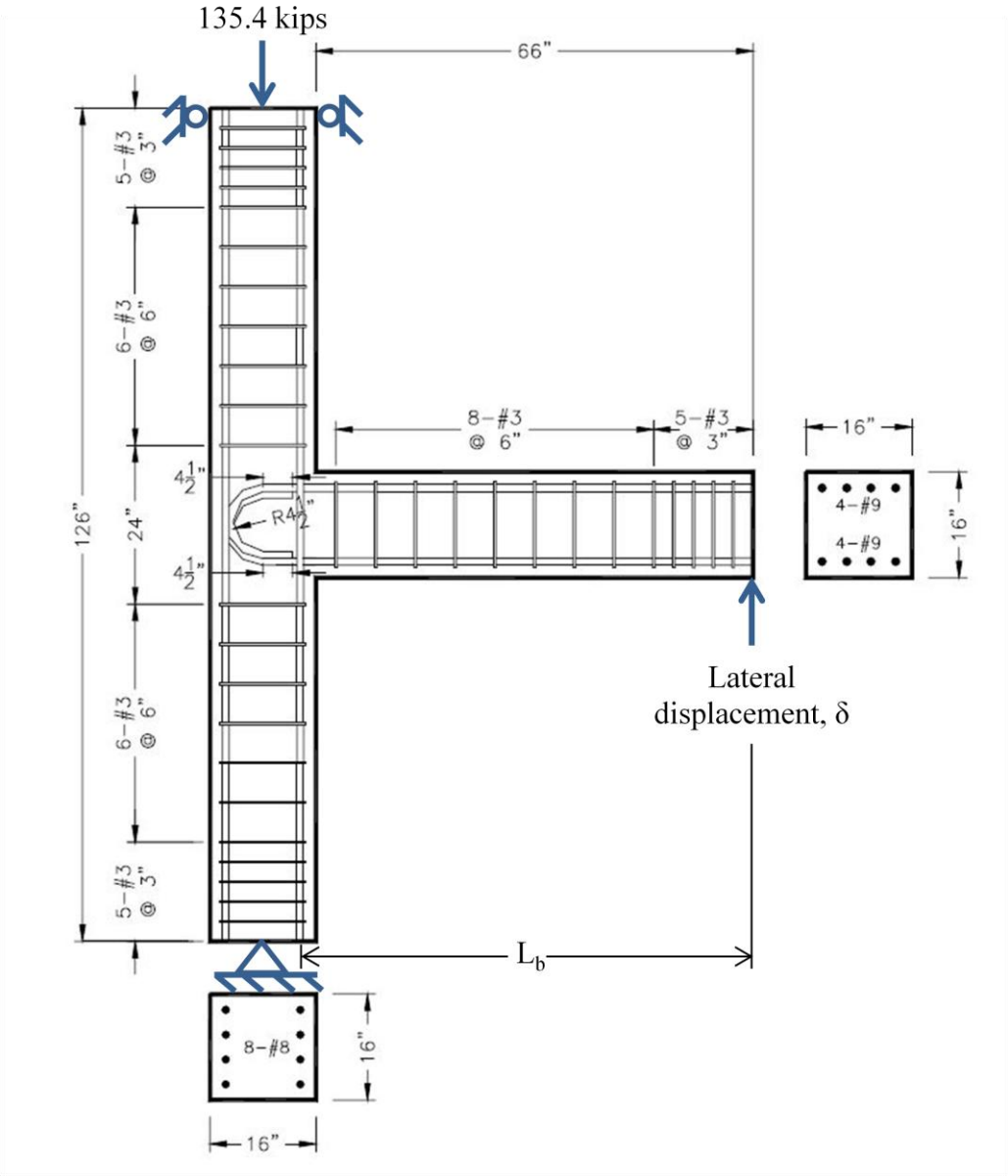

Figure 4.15 Reinforcement detailing of the exterior joint. Pantelides, C., Hansen, J., Nadauld, J., and Reaveley, L. (2002), "Assessment of Reinforced Concrete Building Exterior Joints with Substandard Details." *Report No. PEER-2002/18,* Berkeley, CA. Figure used under fair use, 2014.

The subassemblage was cast in place with the columns vertical during testing. A compressive axial load level of 10% was maintained during the test while a cyclic lateral load comprised of eleven different drift levels was applied vertically at the beam end, as described in Table 4.4. Drift ratios were calculated as $\theta = \delta / L_b$, where δ is the vertical displacement at the

Table 4.3 Exterior Joint Reinforcement Properties

Reinforcement Type	Bar Size	f_y (ksi)	F_u (ksi)
Beam longitudinal	9	66.5	110.4
Column longitudinal	8	68.1	107.6
Transverse	3	62.0	94.9

Table 4.4 Pantelides Displacement History

Drift Level	Drift Ratio (%)	Displacement at Beam End (in)
1	0.1	0.07
2	0.25	0.17
3	0.5	0.34
4	0.75	0.51
5	1	0.68
6	1.5	1.02
7	2	1.37
8	3	2.05
9	5	3.42
10	7	4.78
11	10	6.83

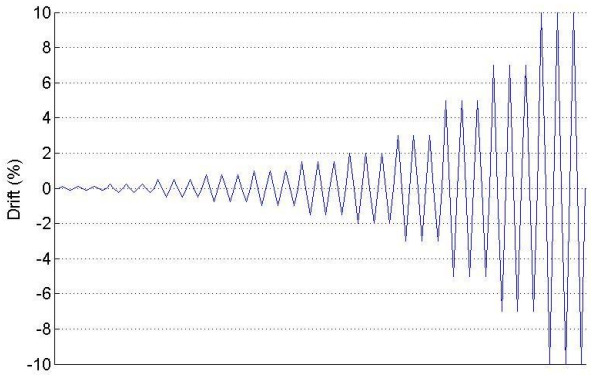

Figure 4.16 Applied drift history for the specimen tested by Pantelides et al. (2002)

beam tip and L_b is the length of the beam, shown in Figure 4.15. Each loading at the different drift levels consisted of three positive and three negative cycles, as seen in Figure 4.16.

The joint shear strain was measured with diagonal gauges, as in Alire (2002). However, the shear strain tensor was reported as opposed to the engineering strain (see Figure 4.5). Thus, the calculation of joint shear strain follows Eq. 4.1, but is halved. The joint shear calculations follow Eq. 4.2, but are normalized by the square root of f'_c.

4.2.2 Model Description

The modeling layout of the joint can be found in Figure 4.17. Nonlinear force-based beam-column elements have been used for the beam and columns and a refined joint subassembly has been defined. The top node of the upper column is fixed against horizontal

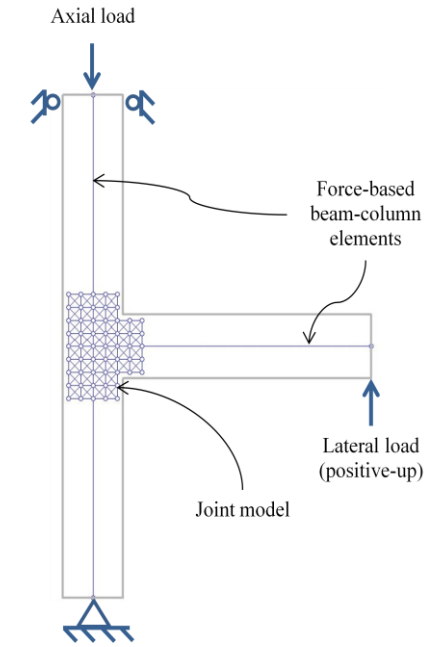

Full model layout

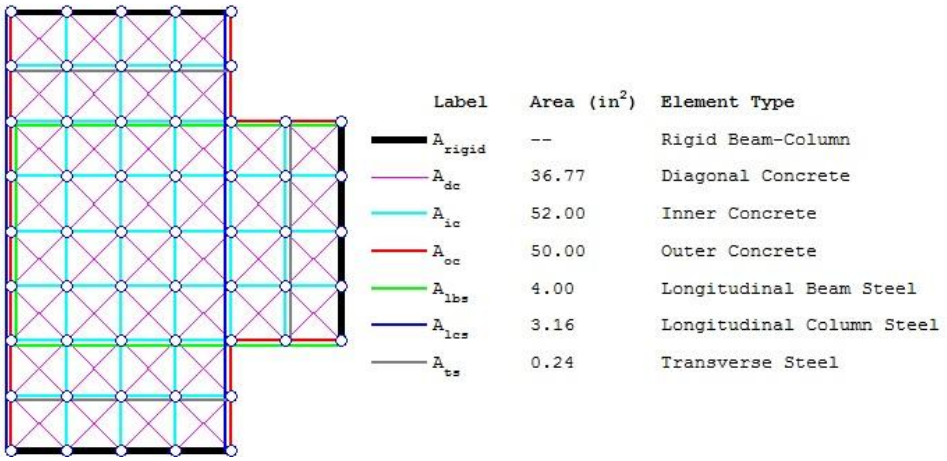

a) Joint element labels by area

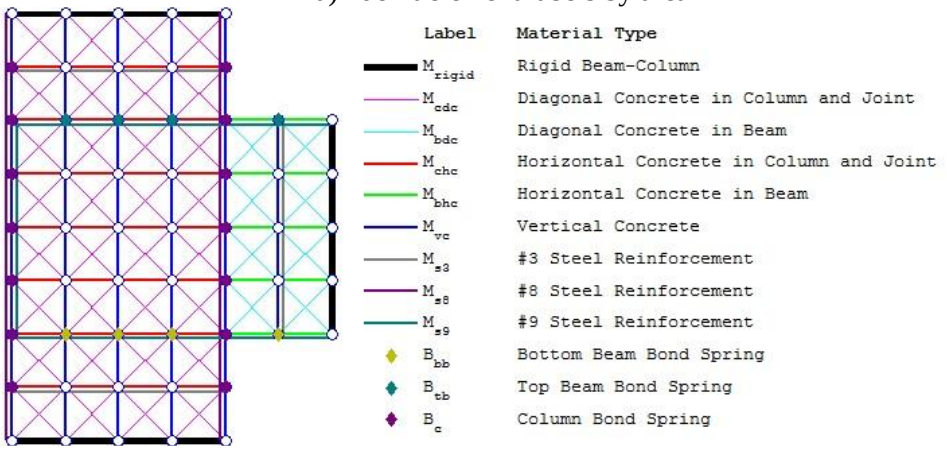

b) Joint element labels by material type

Figure 4.17 Exterior joint model layout

translation and a vertical load is applied to represent the compressive column axial load. The bottom node of the lower column is pinned and the vertical reaction at this node will be used to find the lateral load on the system. The lateral displacement will be applied at the right node of the beam, which will be otherwise free to rotate or translate. The fixity and loading conditions have been detailed in Figure 4.17a.

Figure 4.17b and c detail the model layout of the joint subassembly. All elements are nonlinear truss elements except for the beam and column interface elements, which are rigid beam-columns. The cross-sectional areas of the truss elements can be found in Figure 4.17b. A 4 cell by 4 cell joint core mesh has been selected, giving vertical and horizontal truss element

lengths of 3.25” and an incline angle of 45°. Column longitudinal, beam longitudinal, and transverse steel elements are given No. 8, No. 9, and No. 3 steel reinforcement properties, respectively. Differing material properties are ascribed to the horizontal and diagonal concrete elements to represent given confining pressures, whereas the material properties are ascribed similarly for all vertical concrete elements. Bond-slip is modeled with zero-length springs and the properties are dependent on location, type, and surface area of reinforcing bars.

4.2.3 Discussion of Results

Comparison of the lateral load-drift responses of the experimental results and the simulated results can be found in Figure 4.18. The model presents good agreement with the initial stiffness and peak strength of the measured data. The first yield of longitudinal reinforcement in the model coincides with the first measured yield in longitudinal reinforcement in the specimen. The onset of diagonal concrete crushing in the compression strut of the model, illustrated in Figure 4.20, also coincides with the formation of the joint shear mechanism in the specimen, pictured in Figure 4.19. Though the specimen degradation pattern is not well captured in the cyclic simulation, the onset of significant concrete spalling in the specimen is well approximated by the degradation of the monotonic curve, as seen in Figure 4.18.

A comparison of the normalized joint shear stress-joint shear strain of the measured response and of the joint model, as seen in Figure 4.21, shows a good prediction of the peak strength. The initial tangent modulus is slightly more steep in the measured response as compared with the simulated response, however the simulation has a steeper tangent modulus in the post-peak portion of the response compared with the envelope of the measured response. The crushing of concrete along the primary compression strut within the model leads to a rapid loss of shear strength and large shear deformations within the joint.

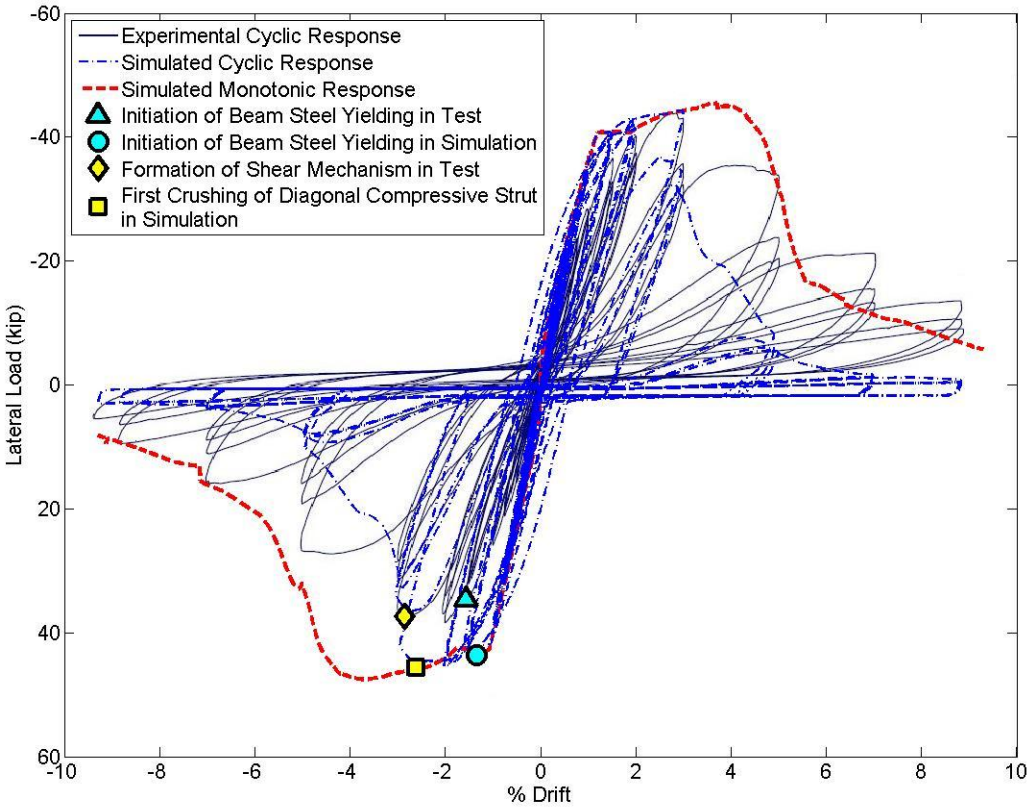

Figure 4.18 Lateral load-drift responses for the exterior joint

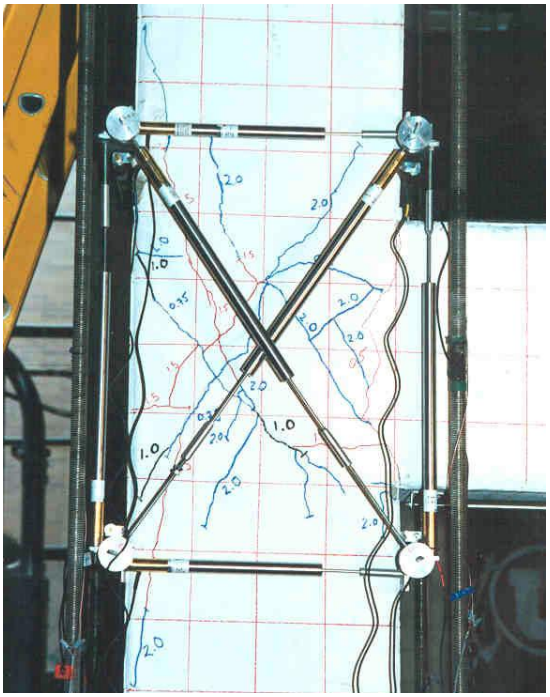

Figure 4.19 Observed cracking pattern at formation of joint shear mechanism. Pantelides, C., Hansen, J., Nadauld, J., and Reaveley, L. (2002), "Assessment of Reinforced Concrete Building Exterior Joints with Substandard Details." *Report No. PEER-2002/18*, Berkeley, CA. Photo used under fair use, 2014.

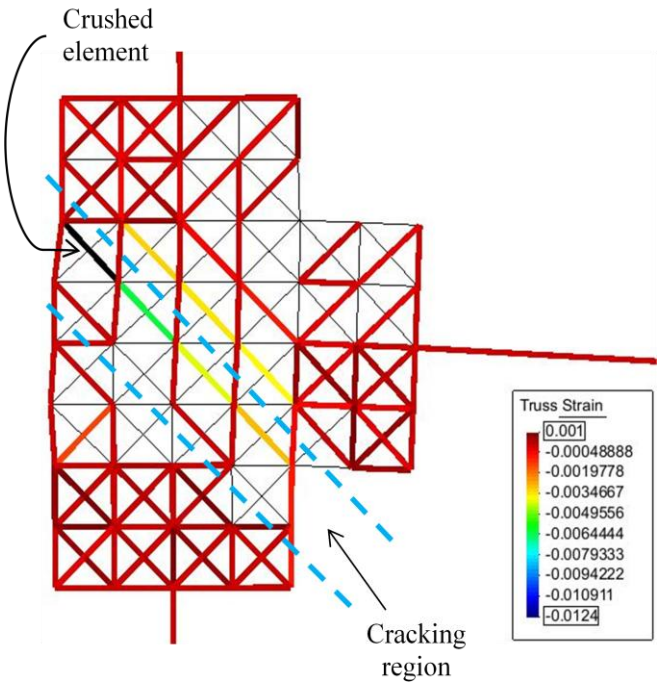

Figure 4.20 Simulated crack pattern at first concrete crushing

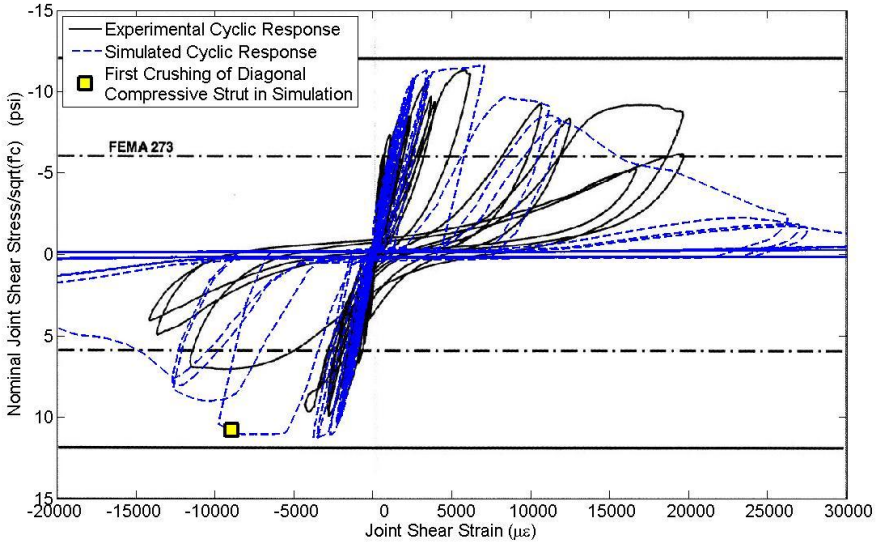

Figure 4.21 Normalized joint shear stress-joint shear strain responses for the exterior joint

4.3 Effects of Key Model Assumptions

The effects of bond-slip and joint confinement on the initial stiffness, peak strength, and ductility of the modeling scheme were investigated in this study. Bond-slip was modeled with zero-length elements at all nodes where longitudinal steel elements came into contact with concrete elements. The constitutive model developed by Mitra and Lowes (2007) was utilized for this study. Confinement parameters as a function of column axial load were calculated based on the expressions of Mander et al. (1988). The column axial load provided the confining pressure for the horizontal and diagonal elements within the columns and the joint. No confining effect was considered for vertical elements or for elements within the beams.

As can be seen in Figure 4.22, bond-slip had a positive effect on all specimens. It had very little effect on initial stiffness, but in all specimens it improved ductility. This is likely due to the steel elements' ability to undergo greater yielding without causing excessive deformation

in the concrete elements. In the second interior joint and the exterior joint, pictured in Figure 4.22b and c, it also improved the approximation of peak strength.

The concrete confinement due to axial column load also had a clear positive effect on the exterior joint, as is evident in Figure 4.23c. The strength has significantly improved, with the simulated peak positive strength coming to within 1.5% of the measured peak strength, both

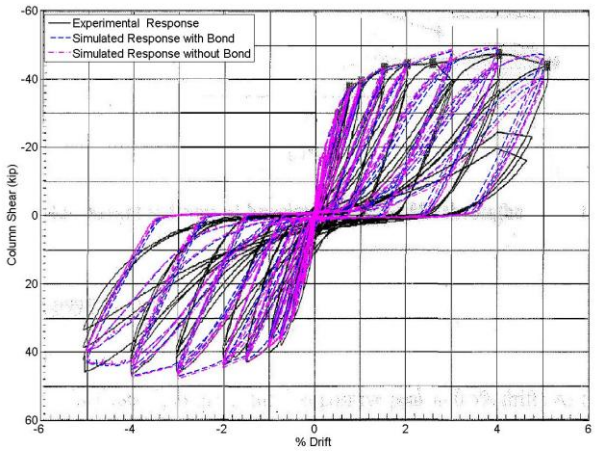

a) First interior joint

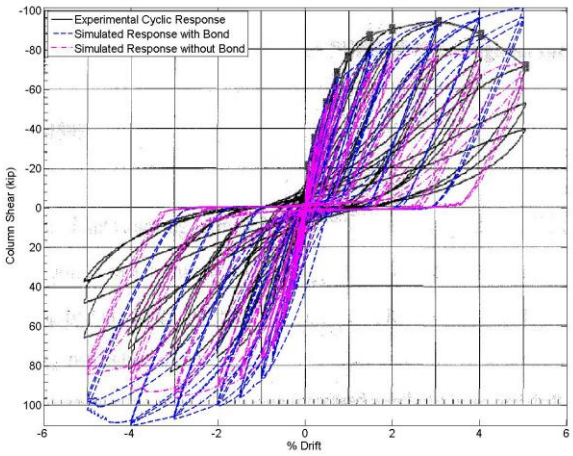

b) Second interior joint

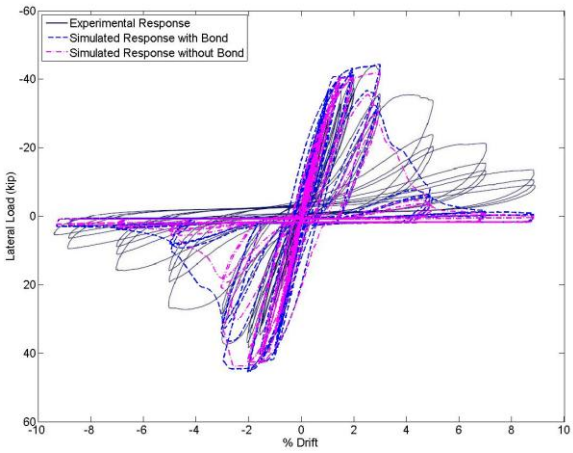

c) Exterior joint

Figure 4.22 Comparison of experimental lateral load-drift response to simulated lateral load-drift responses with and without bond-slip effect

occurring at the same interstory drift. The degradation curve was also improved, leading to a less sharp decline after the crushing of joint core concrete. The simulated response of the first interior joint was also positively in terms of ductility approximations, as seen in Figure 4.23a. For the second interior joint, the confinement lead to an over prediction of system ductility because of the increased concrete strength, as is evident in Figure 4.23b.

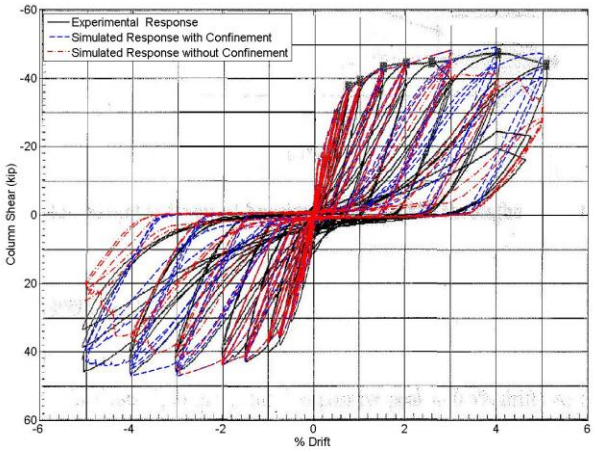

a) First interior joint

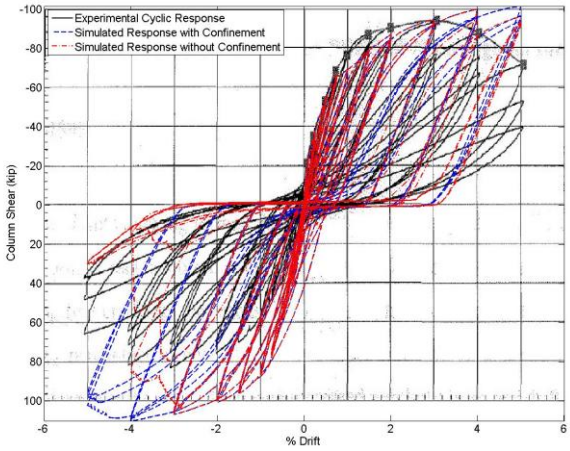

b) Second interior joint

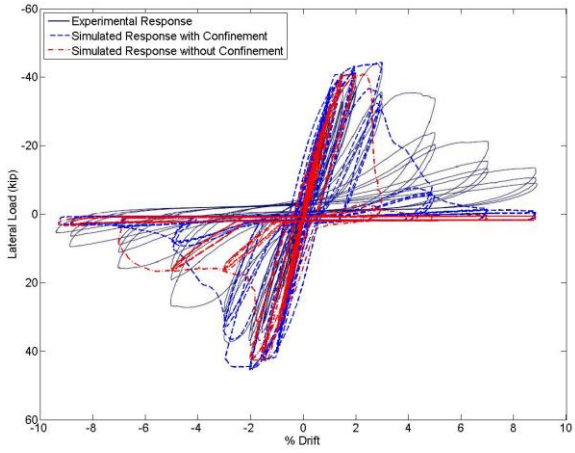

c) Exterior joint

Figure 4.23 Comparison of experimental lateral load-drift response to simulated lateral load-drift responses with and without confinement effect

Chapter 5. Conclusions and Recommendations for Future Research

This thesis has described a nonlinear truss modeling approach for non-ductile beam-to-column joints, for which strength degradation occurs due to diagonal cracks. Concrete and steel have been represented by truss elements that formed a lattice structure. Diagonal concrete elements have accounted for the transverse strain effect in compression members, having reduced compressive strength depending on the orthogonal tensile strain. An accurate steel constitutive model has been implemented that accounts for distinct elastic, yield plateau, and strain hardening regions, as well as having accurately represented the Bauschinger effect in unloading. The reinforcing bar bond-slip relationship has been represented using zero-length springs to connect concrete and steel elements. The model has been verified by comparing the simulated responses to the experimentally measured responses of three poorly detailed beam-to-column joints: two interior joints and one exterior joint.

5.1 Conclusions

1. The proposed model has predicted well the cyclic response of beam-to-column connections with shear-dominated failures, especially in terms of the initial stiffness and strength in the direction of first loading. The model has overestimated the stiffness and strength in the negative loading direction compared with the experimentally measured results, having given strengths in the negative loading direction that are up to 24% higher than the measured values.
2. The onset of longitudinal beam steel yielding and diagonal compression strut crushing, as well as the crack pattern formation, have been well predicted by the model. The onset of these events has typically occurred within the same loading cycle in both the experimental tests and the simulations.

3. The strength and ductility of the joint have been better captured by including bond-slip in the modeling scheme.
4. The confining pressures of the diagonal and horizontal concrete elements have been well predicted by the vertical pressure due to the column axial load. However, this confining effect has lead to an over prediction of joint ductility.

5.2 Recommendations for Future Research

Future research should include an investigation into the strength and stiffness of the negative loading direction. The formation of cracks during the first positive loading may have an effect on the strength in this negative loading direction.

Degradation in the model occurs very swiftly after the first crushing of a concrete element within the diagonal compression strut. Redundancy to account for this and allow for the greater ductility typically seen in beam-to-column joints should be investigated further. Accounting for dowel action in the reinforcing bars is one suggested approach.

A further refinement of the calculations to determine the confinement of the concrete due to column axial load is suggested. The dependence of confinement on joint concrete spalling and bar buckling is a possible source of variability. A broader range of column axial load levels, including tensile axial loads caused by overturning of the moment frame, should be investigated.

Further research should be conducted to broaden the applicability of the model. Of particular interest would be an investigation into the applicability of the model to well-detailed, modern joints which rely more heavily on the panel-truss shear mechanism. A variety of failure types should also be studied.

A comparison of the modeling scheme to refined finite element models should be made, particularly looking at accuracy and computational efficiency.

References

ACI (1971), *Building Code Requirements for Structural Concrete*, ACI 318-71, American Concrete Institute.

ACI (1985), *Recommendations for Design of Beam-Column Connections in Monolithic Reinforced Concrete Structures*, ACI 352-85, American Concrete Institute.

Alath, S., and Kunnath, S. (1995), "Modeling Inelastic Shear Deformation in RC Beam-Column Joints." *Proceedings of the 10th Engineering Mechanics Conference*, Boulder, CO, 822-825

Alire, D. (2002), "Seismic Evaluation of Existing Unconfined Reinforced Concrete Beam-Column Joints." *M.S. Thesis*, University of Washington, Seattle, WA, 306pp.

Anderson, M., Lehman, D., and Stanton, J. (2008), "A cyclic shear stress-strain model for joints without transverse reinforcement." *Engineering Structures 30, 941-954*

Baglin, R. H., and Scott, P. S. (2000), "Finite Element Modeling of Reinforced Concrete Beam-Column Connections." *ACI Structural Journal* 97(6), 886-894

Beres, A., Pessiki, S., White, R., and Gergely, P. (1991), "Seismic performance of existing reinforced concrete frames designed primarily for gravity loads." *Proceedings of the 6th Canadian Conf. Earthquake Engineering*, Toronto, Canada, 655-662

Beres, A., White, R., Gergely, P., Pessiki, S., and El-Atta, A. (1992), "Behavior of existing non-seismically detailed reinforced concrete frames." *Proceedings of the 10th Earthquake Engineering World Conference*, Balkema, Rotterdam, 3359-3363

Beres, A., Pessiki, S., White, R., and Gergely, P. (1996), "Implications of Experiments on the Seismic Behavior of Gravity Load Designed RC Beam-to-Column Connections." *Earthquake Spectra* 12(2), 185-198

Biddah, A., and Ghobarah, P. (1999), "Modelling of Shear Deformation and Bond Slip in Reinforced Concrete Joints." *Structural Engineering and Mechanics* 7(4), 413-432

Birely, A., Lowes, L., and Lehman, D. (2011), "A model for the practical nonlinear analysis of reinforced-concrete frames including joint flexibility." *Engineering Structures 34*, 455-465

Ciampi, V., Eligehausen, R., Bertero, V., and Popov, E. (1981), "Analytical Model for Deformed Bar Bond under Generalized Excitations." *Proceedings of the IABSE Colloquium on Advanced Mechanics of Reinforced Concrete*, Delft, Netherlands

Comartin, C., Anagnos, T., Faison, H., Greene, M., and Moehle, J. (2008), "The Concrete Coalition: Building a Network to Address Nonductile Concrete Buildings." *Proceedings of the 14th World Conference on Earthquake Engineering*, Beijing, China

Dodd, L., and Restrepo-Posada, J. (1995), "Model for Predicting Cyclic Behavior of Reinforcing Steel." *Journal of Structural Engineering* 121(3), 433-445

Durrani, A., and Zerbe, H. (1987), "Seismic Resistance of R/C Exterior Connections with Floor Slabs." *Journal of Structural Engineering* 113(8), 1850-1864

Ehsani, M., and Wight, J. (1985), "Exterior Reinforced Concrete Beam-to-Column Connections Subjected to Earthquake- Type Loading." *ACI Journal* 82-43, 492-499

Eligehausen, R., Popov, E., and Bertero, V. (1983), "Local Bond Stress-Slip Relationships of Deformed Bars Under Generalized Excitations." *Report No. UCB/EERC-83/23*, Berkeley, CA.

Filippou, F., Popov, E., and Bertero, V. (1983), "Modeling of R/C Joints under Cyclic Excitations." *Journal of Structural Engineering* 109(11), 2666-2684

Filson, J. R., McCarthy, J., Ellsworth, W. L., and Zoback, M. L. (2003), "The USGS earthquake hazards program in NEHRP—Investing in a safer future." *USGS Fact Sheet 017-03*, Reston, VA.

Hassan, W. M., Park, S., Lopez, R. R., Mosalam, K. M., and Moehle, J. P. (2010), "Seismic Response of Older-Type Reinforced Concrete Corner Joints." *Proceedings of the 9th U.S. National and 10th Canadian Conference on Earthquake Engineering*, Toronto, Ontario, Canada, Paper No. 1616

Kashiwazaki, T., Nagai, T., and Noguchi, H. (1996), "Parametric Study on the Shear Strength of RC Interior Beam-Column Joints Using Finite Element Method." *Transactions of the Japan Concrete Institute* 18, 275-282

Kim, J., and LaFave, J. (2006), "Key influence parameters for the joint shear behaviour of reinforced concrete (RC) beam-column connections." *Engineering Structures 29, 2523-2539*

Leon, R. (1989), "Interior Joints with Variable Anchorage Lengths." *Journal of Structural Engineering* 115(9), 2261-2275

Leon, R. (1990), "Shear Strength and Hysteretic Behavior of Interior Beam-Column Joints." *ACI Structural Journal* 87(1), 3-11

Leon, R., Kam, W., and Pampanin, S. (2014), "Performance of Beam-Column Joints in the 2010-2012 Christchurch Earthquakes."*ACI SP-296*-3

Lowes, L., (1999), "Finite element modeling of reinforced concrete beam-column bridge connections." *Ph.D. Dissertation, Univ. of California*, Berkeley, CA

Lowes, L., and Altoontash, A. (2003), "Modeling Reinforced-Concrete Beam-Column Joints Subjected to Cyclic Loading." *Journal of Structural Engineering* 129(12), 1686-1697

Lowes, L., Mitra, N., and Altoontash, A. (2004), "A Beam-Column Joint Model for Simulating the Earthquake Response of Reinforced Concrete Frames." *Report No. PEER-2003/10*, Berkeley, CA.

Lu, Y., and Panagiotou, M. (2013), "Three-Dimensional Cyclic Beam-Truss Model for Non-Planar Reinforced Concrete Walls." *Journal of Structural Engineering*, accepted manuscript

Mander, J. B., Priestley, M. J. N., and Park, R., (1988), "Theoretical Stress-Strain Model for Confined Concrete." *Journal of Structural Engineering* 114(8), 1804-1826

McKenna, F., et al. (2005). "OpenSees: Open system for earthquake engineering simulation." *http://opensees.berkeley.edu*, University of California, Berkeley.

Mitra, N., and Lowes, L. (2007), "Evaluation, Calibration, and Verification of a Reinforced Concrete Beam-Column Joint Model." *Journal of Structural Engineering* 133(1), 105-120

Mosier, W. G. (2000), "Seismic Assessment of Reinforced Concrete Beam-Column Joints." *M.S. Thesis*, University of Washington, Seattle, WA, 218 pp.

Noguchi, H. (1981), "Nonlinear Finite Elements Analysis of Reinforced Concrete Beam-Column Joints." *Reports of the Working Commissions (International Association for Bridge and Structural Engineering* 34, 639-654

Pagni, C., and Lowes, L. (2004), "Predicting Earthquake Damage in Older Reinforced Concrete Beam-Column Joints." *Report No. PEER-2003/17*, Berkeley, CA

Pampanin, S., Magenes, G., and Carr, A. (2003), "Modeling of Shear Hinge Mechanism in Poorly Detailed RC Beam-Column Joints." *FIB Symposium, Concrete Structures in Seismic Regions*, Athens, Greece

Panagiotou, M., and Restrepo, J. I. (2011), "Nonlinear Cyclic Truss Model for Strength Degrading Plane Stress Reinforced Concrete Elements." *Report No. UCB/SEMM-2011/01,* Berkeley, CA.

Panagiotou, M., Restrepo, J. I., Schoettler, M., and Kim, G. (2012), "Nonlinear Cyclic Truss Model for Reinforced Concrete Walls." *ACI Structural Journal* 109(2), 205-214

Pantazopoulou, S. J., and Bonacci, J. F. (1994), "On earthquake-resistant reinforced concrete frame connections." *Canadian Journal of Civil Engineering* 21, 307-328

Pantelides, C., Hansen, J., Nadauld, J., and Reaveley, L. (2002), "Assessment of Reinforced Concrete Building Exterior Joints with Substandard Details." *Report No. PEER-2002/18,* Berkeley, CA

Park, S., and Mosalam, K. (2009), "Shear Strength Models of Exterior Beam-Column Joints without Transverse Reinforcement." *Report No. Peer-2009/106,* Berkeley, CA

Paulay, T., Park, R., and Priestley, M. J. N. (1978), "Reinforced Concrete Beam-Column Joints Under Seismic Actions." *Journal of the American Concrete Institute* 75(11), 585-593

Paulay, T., and Scarpas, A. (1981), "The Behavior of Exterior Beam-Column Joints." *Bulletin of the New Zealand National Society for Earthquake Engineering* 14(3), 131-144

Raynor, D. J. (2000), "Bond Assessment of Hybrid Frame Continuity Reinforcement." *M.S. Thesis,* University of Washington, Seattle, WA, 248 pp.

Restrepo-Posada, J. I., Dodd, L. L., and Cooke, N. (1994), "Variables Affecting Cyclic Behavior of Reinforcing Steel." *Journal of Structural Engineering* 120(11), 3178-3196

Sezen, H., Elwood, K. J., Whittaker, A. S., Mosalam, K. M., Walace, J. W., and Stanton, J. F., (2000), "Sezen - Structural Engineering Reconnaissance of the August 17, 1999, Kocaeli (Izmit), Turkey, Earthquake." *Report No. PEER-2000/09*, Berkeley, CA

Sharma, A., Eligehausen, R., and Reddy, G. (2011), "A new model to simulate joint shear behavior of poorly detailed beam-column connection in RC structures under seismic loads, Part I: Exterior joints." *Engineering Structures* 33, 1034-1051

Shin, M., and LaFave, J. (2004), "Testing and Modeling for Cyclic Joint Shear Deformations in RC Beam-Column Connections." *Proceedings of the 13th World Conference on Earthquake Engineering,* Vancouver, Canada

Vecchio, F., and Collins, M. (1986), "The modified compression field theory for reinforced concrete elements subjected to shear." *Journal of the American Concrete Institute* 83(2), 219-231

Appendix A. DoddRestr Steel Constitutive Model Source Code

```
function hr = Doddrestr(e_s,hr,d)
% Function to define stress-strain behavior of steel under cyclic loading.
% List of variables
%   ep_a = natural strain at initiation of Bauschinger effect
%   ep_M = maximum plastic strain defined as greater of |ep_o(1)| or ep_o(2)
%   epp_N = transformed-normalized natural strain
%   ep_o(k) = "shifted" origin strain (k = 1 for compression, 2 for tension)
%   ep_p = strain magnitude between inclined envelope and point at initiaion
%      of Bauschinger effect in natural coordinate system
%   ep_r(m) = natural strain at reversal point (m = 1 for max tension, m = 2
%      for max compression)
%   e_s = steel strain in engineering coordinate system
%   ep_s = steel strain in natural coordinate system
%   ep_sh = natural strain at initiation of work hardening
%   ep_sh1 = arbitrary natural strain in work hardening region of tension
%      monotonic curve
%   ep_su = "ultimate" strain in natural coordinate system
%   ep_sushift(k) = natural strain associated with "ultimate" true stress
%   Ep_u = natural coordinate unload modulus
%   Em_s = initial elastic modulus
%   fp_a = true stress at initiation of Bauschinger effect
%   fp_p = stress magnitude between inclined envelope and point at initiation
%      of Bauschinger effect in natural coordinate system
%   fp_r(m) = true stress at reversal point (m = 1 for max tension, m = 2
%      for max compression)
%   f_s = engineering stress of steel
%   fp_s = true stress of steel
%   fp_sh = true stress at onset of strain hardening
%   fp_sh1 = true stress at arbitrary point ep_sh1
%   fp_su = "ultimate stress" in natural coordinates
%   fps_su = slope at "ultimate stress" in natural coordinates, numerically
%      equal to fo_su
%   fp_t = stress magnitude between top and bottom inclined envelopes in
%      natural coordinate system
%   f_y = yield stress of steel in engineering coordinate system
%   load = loading direction (1 for compression, 2 for tension)
%   P = exponential factor to define work hardening region of skeleton curve
%      and shape of Bauschinger effect
%   region = region of model
%   region = 0: We load along the skeleton curve, we do not store any
%             unloading-reloading points
%   region = 1: Major reversal, (s1 = -1)
%   region = 2: Major reversal, (s1 = 1)
%   region = 3: Minor reversal, "minor point" on positive side (s1 = -1)
%   region = 4: Minor reversal, "minor point" on negative side (s1 = 1)
%   region = 5: Simple reversal, s1 = -1,inside a "region3"
%   region = 6: Simple reversal, s1 = -1,inside a "region4"
%   region = 7: Simple reversal, s1 = 1,inside a "region3"
%   region = 8: Simple reversal, s1 = 1,inside a "region4"
%   point: array with dimension (6x3), row = point number
%             column: 1 = strain, 2 = stress, 3 = slope
%             row: 1=largest tensile major reversal or farthest tensile point
%                  2=largest compressive major reversal or farthest
%                    compressive point
```

```
%                   3=immediate tensile reconnect point
%                   4=immediate compressive reconnect point
%                   5=last tensile reversal
%                   6=last compressive reversal

%   s1 = strain direction factor (1 for tension, -1 for compression)
%   virgin = 1 for virgin loading, 0 for non-virgin
%   W = (omega) partial area under normalized Bauschinger curve

% -------------------------------------------------------------------------
% -------------------------------------------------------------------------
% Reading history variables
e_so = hr(1);
f_so = hr(2);
yield1 = hr(3);
region = hr(4);
point(1,1) = hr(5);
point(1,2) = hr(6);
point(1,3) = hr(7);
point(2,1) = hr(8);
point(2,2) = hr(9);
point(2,3) = hr(10);
point(3,1) = hr(11);
point(3,2) = hr(12);
point(3,3) = hr(13);
point(4,1) = hr(14);
point(4,2) = hr(15);
point(4,3) = hr(16);
point(5,1) = hr(17);
point(5,2) = hr(18);
point(5,3) = hr(19);
ep_o(1) = hr(20);
ep_o(2) = hr(21);
ep_M = hr(22);
fps_so = hr(23);
hist1(1) = hr(24);
hist1(2) = hr(25);
point(6,1) = hr(26);
point(6,2) = hr(27);
point(6,3) = hr(28);
sim1 = hr(29);
stiff = hr(30);

% Reading material properties
Em_s = d(1);
f_y = d(2);
e_sh = d(3);
e_sh1 = d(4);
f_sh1 = d(5);
e_su = d(6);
f_su = d(7);
P_major = d(8);
P_minor = d(9);

% Converting from engineering strain to true strain
ep_sh = log(1+e_sh);
```

```
fp_sh = f_y*exp(ep_sh);
ep_sh1 = log(1+e_sh1);
fp_sh1 = f_sh1*exp(ep_sh1);
ep_su = log(1+e_su);
fp_su = f_su*exp(ep_su);
fps_su = exp(ep_su)*f_su;
ep_s = log(1+e_s);
ep_so = log(1+e_so);
fp_so = f_so*(1+e_so);

% Calculate Ep_u (unloading-Reloading modulus)
if (yield1 > 0.5)
    Ep_u = Em_s*(0.82+1/(5.55+1000*ep_M));
else
    Ep_u = Em_s;
end

% Calculate shifted ultimate strain
ep_sushift(1) = ep_su+ep_o(1);
ep_sushift(2) = -ep_su+ep_o(2);

% Give positive value if you want to set a constant P = P_major,
% otherwise use Eq 36 (Dodd and Restrepo, 1995) to solve for P
if (P_major > 0)
    icheat = 1;
else
    icheat = 0;
end

if((ep_s >= point(1,1)) || (ep_s <= point(2,1))...
        || ep_s >= ep_sushift(1) || ep_s <= ep_sushift(2))
    if(ep_s >= point(1,1) || (ep_s) >= ep_sushift(1)) %if in tension
        ep_o1 = ep_o(1);
        if(hist1(1) > 0.5)
            s1 = 1;
            k = 1;
            ep_a = point(2,1)+s1*f_y/Ep_u;
            fp_a = point(2,2)+s1*f_y;
            ep_sushift(k) = s1*ep_su+ep_o(k);
            ep_rejoin = ep_sushift(k);
            fp_rejoin = s1*fp_su;
            fps_rejoin = fps_su;
            if(ep_s >= ep_sushift(k))
                fp_s = s1*fp_su;
                fps_s = fps_su;
                ep_sushift(k) = ep_s;
                ep_o(k) = ep_sushift(k)-s1*ep_su;
            else
                [fp_s,fps_s] = Bauschinger(1,icheat,P_major,P_minor,...
                    ep_sushift,s1,fp_su,Ep_u,ep_a,fp_a,ep_s,k,...
                    ep_rejoin,fp_rejoin,fps_rejoin,ep_o,ep_so,fp_so);
            end
        else
            [fp_s,fps_s] = virginLoading;
        end
    else %if in compression
```

```
        ep_o1 = ep_o(2);
        if(hist1(2) > 0.5)
            s1 = -1;
            k = 2;
            ep_a = point(1,1)+s1*f_y/Ep_u;
            fp_a = point(1,2)+s1*f_y;
            ep_sushift(k) = s1*ep_su+ep_o(k);
            ep_rejoin = ep_sushift(k);
            fp_rejoin = s1*fp_su;
            fps_rejoin = fps_su;
            if(ep_s <= ep_sushift(k))
                fp_s = s1*fp_su;
                fps_s = fps_su;
            else
                [fp_s,fps_s] = Bauschinger(1,icheat,P_major,P_minor,...
                    ep_sushift,s1,fp_su,Ep_u,ep_a,fp_a,ep_s,k,...
                    ep_rejoin,fp_rejoin,fps_rejoin,ep_o,ep_so,fp_so);
            end
        else
            [fp_s,fps_s] = virginLoading;
        end
    end

    region = 0;     %say we are not in a reversal
    point(3,1) = 0; %and erase all of the old reversal stuff
    point(3,2) = 0;
    point(3,3) = 0;
    point(4,1) = 0;
    point(4,2) = 0;
    point(4,3) = 0;
    point(5,1) = 0;
    point(5,2) = 0;
    point(5,3) = 0;

    if(ep_s > point(1,1) || ep_s >= ep_sushift(1))
        point(1,1) = ep_s; %if past the max previous tensile point/max
        point(1,2) = fp_s; %tensile reversal replace point 1
        point(1,3) = fps_s;
    end

    if(ep_s < point(2,1) || ep_s <= ep_sushift(2))
        point(2,1) = ep_s; %if past the max previous compressive point/max
        point(2,2) = fp_s; %compressive reversal, replace point 2
        point(2,3) = fps_s;
    end
elseif(ep_s < point(1,1) && ep_s > point(2,1))
    %-------------------------------------------------------------------
    if(region < 0.5) %Reversal from virgin loading
        if(yield1 < 0.5)%Reversal in elastic branch
            fp_s = Em_s*ep_s;
            fps_s = Em_s;
            %check if greater than previous greatest points
            if(ep_s > point(1,1))
                point(1,1) = ep_s;
                point(1,2) = fp_s;
                point(1,3) = fps_s;
```

```
    end

    if(ep_s < point(2,1))
        point(2,1) = ep_s;
        point(2,2) = fp_s;
        point(2,3) = fps_s;
    end
elseif(yield1 < 1.5) %Reversal in yield plateau
    if(ep_so < point(1,1) && ep_so > point(2,1))
        if(point(5,2) > 0) %if it was a tensile reversal
            s1 = -1;
            k = 2;
            m = 1;
            region = 1;
        else %if it was a compressive reversal
            s1 = 1;
            k = 1;
            m = 2;
            region = 2;
        end
    else %if beyond point of last greatest reversal/max point reached
        point(5,1) = ep_so;
        point(5,2) = fp_so;
        point(5,3) = fps_so;
        if(fp_so > 0)
            s1 = -1;
            k = 2;
            m = 1;
            region = 1;
        else
            s1 = 1;
            k = 1;
            m = 2;
            region = 2;
        end
    end

    ep_r = point(5,1);
    fp_r = point(5,2);
    fp_rejoin = s1*f_y;
    ep_rejoin = point(m,1)+s1*(ep_o(2)-ep_o(1)+2*f_y/Ep_u);
    fps_rejoin = f_y;

    if(s1 < 0)%if we have yielded in tension and now unloading define
              %the "rejoin point" as the minimum attained strain
        point(2,1) = ep_rejoin;
        point(2,2) = fp_rejoin;
        point(2,3) = f_y;
    else %if we have yielded in compression and now unloading
         %define the "rejoin point" as the maximum attained strain
        point(1,1) = ep_rejoin;
        point(1,2) = fp_rejoin;
        point(1,3) = f_y;
    end

    ep_sushift(k) = s1*ep_su+ep_o(k);
```

```
    ep_a = ep_r+s1*f_y/Ep_u;
    fp_a = fp_r+s1*f_y;

    if(abs(ep_s-ep_r) <= abs(ep_a-ep_r)) %if w/in linear portion
        fp_s = fp_r+Ep_u*(ep_s-ep_r);
        fps_s = Ep_u;
    else
        [fp_s,fps_s] = Bauschinger(0,icheat,P_major,P_minor,...
            ep_sushift,s1,fp_su,Ep_u,ep_a,fp_a,ep_s,k,...
            ep_rejoin,fp_rejoin,fps_rejoin,ep_o,ep_so,fp_so);
    end

    %checking if beyond greatest previous reversal
    if(ep_s > point(1,1))
        point(1,1) = ep_s;
        point(1,2) = fp_s;
        point(1,3) = fps_s;
    end

    if(ep_s < point(2,1))
        point(2,1) = ep_s;
        point(2,2) = fp_s;
        point(2,3) = fps_s;
    end

elseif(yield1 > 1.5)
    %   ******      if WE HAVE ENTERED THE STRAIN HARDENING region
    point(5,1) = ep_so;
    point(5,2) = fp_so;
    point(5,3) = fps_so;

    if(ep_s < ep_so) %if in compressive loading
        s1 = -1;
        k = 2;
        region = 1;
        hist1(2) = 1;
        point(1,1) = ep_so;
        point(1,2) = fp_so;
        point(1,3) = fps_so;
    else %if in tensile loading
        s1 = 1;
        k = 1;
        region = 2;
        hist1(1) = 1;
        point(2,1) = ep_so;
        point(2,2) = fp_so;
        point(2,3) = fps_so;
    end

    ep_r = ep_so;
    fp_r = fp_so;
    ep_o(k) = ep_r+s1*fp_r/Ep_u;
    ep_sushift(k) = s1*ep_su+ep_o(k);
    ep_a = ep_r+s1*f_y/Ep_u;
    fp_a = fp_r+s1*f_y;
    ep_rejoin = ep_sushift(k);
```

```
        fp_rejoin = s1*fp_su;
        fps_rejoin = fps_su;

        if(abs(ep_s-ep_r) <= abs(ep_a-ep_r)) %if within linear portion
            fp_s = fp_r+Ep_u*(ep_s-ep_r);    %of reversal
            fps_s = Ep_u;
        else
            [fp_s,fps_s] = Bauschinger(1,icheat,P_major,P_minor,...
                ep_sushift,s1,fp_su,Ep_u,ep_a,fp_a,ep_s,k,...
                ep_rejoin,fp_rejoin,fps_rejoin,ep_o,ep_so,fp_so);
        end
    end
else %reversal from a reversal
    %-----------------------------------------------------------------
    if(region == 1)%Major compressive reversal (unloading in negative
        [fp_s,fps_s] = reverse1;                              %direction)
        %-----------------------------------------------------------------
    elseif(region == 2)%Major tensile reversal (unloading in positive
        [fp_s,fps_s] = reverse2;                              %direction)
        %-----------------------------------------------------------------
    elseif(region == 3) %Minor compressive reversal (unloading in
                        %negative direction)
        if(ep_s > point(5,1) && ep_s <= point(1,1))%if back to major
            point(5,1) = point(2,1);               %reversal from which
            point(5,2) = point(2,2);               %we left and not to
            point(5,3) = point(2,3);               %skeleton curve
            point(4,1) = 0;
            point(4,2) = 0;
            point(4,3) = 0;
            region = 2;
            [fp_s,fps_s] = reverse2;
        else %if still in minor reversal (or back to skeleton curve)
            [fp_s,fps_s] = reverse3;
        end
        %-----------------------------------------------------------------
    elseif(region == 4) %Minor tensile reversal (unloading in
                        %positive direction)
        if(ep_s < point(5,1) && ep_s >= point(2,1))%if back to major
            point(5,1) = point(1,1);               %reversal from which
            point(5,2) = point(1,2);               %we left and not to
            point(5,3) = point(1,3);               %skeleton curve
            point(4,1) = 0;
            point(4,2) = 0;
            point(4,3) = 0;
            region = 1;
            [fp_s,fps_s] = reverse1;
        else %if still in minor reversal
            [fp_s,fps_s] = reverse4;
        end
        %-----------------------------------------------------------------
    elseif(region == 5) %simple reversal unloading in negative direction
                        %within region 3 (region 3 = minor unloading in
                        %negative direction)
        if(ep_s > point(4,1) && ep_s <= point(1,1)) %if we have reversed
            point(5,1) = point(2,1);                %and are now within
            point(5,2) = point(2,2);                %the major reversal
            point(5,3) = point(2,3);                %from which we came
```

```
        point(4,1) = 0;
        point(4,2) = 0;
        point(4,3) = 0;
        region = 2;
        sim1 = 0;
        [fp_s,fps_s] = reverse2;
    else
        [fp_s,fps_s] = reverse5;
    end
    %---------------------------------------------------------------
elseif(region == 6) %simple reversal unloading in negative direction
                    %within region 4 (region 4 = minor unloading in
                    %positive direction)
    if(ep_s < point(4,1) && ep_s >= point(2,1)) %if back to w/in the
        point(5,1) = point(1,1);                %major reversal from
        point(5,2) = point(1,2);                %which we came
        point(5,3) = point(1,3);
        point(4,1) = 0;
        point(4,2) = 0;
        point(4,3) = 0;
        region = 1;
        sim1 = 0;
        [fp_s,fps_s] = reverse1;
    elseif((ep_s > point(5,1) && ep_s < point(1,1)) && sim1 < 0.5)
        point(5,1) = point(4,1); %if we have reversed and are back to
        point(5,2) = point(4,2); %aiming for the major compressive
        point(5,3) = point(4,3); %reversal point
        region = 4;
        sim1 = 0;
        [fp_s,fps_s] = reverse4;
    else
        [fp_s,fps_s] = reverse6;
    end
    %---------------------------------------------------------------
elseif(region == 7) %simple reversal unloading in positive direction
                    %within region 3 (region 3 = minor unloading in
                    %negative direction)
    if(ep_s > point(4,1) && ep_s <= point(1,1)) %if back to w/in the
        point(5,1) = point(2,1);                %major reversal from
        point(5,2) = point(2,2);                %which we came
        point(5,3) = point(2,3);
        point(4,1) = 0;
        point(4,2) = 0;
        point(4,3) = 0;
        region = 2;
        sim1 = 0;
        [fp_s,fps_s] = reverse2;
    elseif(ep_s < point(6,1) && ep_s > point(2,1) && sim1 < 0.5)
        point(5,1) = point(4,1); %if we have reversed and are back to
        point(5,2) = point(4,2); %aiming for the major compressive
        point(5,3) = point(4,3); %reversal point
        region = 3;
        sim1 = 0;
        [fp_s,fps_s] = reverse3;
    else
        [fp_s,fps_s] = reverse7;
    end
```

```
            %-----------------------------------------------------------------
        elseif(region == 8) %simple reversal unloading in positive direction
                            %within region 4 (region 4 = minor unloading in
                            %positive direction)
            if(ep_s < point(4,1) && ep_s >= point(2,1)) %if we have reversed
                point(5,1) = point(1,1);                %and are now within
                point(5,2) = point(1,2);                %the major reversal
                point(5,3) = point(1,3);                %from which we came
                point(4,1) = 0;
                point(4,2) = 0;
                point(4,3) = 0;
                region = 1;
                sim1 = 0;
                [fp_s,fps_s] = reverse1;
            else
                [fp_s,fps_s] = reverse8;
            end
        end
    end
end

%-----------------------------------
%   UPDATE HISTORY VARIABLES
f_s = fp_s/exp(ep_s);

if stiff
    fs_s = fps_s*(1/(e_s+1))^2;
else
    fs_s = Em_s;
end

if(yield1 > 0.5 && ep_s < 0 && ep_s <= point(2,1)...
        && ((ep_s+0.002) < (-1*ep_M)))
    ep_M = abs(ep_s+0.002);
end

if(yield1 > 0.5 && ep_s > 0 && ep_s >= point(1,1)...
        && ((ep_s-0.002) > ep_M))
    ep_M = (ep_s-0.002);
end

if(yield1 > 0.5)
    Ep_u = Em_s*(0.82+1./(5.55+1000.*ep_M));
else
    Ep_u = Em_s;
end

if(yield1 > 0.5 && yield1 < 1.5 && region < 0.5)
    ep_o(2) = point(1,1)-point(1,2)/Ep_u;
    ep_o(1) = point(2,1)-point(2,2)/Ep_u;
end

%Update history variables
hr(1) = e_s;
hr(2) = f_s;
```

```
hr(3) = yield1;
hr(4) = region;
hr(5) = point(1,1);
hr(6) = point(1,2);
hr(7) = point(1,3);
hr(8) = point(2,1);
hr(9) = point(2,2);
hr(10) = point(2,3);
hr(11) = point(3,1);
hr(12) = point(3,2);
hr(13) = point(3,3);
hr(14) = point(4,1);
hr(15) = point(4,2);
hr(16) = point(4,3);
hr(17) = point(5,1);
hr(18) = point(5,2);
hr(19) = point(5,3);
hr(20) = ep_o(1);
hr(21) = ep_o(2);
hr(22) = ep_M;
hr(23) = fps_s;
hr(24) = hist1(1);
hr(25) = hist1(2);
hr(26) = point(6,1);
hr(27) = point(6,2);
hr(28) = point(6,3);
hr(29) = sim1;
hr(31) = fs_s;

% ========================================================================

function [fp_s,fps_s] = reverse1
    f_y = d(2);
    e_su = d(6);
    f_su = d(7);
    P_major = d(8);
    P_minor = d(9);
    ep_su = log(1+e_su);
    fp_su = f_su*exp(ep_su);
    fps_su = exp(ep_su)*f_su;
    s1 = -1;
    k = 2;
    m = 1;

%************************************************************************

    if(yield1 < 1.5)
        if((ep_s-ep_so) <= 0.0) %We continue unloading
            ep_sushift(k) = s1*ep_su+ep_o(k);
            ep_a = point(5,1)+s1*f_y/Ep_u;
            fp_a = point(5,2)+s1*f_y;

            if((point(5,1)-ep_s) <= (point(5,1)-ep_a))
                fp_s = point(5,2)+Ep_u*(ep_s-point(5,1));
                fps_s = Ep_u;
            else
```

```
                fp_rejoin = s1*f_y;
                ep_rejoin = point(m,1)+s1*(ep_o(2)-ep_o(1)+2*f_y/Ep_u);
                fps_rejoin = f_y;
                [fp_s,fps_s] = Bauschinger(0,icheat,P_major,P_minor,...
                    ep_sushift,s1,fp_su,Ep_u,ep_a,fp_a,ep_s,k,...
                    ep_rejoin,fp_rejoin,fps_rejoin,ep_o,ep_so,fp_so);
            end
        else
            ep_a = point(5,1)+s1*f_y/Ep_u;
            fp_a = point(5,2)+s1*f_y;
            if(((point(5,1)-ep_so) <= (point(5,1)-ep_a)) &&...
                    ((point(5,1)-ep_s) <= (point(5,1)-ep_a)))
                fp_s = point(5,2)+Ep_u*(ep_s-point(5,1));
                fps_s = Ep_u;
            else %We have a MINOR reversal
                point(3,1) = point(5,1);
                point(3,2) = point(5,2);
                point(3,3) = point(5,3);
                point(4,1) = ep_so;
                point(4,2) = fp_so;
                point(4,3) = fps_so;
                point(5,1) = ep_so;
                point(5,2) = fp_so;
                point(5,3) = fps_so;
                region = 4;
                [fp_s,fps_s] = reverse4;
            end
        end

%*************************************************************************

    else
        ep_a = point(5,1)+s1*f_y/Ep_u;
        fp_a = point(5,2)+s1*f_y;
        if(ep_s <= ep_so)
            ep_sushift(k) = s1*ep_su+ep_o(k);
            ep_a = point(5,1)+s1*f_y/Ep_u;
            fp_a = point(5,2)+s1*f_y;
            ep_rejoin = ep_sushift(k);
            fp_rejoin = s1*fp_su;
            fps_rejoin = fps_su;
            if((point(5,1)-ep_s) <= (point(5,1)-ep_a))
                fp_s = point(5,2)+Ep_u*(ep_s-point(5,1));
                fps_s = Ep_u;
            else
                [fp_s,fps_s] = Bauschinger(1,icheat,P_major,P_minor,...
                    ep_sushift,s1,fp_su,Ep_u,ep_a,fp_a,ep_s,k,...
                    ep_rejoin,fp_rejoin,fps_rejoin,ep_o,ep_so,fp_so);
            end
        else
            if(((point(5,1)-ep_so) <= (point(5,1)-ep_a)) && ...
                    ((point(5,1)-ep_s) <= (point(5,1)-ep_a)))
                fp_s = point(5,2)+Ep_u*(ep_s-point(5,1));
                fps_s = Ep_u;
            else
                if((point(5,2)-fp_so) >= 2*f_y) %We have a MAJOR reversal
```

```
                    point(5,1) = ep_so;
                    point(5,2) = fp_so;
                    point(5,3) = fps_so;
                    point(2,1) = ep_so;
                    point(2,2) = fp_so;
                    point(2,3) = fps_so;
                    region = 2;
                    s1 = 1;
                    k = 1;
                    ep_o(k) = ep_so-s1*fp_so/Ep_u;
                    ep_sushift(k) = s1*ep_su+ep_o(k);
                    ep_o(1) = ep_so+fp_so/Ep_u;
                    ep_sushift(1) = ep_o(1)+ep_su;
                    if(hist1(1) < 0.5)
                        hist1(1) = 1;
                    end
                    [fp_s,fps_s] = reverse2;
                else %We have a MINOR reversal
                    region = 4;
                    point(3,1) = point(5,1);
                    point(3,2) = point(5,2);
                    point(3,3) = point(5,3);
                    point(4,1) = ep_so;
                    point(4,2) = fp_so;
                    point(4,3) = fps_so;
                    point(5,1) = ep_so;
                    point(5,2) = fp_so;
                    point(5,3) = fps_so;
                    [fp_s,fps_s] = reverse4;
                end
            end
        end
    end
end

% ========================================================================

function [fp_s,fps_s] = reverse2
    f_y = d(2);
    e_su = d(6);
    f_su = d(7);
    P_major = d(8);
    P_minor = d(9);
    ep_su = log(1+e_su);
    fp_su = f_su*exp(ep_su);
    fps_su = exp(ep_su)*f_su;
    s1 = 1;
    k = 1;
    m = 2;

%************************************************************************

    if(yield1 < 1.5)
        if(ep_s >= ep_so) % we continue unloading
            ep_sushift(k) = s1*ep_su+ep_o(k);
            ep_a = point(5,1)+s1*f_y/Ep_u;
```

```
            fp_a = point(5,2)+s1*f_y;

            if(((point(5,1)-ep_s) >= (point(5,1)-ep_a)))
                fp_s = point(5,2)+Ep_u*(ep_s-point(5,1));
                fps_s = Ep_u;
            else
                fp_rejoin = s1*f_y;
                ep_rejoin = point(m,1)+s1*(ep_o(2)-ep_o(1)+2*f_y/Ep_u);
                fps_rejoin = f_y;
                [fp_s,fps_s] = Bauschinger(0,icheat,P_major,P_minor,...
                    ep_sushift,s1,fp_su,Ep_u,ep_a,fp_a,ep_s,k,...
                    ep_rejoin,fp_rejoin,fps_rejoin,ep_o,ep_so,fp_so);
            end
        else
            ep_a = point(5,1)+s1*f_y/Ep_u;
            fp_a = point(5,2)+s1*f_y;

            if(((point(5,1)-ep_so) >= (point(5,1)-ep_a)) && ...
                    ((point(5,1)-ep_s) >= (point(5,1)-ep_a)))
                fp_s = point(5,2)+Ep_u*(ep_s-point(5,1));
                fps_s = Ep_u;
            else %We have a MINOR reversal
                point(3,1) = point(5,1);
                point(3,2) = point(5,2);
                point(3,3) = point(5,3);
                point(4,1) = ep_so;
                point(4,2) = fp_so;
                point(4,3) = fps_so;
                point(5,1) = ep_so;
                point(5,2) = fp_so;
                point(5,3) = fps_so;
                region = 3;
                [fp_s,fps_s] = reverse3;
            end
        end

%************************************************************************

    else
        ep_a = point(5,1)+s1*f_y/Ep_u;
        fp_a = point(5,2)+s1*f_y;

        if(ep_s >= ep_so)
            ep_sushift(k) = s1*ep_su+ep_o(k);
            ep_a = point(5,1)+s1*f_y/Ep_u;
            fp_a = point(5,2)+s1*f_y;
            ep_rejoin = ep_sushift(k);
            fp_rejoin = s1*fp_su;
            fps_rejoin = fps_su;
            if(((point(5,1)-ep_s) >= (point(5,1)-ep_a)))
                fp_s = point(5,2)+Ep_u*(ep_s-point(5,1));
                fps_s = Ep_u;
            else
                [fp_s,fps_s] = Bauschinger(1,icheat,P_major,P_minor,...
                    ep_sushift,s1,fp_su,Ep_u,ep_a,fp_a,ep_s,k,...
                    ep_rejoin,fp_rejoin,fps_rejoin,ep_o,ep_so,fp_so);
```

```
            end
        else
            if(((point(5,1)-ep_so) >= (point(5,1)-ep_a)) && ...
                    ((point(5,1)-ep_s) >= (point(5,1)-ep_a)))
                fp_s = point(5,2)+Ep_u*(ep_s-point(5,1));
                fps_s = Ep_u;
            else
                if((fp_so-point(5,2)) >= 2*f_y) %We have a MAJOR reversal!
                    point(5,1) = ep_so;
                    point(5,2) = fp_so;
                    point(5,3) = fps_so;
                    point(1,1) = ep_so;
                    point(1,2) = fp_so;
                    point(1,3) = fps_so;

                    if(hist1(2) < 0.5)
                        hist1(2) = 1;
                    end

                    region = 1;
                    s1 = -1;
                    k = 2;
                    ep_o(k) = ep_so+s1*fp_so/Ep_u;
                    ep_sushift(k) = s1*ep_su+ep_o(k);
                    [fp_s,fps_s] = reverse1;
                else %We have a MINOR reversal
                    point(3,1) = point(5,1);
                    point(3,2) = point(5,2);
                    point(3,3) = point(5,3);
                    point(4,1) = ep_so;
                    point(4,2) = fp_so;
                    point(4,3) = fps_so;
                    point(5,1) = ep_so;
                    point(5,2) = fp_so;
                    point(5,3) = fps_so;
                    region = 3;
                    [fp_s,fps_s] = reverse3;
                end
            end
        end
    end
end

% ========================================================================

function [fp_s,fps_s] = reverse3
    f_y = d(2);
    e_su = d(6);
    f_su = d(7);
    P_major = d(8);
    P_minor = d(9);
    ep_su = log(1+e_su);
    fp_su = f_su*exp(ep_su);
    fps_su = exp(ep_su)*f_su;
    s1 = -1;
    k = 2;
```

```
    m = 1;

%************************************************************************

    if(ep_s <= ep_so)
        ep_sushift(k) = s1*ep_su+ep_o(k);
        ep_a = point(5,1)+s1*f_y/Ep_u;
        fp_a = point(5,2)+s1*f_y;
        ep_rejoin = point(3,1);
        fp_rejoin = point(3,2);
        fps_rejoin = point(3,3);
        if(((point(5,1)-ep_s) <= (point(5,1)-ep_a)))
            fp_s = point(5,2)+Ep_u*(ep_s-point(5,1));
            fps_s = Ep_u;
        else
            [fp_s,fps_s] = Bauschinger(0,icheat,P_major,P_minor,...
                ep_sushift,s1,fp_su,Ep_u,ep_a,fp_a,ep_s,k,...
                ep_rejoin,fp_rejoin,fps_rejoin,ep_o,ep_so,fp_so);
        end
    else
        ep_a = point(5,1)+s1*f_y/Ep_u;
        fp_a = point(5,2)+s1*f_y;
        if(((point(5,1)-ep_so) <= (point(5,1)-ep_a)) && ...
                ((point(5,1)-ep_s) <= (point(5,1)-ep_a)))
            fp_s = point(5,2)+Ep_u*(ep_s-point(5,1));
            fps_s = Ep_u;
        else %We have a SIMPLE reversal
            point(4,1) = point(5,1);
            point(4,2) = point(5,2);
            point(4,3) = point(5,3);
            point(6,1) = ep_so;
            point(6,2) = fp_so;
            point(6,3) = fps_so;
            region = 7;
            [fp_s,fps_s] = reverse7;
        end
    end
end

% ========================================================================

function [fp_s,fps_s] = reverse4
    f_y = d(2);
    e_su = d(6);
    f_su = d(7);
    P_major = d(8);
    P_minor = d(9);
    ep_su = log(1+e_su);
    fp_su = f_su*exp(ep_su);
    fps_su = exp(ep_su)*f_su;
    s1 = 1;
    k = 1;
    m = 2;

%************************************************************************
```

```
    if(ep_s >= ep_so)
        ep_sushift(k) = s1*ep_su+ep_o(k);
        ep_a = point(5,1)+s1*f_y/Ep_u;
        fp_a = point(5,2)+s1*f_y;
        ep_rejoin = point(3,1);
        fp_rejoin = point(3,2);
        fps_rejoin = point(3,3);
        if(((point(5,1)-ep_s) >= (point(5,1)-ep_a)))
            fp_s = point(5,2)+Ep_u*(ep_s-point(5,1));
            fps_s = Ep_u;
        else
            [fp_s,fps_s] = Bauschinger(0,icheat,P_major,P_minor,...
                ep_sushift,s1,fp_su,Ep_u,ep_a,fp_a,ep_s,k,...
                ep_rejoin,fp_rejoin,fps_rejoin,ep_o,ep_so,fp_so);
        end
    else
        ep_a = point(5,1)+s1*f_y/Ep_u;
        fp_a = point(5,2)+s1*f_y;
        if(((point(5,1)-ep_so) >= (point(5,1)-ep_a)) && ...
                ((point(5,1)-ep_s) >= (point(5,1)-ep_a)))
            fp_s = point(5,2)+Ep_u*(ep_s-point(5,1));
            fps_s = Ep_u;

        else %We have a SIMPLE reversal
            point(4,1) = point(5,1);
            point(4,2) = point(5,2);
            point(4,3) = point(5,3);
            point(5,1) = ep_so;
            point(5,2) = fp_so;
            point(5,3) = fps_so;
            region = 6;
            [fp_s,fps_s] = reverse6;
        end
    end
end

% ========================================================================

function [fp_s,fps_s] = reverse5
    f_y = d(2);
    e_su = d(6);
    f_su = d(7);
    P_major = d(8);
    P_minor = d(9);
    ep_su = log(1+e_su);
    fp_su = f_su*exp(ep_su);
    fps_su = exp(ep_su)*f_su;
    s1 = -1;
    k = 2;
    m = 1;

%************************************************************************

    if(ep_s <= ep_so)
        ep_sushift(k) = s1*ep_su+ep_o(k);
        ep_a = point(5,1)+s1*f_y/Ep_u;
```

```
        fp_a = point(5,2)+s1*f_y;
        ep_rejoin = point(3,1);
        fp_rejoin = point(3,2);
        fps_rejoin = point(3,3);
        if((point(5,1)-ep_s) <= (point(5,1)-ep_a))
            fp_s = point(5,2)+Ep_u*(ep_s-point(5,1));
            fps_s = Ep_u;
        else
            if(sim1 > 0.5)
                sim1 = 0;
                point(6,1) = 0;
                point(6,2) = 0;
                point(6,3) = 0;
            end
            [fp_s,fps_s] = Bauschinger(0,icheat,P_major,P_minor,...
                ep_sushift,s1,fp_su,Ep_u,ep_a,fp_a,ep_s,k,...
                ep_rejoin,fp_rejoin,fps_rejoin,ep_o,ep_so,fp_so);
        end
    else
        ep_a = point(5,1)+s1*f_y/Ep_u;
        fp_a = point(5,2)+s1*f_y;
        if(((point(5,1)-ep_so) <= (point(5,1)-ep_a)) && ...
            ((point(5,1)-ep_s) <= (point(5,1)-ep_a)) && ...
            (point(5,1) >= ep_s))
            fp_s = point(5,2)+Ep_u*(ep_s-point(5,1));
            fps_s = Ep_u;
        else %We have a new SIMPLE reversal
            if(sim1 < 0.5)
                point(6,1) = ep_so;
                point(6,2) = fp_so;
                point(6,3) = fps_so;
                sim1 = 1;
            else
                point(5,1) = 0;
                point(5,2) = 0;
                point(5,3) = 0;
                sim1 = 0;
            end

            region = 7;
            [fp_s,fps_s] = reverse7;
        end
    end
end

% ========================================================================

function [fp_s,fps_s] = reverse6
    f_y = d(2);
    e_su = d(6);
    f_su = d(7);
    P_major = d(8);
    P_minor = d(9);
    ep_su = log(1+e_su);
    fp_su = f_su*exp(ep_su);
    fps_su = exp(ep_su)*f_su;
```

```
    s1 = -1;
    k = 2;
    m = 1;

%************************************************************************

    if(ep_s <= ep_so)
        ep_sushift(k) = s1*ep_su+ep_o(k);
        ep_a = point(5,1)+s1*f_y/Ep_u;
        fp_a = point(5,2)+s1*f_y;
        ep_rejoin = point(4,1);
        fp_rejoin = point(4,2);
        fps_rejoin = point(4,3);

        if((point(5,1)-ep_s) <= (point(5,1)-ep_a))
            fp_s = point(5,2)+Ep_u*(ep_s-point(5,1));
            fps_s = Ep_u;
        else
            if(sim1 > 0.5)
                sim1 = 0;
                point(6,1) = 0;
                point(6,2) = 0;
                point(6,3) = 0;
            end

            [fp_s,fps_s] = Bauschinger(0,icheat,P_major,P_minor,...
                ep_sushift,s1,fp_su,Ep_u,ep_a,fp_a,ep_s,k,...
                ep_rejoin,fp_rejoin,fps_rejoin,ep_o,ep_so,fp_so);
        end
    else
        ep_a = point(5,1)+s1*f_y/Ep_u;
        fp_a = point(5,2)+s1*f_y;

        if(((point(5,1)-ep_so) <= (point(5,1)-ep_a)) && ...
                ((point(5,1)-ep_s) <= (point(5,1)-ep_a)) && ...
                (point(5,1) >= ep_s))
            fp_s = point(5,2)+Ep_u*(ep_s-point(5,1));
            fps_s = Ep_u;
        else %We have a new SIMPLE reversal in the same region but with
             %the opposite direction
            if(sim1 < 0.5)
                point(6,1) = ep_so;
                point(6,2) = fp_so;
                point(6,3) = fps_so;
                sim1 = 1;
            else
                point(5,1) = 0;
                point(5,2) = 0;
                point(5,3) = 0;
                sim1 = 0.;
            end

            region = 8;
            [fp_s,fps_s] = reverse8;
        end
    end
```

```
end

% ========================================================================

function [fp_s,fps_s] = reverse7
    f_y = d(2);
    e_su = d(6);
    f_su = d(7);
    P_major = d(8);
    P_minor = d(9);
    ep_su = log(1+e_su);
    fp_su = f_su*exp(ep_su);
    fps_su = exp(ep_su)*f_su;
    s1 = 1;
    k = 1;
    m = 2;

%************************************************************************

    if(ep_s >= ep_so)
        ep_sushift(k) = s1*ep_su+ep_o(k);
        ep_a = point(6,1)+s1*f_y/Ep_u;
        fp_a = point(6,2)+s1*f_y;
        ep_rejoin = point(4,1);
        fp_rejoin = point(4,2);
        fps_rejoin = point(4,3);

        if((point(6,1)-ep_s) >= (point(6,1)-ep_a))
            fp_s = point(6,2)+Ep_u*(ep_s-point(6,1));
            fps_s = Ep_u;
        else
            if(sim1 > 0.5)
                sim1 = 0;
                point(5,1) = 0;
                point(5,2) = 0;
                point(5,3) = 0;
            end

            [fp_s,fps_s] = Bauschinger(0,icheat,P_major,P_minor,...
                ep_sushift,s1,fp_su,Ep_u,ep_a,fp_a,ep_s,k,...
                ep_rejoin,fp_rejoin,fps_rejoin,ep_o,ep_so,fp_so);
        end
    else
        ep_a = point(6,1)+s1*f_y/Ep_u;
        fp_a = point(6,2)+s1*f_y;

        if(((point(6,1)-ep_so) >= (point(6,1)-ep_a)) && ...
                ((point(6,1)-ep_s) >= (point(6,1)-ep_a)) && ...
                (point(6,1) <= ep_s))
            fp_s = point(6,2)+Ep_u*(ep_s-point(6,1));
            fps_s = Ep_u;
        else %We have a new SIMPLE reversal inside a region 3, but with
             %the opposite direction
            if(sim1 < 0.5)
                point(5,1) = ep_so;
```

```
                point(5,2) = fp_so;
                point(5,3) = fps_so;
                sim1 = 1;
            else
                point(6,1) = 0;
                point(6,2) = 0;
                point(6,3) = 0;
                sim1 = 0.;
            end

            region = 5;
            [fp_s,fps_s] = reverse5;
        end
    end
end

% ========================================================================

function [fp_s,fps_s] = reverse8
    f_y = d(2);
    e_su = d(6);
    f_su = d(7);
    P_major = d(8);
    P_minor = d(9);
    ep_su = log(1+e_su);
    fp_su = f_su*exp(ep_su);
    fps_su = exp(ep_su)*f_su;
    s1 = 1;
    k = 1;
    m = 2;

%************************************************************************

    if(ep_s >= ep_so)
        ep_sushift(k) = s1*ep_su+ep_o(k);
        ep_a = point(6,1)+s1*f_y/Ep_u;
        fp_a = point(6,2)+s1*f_y;
        ep_rejoin = point(3,1);
        fp_rejoin = point(3,2);
        fps_rejoin = point(3,3);
        if((point(6,1)-ep_s) >= (point(6,1)-ep_a))
            fp_s = point(6,2)+Ep_u*(ep_s-point(6,1));
            fps_s = Ep_u;

        else
            if(sim1 > 0.5)
                sim1 = 0;
                point(5,1) = 0;
                point(5,2) = 0;
                point(5,3) = 0;
            end

            [fp_s,fps_s] = Bauschinger(0,icheat,P_major,P_minor,...
                ep_sushift,s1,fp_su,Ep_u,ep_a,fp_a,ep_s,k,...
                ep_rejoin,fp_rejoin,fps_rejoin,ep_o,ep_so,fp_so);
```

```
        end
    else
        ep_a = point(6,1)+s1*f_y/Ep_u;
        fp_a = point(6,2)+s1*f_y;

        if(((point(6,1)-ep_so) >= (point(6,1)-ep_a)) && ...
                ((point(6,1)-ep_s) >= (point(6,1)-ep_a)) && ...
                (point(6,1) <= ep_s))
            fp_s = point(6,2)+Ep_u*(ep_s-point(6,1));
            fps_s = Ep_u;
        else %We have a new SIMPLE reversal inside a region 3, but with
             %the opposite direction
            if(sim1 < 0.5)
                point(5,1) = ep_so;
                point(5,2) = fp_so;
                point(5,3) = fps_so;
                sim1 = 1;
            else
                point(6,1) = 0;
                point(6,2) = 0;
                point(6,3) = 0;
                sim1 = 0.;
            end

            region = 6;
            [fp_s,fps_s] = reverse6;
        end
    end
end

% ========================================================================

function [fp_s,fps_s] = virginLoading
    if (ep_s >= ep_o1) %if in tensile loading
        s1 = 1;
        k = 1;
    else %if in compressive loading
        s1 = -1;
        k = 2;
    end

%Model modified to account for shift due to reversal in yield plateau

    if ((abs(ep_s-ep_o1) >= 0) && ((abs(ep_s-ep_o1)) < (f_y/Em_s)))
        %Elastic branch
        fp_s = Em_s*ep_s; %Eq 15
        fps_s = Em_s;
        yield1 = 0;
    elseif (((abs(ep_s-ep_o1)) >= (f_y/Em_s)) && ((abs(ep_s-ep_o1)) < ep_sh))
        %Yield plateau
        fp_s = s1*f_y*exp(ep_s); %Eq 16
        fps_s = f_y;
        if(yield1 < 0.5); yield1 = 1; end
    else %Strain hardening or post-ultimate branch
%Eq 18.b - This term provides the initial power of the strain hardening curve
        P = log10((fp_sh1+fps_su*(ep_su-ep_sh1)-fp_su)/(fp_sh+fps_su* ...
```

```
            (ep_su-ep_sh)-fp_su))/log10((ep_su-ep_sh1)/(ep_su-ep_sh));

        aux1 = s1*(fp_sh+fps_su*(ep_su-ep_sh)-fp_su);
        aux2 = (ep_su-s1*(ep_s-ep_o1))/(ep_su-ep_sh);
        fp_s = aux1*(aux2^P)-fps_su*(s1*ep_su-(ep_s-ep_o1))+s1*fp_su;%Eq 18.a
        fps_s = fps_su+aux1*P*(aux2^(P-1))*(-1*s1)/(ep_su-ep_sh);
        yield1 = 2;
    end
end

% ========================================================================

function [fp_s,fps_s] = Bauschinger(major,icheat,P_major,P_minor,...
    ep_sushift,s1,fp_su,Ep_u,ep_a,fp_a,ep_s,k,ep_target,fp_target,...
    fps_target,ep_o,ep_so,fp_so)

    if((ep_target-ep_a) == 0)
        slope2 = fps_target;
    else
        slope2 = 0.8*(fp_target-fp_a)/(ep_target-ep_a);
    end

    if(fps_target < slope2); slope2 = fps_target; end

    if(major == 0)
        P = P_minor;
    else
        if (icheat == 1)
            P = P_major;
        else
            fp_p = fp_su*(s1-ep_sushift(k)+ep_a)-fp_a; %Eq 33.a
            fp_t = fp_su*(2-ep_sushift(1)+ep_sushift(2)); %Eq 33.b
            ep_p = abs((0.2*s1+ep_o(k) - ep_a)/0.2); %Eq 33.c
            fnorm1 = abs(fp_p/fp_t);
            W = ((0.001+0.00108/(1.043-ep_p))/0.18*(fnorm1-...
                0.69)+0.085); %Eq 34
            if (W > 0.30); W = 0.30; end
            if (W < 0.06); W = 0.06; end

            P = 56.689*(W-0.077)^2-4.921*(W-0.077)+0.1; %Eq 36
        end
    end

    %Initialize values for Newton-Raphson algorithm
    R = 1;
    tol = 1.d-9;
    n = 0;
    epp_N = 0.1;
    Bisection = 0;
    while ((abs(R) > tol) && n < 10) %Newton-Raphson algorithm
        if(epp_N < 0);      %switch to bisection algorithm if negative
            Bisection = 1;  %values are obtained
            break;
        end
        R = rcalc(epp_N,P,ep_target,fp_target,slope2,ep_a,fp_a,Ep_u,ep_s);
```

```
    J = -(fp_target-fp_a+Ep_u*(ep_a-ep_target))/(fp_target-fp_a+slope2...
        *(ep_a-ep_target))-P*(1-(epp_N-1)^2)^(P-1)*(2*epp_N-2);
    depp_N = -R/J;
    epp_N = epp_N+depp_N;
    n = n+1;
end

if(n == 10); Bisection = 1; end

if (Bisection == 1)
    %Bisection algorithm initialization
    Ru = 1;
    Rl = 1;
    epp_N = 0;
    n = 0;

    %Bracket solution
    while ((Ru*Rl) > 0 && n < 1000)
        n = n+1;
        valn1 = n;
        epp_Nl = 0;
        epp_Nu = epp_N+0.001*valn1;
        Rl = rcalc(epp_Nl,P,ep_target,fp_target,slope2,ep_a,fp_a,Ep_u,...
            ep_s);
        Ru = rcalc(epp_Nu,P,ep_target,fp_target,slope2,ep_a,fp_a,Ep_u,...
            ep_s);
    end

    if(n == 1000 && (Ru*Rl) > 0)
        disp('could not bracket solution!')
        disp([epp_Nl,Rl])
        disp([epp_Nu,Ru])
        disp([ep_target,fp_target,slope2,ep_a,fp_a,Ep_u,ep_s])
        disp([ix(1,1),ix(2,1),ep_s])
        disp([ep_r(1),fp_r(1),ep_r(2),fp_r(2),P])
        stop
    end

    if (abs(Rl) < tol) %if the lower bound is a root
        epp_N = epp_Nl;
    elseif (abs(Ru) < tol) %or if the upper bound is a root
        epp_N = epp_Nu;
    else %otherwise do the bisectional algorithm
        tol = 1.d-10;
        tol12 = 1.d-4;
        Rm = 1; %just give initial value higher than tolerance
        iter = 0;

        while ((epp_Nu-epp_Nl) > tol && iter < 10000 && abs(Rm) > tol12)
            iter = iter+1;
            epp_Nm = (epp_Nl+epp_Nu)/2;
            Rm = rcalc(epp_Nm,P,ep_target,fp_target,slope2,...
                ep_a,fp_a,Ep_u,ep_s);
            if ((Rl*Rm) < 0)
                epp_Nu = epp_Nm;
                Ru = Rm;
```

```
                elseif ((Rl*Rm) > 0)
                    epp_Nl = epp_Nm;
                    Rl = Rm;
                end
            end

            if(iter == 10000)
                disp(['maximum number of iterations in Bisection method',...
                    ' exceeded'])
                disp([epp_Nu,epp_Nl,Rl,Ru,epp_Nm,Rm,iter])
                disp(' ')
                disp([ep_target,fp_target,slope2,ep_a,fp_a,Ep_u,ep_s])
                disp(ep_s)
                stop
            end
            epp_N = epp_Nm;
        end
    end

    fp_s = (epp_N*((fp_target-fp_a)-Ep_u*(ep_target-ep_a))+Ep_u* ...
        (ep_s-ep_a)+fp_a);

    if (epp_N < 0.0001 || (Ep_u-slope2)/Ep_u < 0.01)
        fps_s = Ep_u;
    else
        fps_s = 2*P*(1-(1-epp_N)^2)^(P-1)*(1-epp_N);
        fps_s = fps_s*((fp_target-fp_a)-slope2*(ep_target-ep_a))/...
            (((ep_target-ep_a)*Ep_u-(fp_target-fp_a))/(Ep_u-slope2));
        fps_s = fps_s*Ep_u/(fps_s+Ep_u) + slope2;
    end

    if(fps_s < 0.) %if derivative is negtive, use tangent slope of curve
        fps_s = (fp_s-fp_so)/(ep_s-ep_so);
    end
end

% ========================================================================

function R=rcalc(epp_N,P,ep_target,fp_target,fps_target,ep_a,fp_a,Ep_u,ep_s)
    val2 = (fp_target-fp_a)-fps_target*(ep_target-ep_a);
    val1 = epp_N*((fp_target-fp_a)-Ep_u*(ep_target-ep_a))...
        +(Ep_u-fps_target)*(ep_s-ep_a);
    %Eq 29, moved all to the righthand side to solve for r = 0
    R = (1-(1-epp_N)^2)^P-val1/val2;
end
end
```